LASER MILLING: SURFACE INTEGRITY, REMOVAL STRATEGIES AND PROCESS ACCURACY

A thesis

submitted to the

Cardiff University

for the degree of

Doctor of Philosophy

by

Petko Petkov

Manufacturing Engineering Centre

School of Engineering

Cardiff University

United Kingdom

May, 2011

Abstract

Laser milling is capable of processing a large range of materials which are not machinable with conventional manufacturing processes. Engineering materials such as glass, metals and ceramics can be machined without requiring expensive special tools and without any limitations on the 3D complexity of the component.

Laser milling is still in its infancy. Laser material interactions are not yet fully understood. Much effort in research and development of the available laser sources is still needed. Ultrafast lasers are beginning to be applied. They can offer more precise machining without the thermal damage that accompanies long-pulse laser manufacturing.

Laser pulse duration and its effect on resulting surface integrity has been studied as well as material removal strategy and process accuracy.

In order to characterise the resulting surface after laser ablation, the heat affected zone is usually specified. In most cases, visual inspection would be performed without further analysis, resulting in variance of the findings attributed to the operator.

A new methodology was required to accurately and impartially assess the heat penetration and quantify the findings. Based on material grain refinement, a comprehensive new methodology was created. By monitoring the changes in grain sizes, a chart of the heat penetration could be created accurately with automated routines.

Surface integrity is a critical factor for many applications and a methodology based on analysis of grain refinement in the vicinity of the processed area would create a full map of

the changes happening after laser ablation. Furthermore, the impact of the laser pulse duration is studied utilising the above mentioned development. Further to the surface roughness and heat affected zone, an in-depth analysis was completed on the micro hardness of the material in order to create a comprehensive chart of the changes induced by the laser milling process.

Material removal is based on the overlapping of single craters, and the way the craters overlap is referred to as material removal strategy. Generally there are many strategies formulated for material removal but none of them takes into account the specifics of laser milling. Based on surface orientation, dimensions and feature importance, an assessment of material removal strategies is presented. Although 'laser milling' is a term used for a number of material removal processes, there are significant differences between them. New strategies for material removal are formulated and reported based on surface topography and orientation. Advanced programming is realised using a commercially available generic CAM package but taking into account the specifics of the laser milling process.

The accuracy of the laser milling process depends on the laser-material interaction, and also on the machine hardware, control system and software. Most of the factors affecting accuracy cannot be changed once the machine is built, but there are some that can be optimised to improve process accuracy. The laser source with its characteristics is as important as the material being processed. The relationship between pulse duration, pulse shape and accuracy of the process was demonstrated through a series of experiments designed to expose the correlation between, and impact of, these parameters.

Acknowledgements

I would like to express my thanks to my supervisor and Director of the Manufacturing Engineering Centre, Professor D. T. Pham, for giving me this opportunity and for his valued supervision and support during my research.

To all colleagues and friends at the Manufacturing Engineering Centre, I would like to express my gratitude for their patience and continuous support. Special thanks go to Prof. S Dimov, Dr R. Minev, Dr K. Popov and Dr. T Dobrev for their constant assistance through technical help, countless discussions and unquestionable support.

My deepest gratitude goes to my family and friends that have supported me through this journey.

Declaration

This work has not previously been accepted in substance for any degree and is not being concurrently submitted in candidature for any degree.

Signed: .....(Petko Petkov, Candidate) Date: .....

Statement 1

This thesis is being submitted in partial fulfilment of the requirements for the degree of PhD.

Signed: .....(Petko Petkov, Candidate) Date: .....

Statement 2

This thesis is the result of my own investigations, except where otherwise stated. Other sources are acknowledged by giving explicit references. A bibliography is appended.

Signed: .....(Petko Petkov, Candidate) Date: .....

Statement 3

I hereby give my consent for my thesis, if accepted, to be available for photocopying and for interlibrary loan, and for the title and summary to be made available to outside organisations.

Signed: .....(Petko Petkov, Candidate) Date: .....

LIST OF TABLES

LIST OF FIGURES

ABBREVIATIONS

2D	Two dimensional
3D	Three dimensional
CAD	Computer aided design
CAM	Computer aided manufacturing
CL	Cutter location
CNC	Computer numerical control
CO_2	Carbon dioxide laser (CO_2 laser)
CW	Continuous wave
EXCIMER	EXCIted diMER
FIB	Focused ion beam
FWHM	Full width at half-maximum
HAZ	Heat affected zone
HeNe	Helium-neon laser
IEEE 1394	Serial bus interface standard
IGS	Initial graphics exchange specification
I/O	Input/Output
IR	Infrared
ISO	International organization for standardization
IT	International tolerance grade
MOPA	Master oscillator power amplifier
NC	Numerical control
Nd:YAG	Neodymium-doped yttrium aluminium garnet; $Nd:Y_3Al_5O_{12}$
PSO	Position synchronized output
QS	Q Switched (pulsed mode)

SEM	Scanning electron microscope
STL	Stereolithography file format
STP	ISO10303: Automation systems and integration — product data representation and exchange
UV	Ultraviolet

NOMENCLATURE

α	[-]	material phase
γ	[-]	material phase
$2w_o$	[μm]	laser spot
λ	[nm]	wavelength
π	[-]	3.14159
τ_e	[s]	electron cooling time
τ_i	[s]	lattice heating time
τ_L	[s]	laser pulse duration
D	[mm]	input beam diameter
f	[mm]	focal length
M^2	[-]	laser beam quality factor
P	[W]	laser average power
P_{max}	[W]	maximum power output
R_a	[μm]	surface roughness
W	[Wcm^{-2}]	peak power

Chapter 1 Introduction

1.1 Motivation

Since their discovery, lasers have attracted the attention of researchers in different domains because of their ability to concentrate significant amounts of energy onto a very small area. They provide extremely high power densities that can be utilised in various manufacturing applications. Lasers are used in welding, cutting, cladding, hardening, heating and drilling (Steen, 1998). Also, lasers are easily integrated in CNC machines, which make them a flexible and efficient material processing technology.

A new laser-based manufacturing process was developed in the last two decades and has recently become commercially available. The process is called laser milling and is also known as laser ablation. This is a process for direct material removal in a layer-by-layer fashion. 3D CAD data is used to generate CNC machining programs. The process is flexible and can be employed in a wide range of applications from one-off part production to the manufacture of small batches. Development in laser technology has been progressing rapidly in the last decade but when it comes to the development of new applications, new challenges have arisen as this new technology has been utilized for micro manufacturing. In the world of micro components/features where feature sizes are comparable with the topography (roughness for example), surface integrity and strategies for retaining desired properties need to be addressed.

1.2 Aim and objectives

The aim of this work was to investigate the effects on the substrate caused by laser ablation when utilized in ‘milling’ fashion and, in particular the heat affected zones created. Then,

through material removal strategy and accuracy estimation, to apply process optimization for the material removal when utilized in micro structuring applications.

The main objectives were:

- To find suitable method for heat affected zone analysis
- To formulate material removal strategies
- To analyze material removal process accuracy

1.1.1 Research questions

This thesis aims to answer the following research questions:

1. How does the laser material interaction change the surface integrity and is there a method for analysis?
2. How does the way the material is removed influence the outcome of the process?
3. Which factors influence the process accuracy and is there a way to improve the overall accuracy?

1.1.2 Methodology

The project covered the investigation of the heat affected zones and a method for quality analysis of resultant surfaces after laser ablation, as required by many aerospace applications and applications involving multiple heating/cooling cycles.

The expected quality aspects include:

- Thermal penetration
- Grain refinement

- Hardness change

After developing a suitable method for quality analysis of the resulting surface, experiments will be carried out to analyze the effects of the pulse duration on the substrate. A series of experiments will be carried out utilizing laser sources with different pulse durations, the results will then be processed and compared.

Material removal strategy will be under investigation. By changing the order in which the material is removed – often referred to as removal strategy- different results can be obtained. Although referred to as laser milling this process inherits a lot of specifics of the laser ablation and widely used ‘milling’ strategies are not applicable.
New laser milling strategies will be identified and verified through experiments for particular applications with regard to the micro manufacturing of components and features.

The next objective was to investigate the overall accuracy of the laser milling process and to identify the laser parameters that are influencing it. Laser pulse duration will be investigated as well as pulse energy and pulse shape through series of experiments.

1.2 Outline of thesis

Chapter 2 presents an in depth review of the physical phenomena of laser ablation with a focus on laser radiation, substrate material characteristics and absorption of the laser light. Important characteristics of the laser source like wavelength, spot size, pulse duration and beam intensity are reviewed. The chapter continues with a review of the most commonly utilized machining techniques for material removal and a description of one of the most

advanced laser machining systems. Chapter 2 concludes by identifying advantages and disadvantages of the laser milling process.

Chapter 3 takes a closer look at the resulting surface of the laser ablation process. Laser sources and substrate materials are reviewed in the context of laser material interaction. Material removal mechanisms are discussed as well as the effect they have on the resulting surface. A novel approach was developed for heat affected zone analysis based on the changes in grain microstructure of the steel substrates.

In chapter 4, the focus is on the strategies for material removal as the factors influencing the laser milling process, such as CAD data, tool path generation, and machine set-up are discussed. In this chapter a new approach is defined for identifying the most suitable strategy for material removal based on the topography of the model and laser – substrate coupling characteristics.

Chapter 5 further discusses the accuracy of the laser milling process and its most influential factors. The optimization of accuracy, based on process optimization and control is reviewed as machine factors influencing accuracy of the laser milling process are very difficult to change.

Chapter 6 summarizes the contributions in the presented work with major outcomes. The chapter concludes with suggestions for further research.

Chapter 2 Background

This chapter provides an overview of the characteristics of the process and discusses its application aspects. The chapter starts with a description of the physical phenomena underlying the process. It then outlines the machining techniques that are employed in laser milling.

2.1 Physical phenomena

The laser milling process removes material as a result of interaction between the laser beam and the substrate or workpiece. Several removal mechanisms can take place, depending on a number of process parameters related to the beam and the workpiece material. The following sub-sections describe the factors influencing the laser milling process.

2.1.1 Laser radiation

Laser radiation has a number of characteristics that make it applicable to manufacturing. The focus is on those characteristics relating to material removal capabilities.

Laser radiation can be delivered to the workpiece in an ordered sequence of pulses with a predetermined pulse length (duration) and repetition rate (frequency). This allows the accumulated energy to be released in very short time intervals, which is a prerequisite for the formation of extremely high peak power. Additionally, the laser beam can be focused on a spot with very small dimensions (1-50 μm), which leads to a significant energy density (fluence) and intensity (power density) in the spot area. As a result, an extremely high density

(10^{17}-10^{22} W/m^2) can be released in the laser-material interaction zone that could not be achieved by any conventional machining technology. This explains the capability of laser milling to process materials that are difficult to machine (Hellrung et al, 1999).

Laser radiation is monochromatic, which means that the substrate response and substrate properties remain relatively uniform and a stable process can be easily achieved. Another important laser radiation feature that affects the ablation mechanism is photon energy. For example, for the UV excimer laser radiation, photon energy is comparable to the material bonding energy of semiconductors and polymers. Therefore, these lasers produce clean ablation and minimal heat effects and are preferred for such materials (Leong, 2000). Interaction between the laser radiation and the plasma formed during the process must be noted as a factor reducing the overall machining efficiency (Dörbecker et al, 1996).

1.1.1 Substrate material

The response of the substrate to laser radiation is influenced by a number of material characteristics. Laser ablation occurs only at wavelengths for which the particular material is strongly absorptive. Hence, for optimal machining results a proper match of laser source and material should be achieved. Generally, higher absorption efficiency leads to a more effective laser milling process. A number of ways exist to increase laser absorptivity, in particular, creating an appropriate surface finish prior to laser milling or applying a suitable surface coating. Laser ablation efficiency canalso be increased by performing the process at elevated temperatures or under water (Geiger et al, 1996).

Thermal conductivity is another key material factor. This affects the dissipation of the absorbed energy into the bulk of the material, the energy losses, the material removal efficiency and the dimensions of the heat affected zone (HAZ). For example, ceramic materials, which have the highest melting and vaporisation temperatures, have low thermal conductivity which makes them easily machinable by laser radiation (Tsai et al, 2003; Moldovan et al, 2005; Karnakis et al, 2005; Knowles et al, 2006; Pham et al, 2007).

During laser ablation, the material passes through several phase transitions, depending on the process parameters. Thus, relevant material characteristics are transition energies such as evaporation energy and melting energy. This can be illustrated by the fact that compared with ceramics, metals are easy to melt, but are relatively more difficult to evaporate, which influences the laser ablation mechanism.

1.1.2 Absorption of laser radiation

During interaction between the laser radiation and the material, electrons in the substrate are excited by the laser photons. As a result, the electron subsystem is heated to a high temperature and the absorbed energy is transferred to the atomic lattice (Shirk et al, 1998; Lunney et al, 1998; Meijer et al, 2004; Weaver et al, 1981; Wilson et al, 1987). Energy losses are caused by heat transport via electrons into the bulk of the substrate. According to classical linear theory, light absorption is described by the Beer-Lambert law, which states that the absorption of a particular wavelength of light transmitted through a material is a function of the material path length and is independent of the incident intensity. For the very high intensities which can be achieved in laser processing, non-linear phenomena take place and

cause stronger energy absorption. According to the linear absorption model, electrons excited by photon absorption transfer heat energy to the lattice and cause melting or vaporisation. In the case of extreme intensities, as with ultrashort pulse ablation, the bound electrons of the material can be directly freed (Shirk et al, 1998). Effects such as multiphoton absorption and avalanche ionisation can be observed. Thermal conduction in the material draws energy away from the focal spot and leads to heat affected zones (Yilbas et al, 2000; P V Petkov et al, 2008).

For metals, laser light absorption is not a major problem, because the band structure of the material allows the absorption of most low-to-moderate energy photons. Metals absorb laser radiation with their electrons in the conduction band and near to the Fermi level. For semiconductors and insulators, including ceramics and polymers, the Fermi level is between the valence and conduction bands. The requirement that an electron has to absorb enough energy to pass through the forbidden region between the valence and conduction bands sets a limit on the photon energies that can be absorbed by a linear process. There are two methods for non-linear absorption: an electron avalanche and a strong multiphoton absorption (Shirk et al, 1998).

In the case of an electron avalanche, some electrons with intermediate energies are excited into the conduction band by single photon absorption. The electrons in the conduction band can absorb single photons of the incident light, which will increase their energy. These electrons collide with bound electrons, which lead to avalanche ionisation.

Multiphoton absorption is another mechanism for non-linear absorption in which an electron transfers from the valence band to the conduction band by absorbing several photons.

In general, as materials reach a critical density of electrons they start absorbing sufficient photon energy to undergo ablation (Shirk et al, 1998). It is important to note that there is a material dependent ablation threshold fluence (Shirk et al, 1998, Petzoldt et al, 1996; Zhu et al, 2000), below which the laser ablation cannot start and material removal is not feasible.

1.1.3 Laser ablation mechanisms

For pulsed laser machining the actual process of removing the substrate takes place within the laser pulse. Several mechanisms exist for material removal, depending on the laser pulse duration and some material specific time parameters (Chichkov et al, 1996; Momma et al, 1997). The following important material dependent time parameters are considered:

- τ_e - electron cooling time;
- τ_i - lattice heating time;
- τ_L - laser pulse duration.

As a rule $\tau_e << \tau_i$ and for most materials τ_i is in the picosecond range. Three different ablation regimes exist according to the laser pulse length:

- femtosecond pulses - $\tau_L < \tau_e < \tau_i$;
- picosecond pulses - $\tau_e < \tau_L < \tau_i$;
- nanosecond and longer pulses - $\tau_e < \tau_i < \tau_L$.

The laser ablation mechanisms for femtosecond and picosecond pulses are alike and are shown in Figure 2.1. For these regimes, the ablation process can be regarded as a direct solid-

vapour transition (sublimation), with negligible thermal conduction into the substrate and almost no HAZ (Shirk et al, 1998; Kautek et al, 1994; Preuss et al, 1995; von den Linde, 2000; Liu et al, 1997; Nikumb et al, 2004; D.M. Karnakis et al, 2004).

The laser pulse duration is much shorter than the time required for the absorbed energy to be transferred into the substrate in the form of heat. Each pulse creates some "solid plasma", a substance consisting of loosely bound ions and electrons on the material surface. The solid plasma leaves the material after the end of the pulse, expanding in a highly ionized state. During this expansion the solid plasma takes most of the energy with it and consequently very little energy remains in the substrate.

After the solid plasma leaves the substrate it becomes very energetic containing highly ionized atoms (ions) and electrons. The electrons are lighter and are the first to go away from the substrate followed by the ions and because the latter all have positive charges they repel one another, which helps their removal from the substrate.
For picosecond pulse ablation, in spite of the formation of a molten zone and some heat transfer, the dominant removal mechanism is still a solid-vapour transition.

For nanosecond and longer pulses, the process conditions are summarised in Figure 2.2. In this case, the absorbed energy from the laser pulse melts the material and heats it to the vaporisation temperature. There is enough time for a thermal wave to propagate into the material. Evaporation occurs from the liquid material. The molten material is partially ejected from the cavity by the vapour and plasma pressure, but a part of it remains near the surface, held by surface tension forces. After the end of a pulse, the heat quickly dissipates into the

bulk of the material and a recast layer is formed (Leong et al, 2000; Gotz et al, 1996; Petkov et al, 2007).

Secondary effects for machining regimes with nanosecond and longer pulses are a heat affected zone, a recast layer, microcracks, shock wave surface damage and debris from ejected material. Additionally, the vaporised material forms a plasma from the leading edge of the pulse and this is sustained during the rest of the pulse (Cline et al, 1977; Costa et al, 2003). Due to the plasma shielding effect (the plasma absorbs and defocuses the pulse energy) a higher irradiance (fluence) is required for deeper penetration (Leong et al, 2000; Kautek et al, 1994).

In the case of femtosecond pulse ablation, the plasma is formed after the end of the pulse, which means that the shielding effect is avoided. It is important to note that for the femto- and picosecond regimes, the fluence should only vary within predefined limits. Exceeding these limits causes undesirable secondary effects as shown in Figure 2.3 (Leong et al, 2000; Kautek et al, 1994).

Another mechanism of laser ablation can take place under the following conditions: oxygen environment, low scanning speeds and nano-to-microsecond laser pulses. This mechanism involves four steps (Schubart et al, 1997):

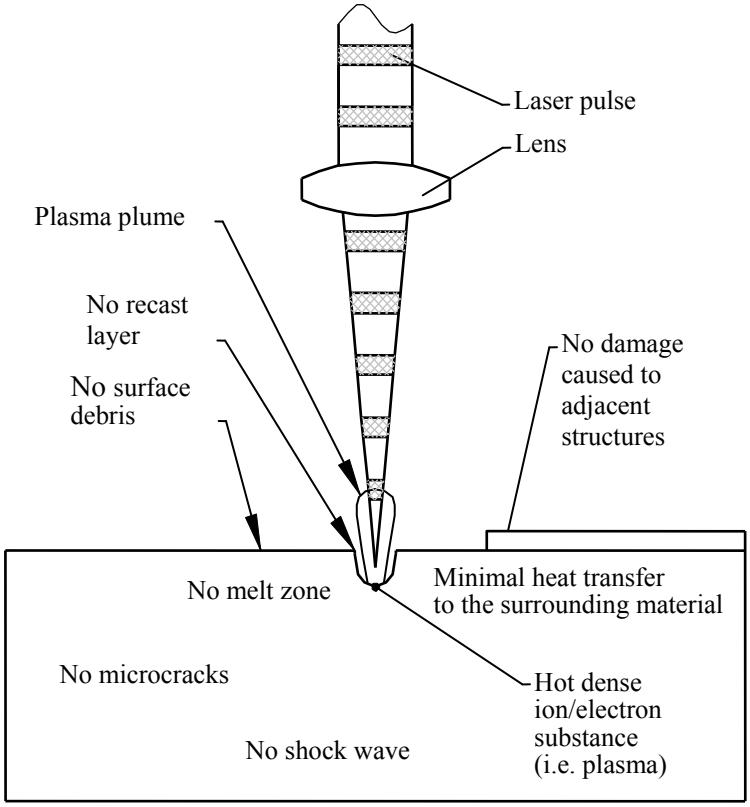

Figure 2.1 Femto and picosecond pulsed laser ablation

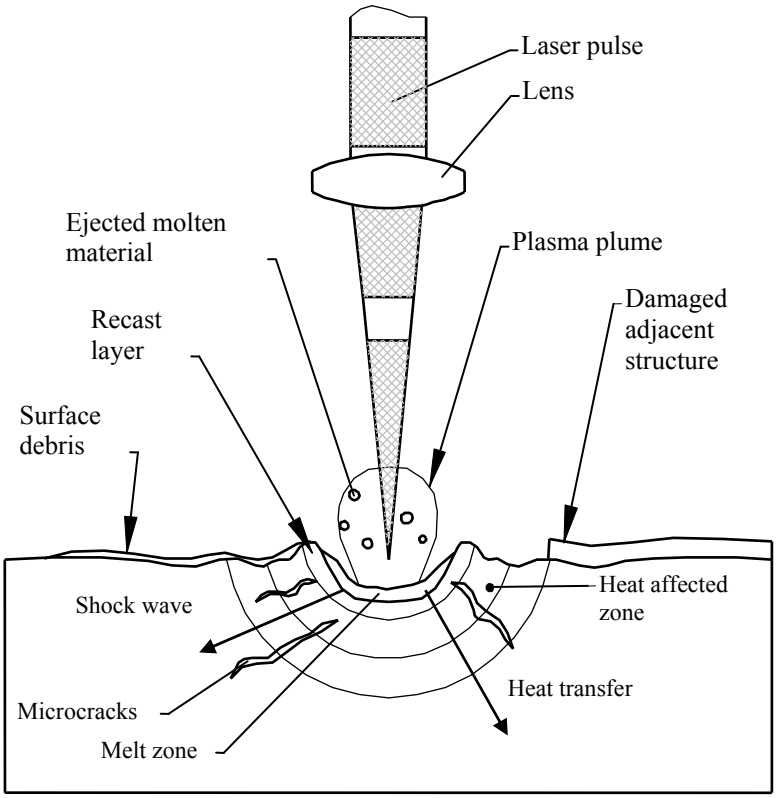

Figure 2.2 Nanosecond and longer pulse laser ablation

- The laser heats the material surface in the oxygen environment and as a consequence the surface oxidises. The oxygen layer grows, which results in increased laser light absorption.
- The surface temperature reaches the ignition temperature and burning begins. The temperature rises additionally due to the laser heating and the exothermal reaction. As a result, the oxide melts and undergoes a phase transition leading to a volume increase.
- After the end of the laser pulse, the liquid oxide cools and solidifies, causing thermal stresses that separate the oxide from the base material.
- The oxide bends in a direction perpendicular to the workpiece due to the remaining temperature gradient.

Several formal models have been proposed to explain the different laser ablation mechanisms in quantitative terms (Geiger et al, 1996; Pronko et al, 1995; Koc et al, 1998; Yilbas et al, Dobrev et al, 2008; Fahler et al, 1996).

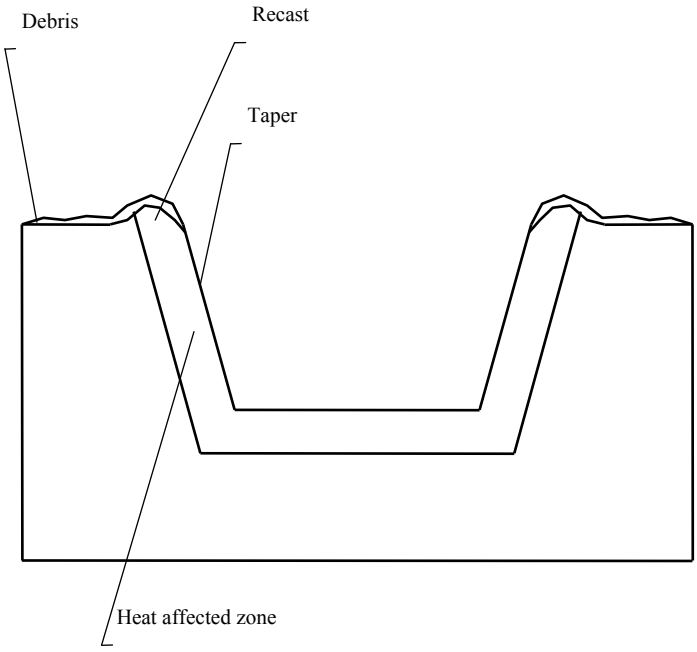

Figure 2.3 Secondary effects of laser machining

2.2 Laser source characteristics

There are three types of laser source: semiconductor-diode, solid-state and gas lasers. Table 2.1 (Fraunhofer, 2011) lists the operating mode, wavelength, power and typical applications of commonly used lasers. In manufacturing, the most widely employed lasers are the CO_2 laser, the Nd:YAG laser and the excimer laser.

The CO_2 laser is an example of a gas laser that employs a mixture of helium and nitrogen as the protective atmosphere, and carbon dioxide as the laser emitting material. The CO_2 laser produces a collimated coherent beam in the infrared region (10.6 μm), which is characteristic for the active material. The wavelength is strongly absorbed by glass or polymers, so either mirrors or ZnSe lenses with excellent infrared transparency are used to handle the beam (Madou et al, 2001).

The Nd:YAG laser is a solid-state laser producing a collimated coherent beam in the near-infrared region of wavelength 1064 nm that can be either pulsed or continuous. In pulsed mode, peak-power pulses of up to 20 kW are now available. The shorter wavelength allows the adoption of optical glasses to control the beam position. By means of optical conversion techniques, it is possible to double, triple (Hayl et al, 2001; Hellrung et al, 1999) and even quadruple the fundamental emission frequency, thereby obtaining higher harmonics of wavelengths equal to 532, 355 and 266 nm, respectively.

Some laser applications, such as micromachining (Rizvi et al, 2002; Pham et al, 2004; Pham et al, 2005) or direct ablation of hard materials, need high laser intensity or fluence, so usually

Table 2.1 Types of laser sources (Fraunhofer, 2011)

	Wavelength	**Power**	**Operating mode**	**Applications**
Semiconductor diode lasers				
Single diodes	Infrared to visible	1 mW - 100 mW	Continuous and pulsed modes	Optoelectronics
Diode laser bars	Infrared to visible	up to 100 W	Continuous and pulsed modes	Pumping light source for solid state lasers
Solid state lasers				
Nd:YAG laser	1.06 µm	1 W - 3 kW	Continuous and pulsed modes	Materials processing, dimensional metrology, medicine
Ruby laser	Red	Several MW	Pulsed mode	Dimensional metrology, pulse holography
Gas lasers				
CO_2-Laser	10.6 µm	1 W – 40 kW (100 MW in pulsed mode)	Continuous and pulsed modes	Materials processing, medicine, isotope separation
Excimer laser	193 nm, 248 nm, 308 nm (and others)	1 kW - 100 MW	Pulsed mode, 10 ns - 100 ns	Micro-machining, laser chemistry, medicine
HeNe laser	632.8 nm (most prominent)	1 mW - 1 W	Continuous mode	Dimensional metrology, holography
Argon ion laser	515 & 458 nm (several)	1 mW - 150 W	Continuous and pulsed modes	Printing technology, pumping laser for dye laser stimulation, medicine
Dye laser	Continuous between infrared and ultraviolet (different dyes)	1 mw - 1 W	Continuous and pulsed modes	Dimensional metrology, spectroscopy, medicine

only excimer lasers, which can produce it, are employed. EXCIMER (EXCIted diMER) lasers, invented in 1975, are a family of pulsed lasers with a fast electrical discharge in a high-pressure mixture of a rare gas (krypton, argon or xenon) and a halogen gas (fluorine or hydrogen chloride) as the source of light emission. The particular combination of rare gas and halogen determines the output wavelength.

The laser source is characterised by its wavelength, spot size (i.e. the minimum diameter of the focused laser beam), average beam intensity and pulse duration.

There are three types of interaction between laser and material: the light can be reflected, transmitted or absorbed. In reality, all three occur to some degree. In order for laser milling to be possible, the material must absorb the laser light. Reflected and transmitted light represents energy that is lost to the manufacturing process. Only absorbed light is used to perform material removal.

2.2.1 Laser wavelength

The most important parameter affecting good material processing is the wavelength of the light used. Different materials absorb light at different parts of the electromagnetic spectrum. It is necessary to choose the correct laser wavelength so absorption of the photons can occur. On a molecular level, infrared photons, like those emitted from a CO_2 or Nd:YAG laser, interact with materials by influencing the way the molecules vibrate internally. Infrared photon energies are matched very closely to quantized vibrational energy levels. Ultraviolet (UV) photons, on the other hand, have a much shorter wavelength and therefore higher

photon energy. Consequently, UV photons can break electronic bonds directly and therefore the material removal mechanism is primarily not a thermal one. It is also important to note that when a material has a very high absorption characteristic, the penetration depth and, therefore, the interaction volume is generally small, slowing the material removal process. The result is that, unless secondary thermal effects are observed, much cleaner and more precise processing can be done with shorter wavelength light, but at the expense of speed.

2.2.2 Laser spot size

In laser milling, when the objective is to manufacture the smallest possible feature, it is important to be able to focus the laser beam down to the smallest spot size. This depends on several factors but, typically, the smallest spot diameter that can be obtained is about half the wavelength of the light used. The calculation formula (Madou, 2001) for the spot size $2w_o$ is given below:

$$2w_o = \frac{4M^2\lambda f}{\pi D}$$

Where: λ is the wavelength of the laser source,

f is the focal length of the lens,

D is the input beam diameter,

M^2 is the beam quality factor

Lasers with ultrashort pulses can create features substantially below the laser spot size (Hellrung et al, 1999). Pronko et *al, 1995* have produced holes with a laser spot size of the order of 3 μm, whereas the diameter of the pit generated was 300 nm. Given that laser beam intensity distribution is Gaussian, with a maximum intensity in the centre of the beam, one can adjust the beam so that only the intensity in its central region is above the threshold for the given material (see Figure 2.4). In this way, material will be removed only in a fraction of

the beam spot area, resulting in an affected area as small as one-tenth of the size of the spot itself.

As can be seen inTable 2.1, both ultrafast pulse lasers and long pulse lasers can produce wavelengths of around 0.5 μm and therefore spot sizes of the order of 0.2 μm. However, unlike the case of ultrafast lasers, with long-pulsed lasers the smallest pit diameter that can be achieved is much larger than the spot size (in the order of 10 μm). This is due to the thermal nature of the laser-material interaction and heat diffusion into the surrounding material.

2.2.3 Laser pulse length

Another influential characteristic in laser-material interaction is the laser pulse length. There are two major considerations: laser pulse energy and heat diffusion time. Generally, for a given amount of energy, the shorter the pulse is, the higher the peak power delivered to the target will be.

In general, to perform processing at atomic cluster level with pulsed lasers, τ_L should be shorter than the time necessary to achieve thermodynamic equilibrium between the electron system and the atomic lattice. For example, for metals with strong electron-phonon coupling such as steel τ_L should be in the range from 3 to 5 ps, while for aluminium and copper, materials with weak coupling, it needs to be one or two orders of magnitude higher (Breitlung et al, 2004). A further reduction of τ_L would not bring additional benefits in terms of material machining response. Nonlinear effects, due to interactions between the ultra-short laser pulse and atmospheric gas in the focal region, occur that lead to a wave-front disruption of the

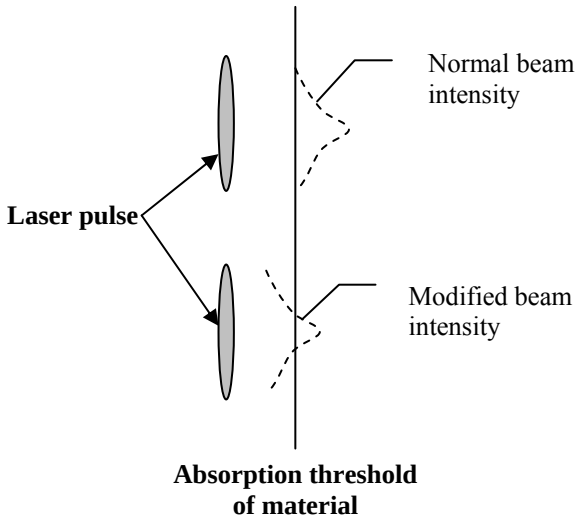

Figure 2.4 Creating sub-spot size features by adjusting the laser beam intensity

beam, profile distortion and increased beam divergence. In particular, these are the side effects when performing laser ablation in the femtosecond regime (Breitlung et al, 2004; Harzic et al,2005).

Once applied, the heat energy does not stay localised at the point where it was initially deposited. The heat diffusion time is the time required for a given amount of energy to dissipate into the surrounding material and is specific for that material. Depending on the heat diffusion time of the material, the laser pulse duration is somewhat arbitrarily divided into two time regimes: long and ultrafast. Long pulse lasers are lasers with pulse duration longer than 10 picoseconds. These are the most widely used commercial lasers in industry today. Ultrafast, or ultrashort, lasers have pulses shorter than 10 picoseconds – usually in the femtosecond range.

In the long-pulse regime, the heat deposited in the substrate diffuses away within the pulse duration. This has a detrimental effect on the quality of the machining, because heat diffusion reduces the efficiency of the laser machining process, through draining energy away from the work spot – energy that would otherwise go into removing material. As a result, the temperature at the focal spot reaches a working level not much above the melting point of the material. Since evaporation of the material does not occur, only molten material is produced. The molten material is then ejected in the form of drops away from the work zone. These drops fall back onto the surface and create debris, which spoil the quality of the machined surface.

Another negative effect of long-pulse machining is the formation of a heat-affected zone (HAZ). The heat energy that dissipates into the surrounding material can produce a

neighbouring zone of mechanical stresses and microcracks. A closely associated phenomenon is the formation of a recast layer around the work spot. This is resolidified material that often has physical characteristics different from those of the unmelted material. This recast layer usually has to be removed in post-process cleaning (Good et al, 1998; Hatano et al, 1996; Hocheng et al, 2003; Kao et al, 2003; Kim et al, 1999; Li et al, 2003; Hsu et al, 2005; Shao et al, 2005; Tam et al, 1992).

In the ultrafast regime however, the laser pulses are so short that the heat energy deposited by the laser into the material does not have time to dissipate into the surrounding material. Therefore, all the energy is used efficiently for heating the material well beyond the evaporation point into the plasma formation state. The plasma expands outward from the surface in a plume of highly ionised atoms. Consequently, there are no droplets that solidify onto the surrounding material. Additionally, since there is no time for the heat to dissipate into the neighbouring material, there is no HAZ.

2.2.4 Laser beam intensity

Table 2.1 gives typical values for the output power of the different laser sources. However, in laser milling, a more important characteristic is laser beam intensity.

The laser intensity (Wcm^{-2}) is defined as the peak power (W) divided by the focal spot area (cm^2), and the peak power (W) is computed as the pulse energy (J) divided by pulse duration(s). The peak power must be large enough to vaporise the material in the laser beam spot. For each material, there exists a threshold value of laser beam intensity below which no melting or evaporation will occur. For example, for a copper substrate if the laser beam intensity is below 4.3×10^9 Wcm^{-2}, the target surface will remain below the melting point and

no material removal will occur (Jandeleit et al, 1998). In order to heat the surface region of the material sufficiently so that melting and/or evaporation can occur, a higher power density is required.

2.3 Machining techniques

A number of techniques for laser milling have been developed. These techniques differ from one another in the applied laser source, the relative beam-workpiece movements and the laser spot characteristics. A common feature of all laser milling techniques is that the final part geometry is created in a layer-by-layer fashion by generating overlapping craters. Within a single layer, these simple volumes are arranged in such a manner that each slice has a uniform thickness. Through relative movements of the laser beam and the workpiece the micro craters produced by individual laser pulses sequentially cover complete layers of the part. Two main machine designs exist:

2.3.1 Fixed laser beam and CNC controlled moving table

This was the layout adopted in the first laser milling machines (Schubart et al, 1997) where conventional CNC milling platforms were integrated with lasers. This design provides accurate positioning and precise toolpaths, but is limited to low scanning speeds due to the machine dynamics. The main advantage of this method is that the laser spot is positioned very accurately in the working area and the energy delivered on the layer surfaces is independent of the beam position. Thus, more uniform layer thicknesses can be achieved. This machine design is the only one possible for some high-power laser systems where the use of scanning optics is not feasible due to the material damage induced by the laser (Toenshoff et al, 1998)

and also for certain very complex laser installations. Typical examples of such a design are some UV excimer laser machining systems and some ultrashort pulse set-ups. This design is also widely used in laser drilling machines.

2.3.2 Scanning laser and CNC controlled focusing

This design was adopted in the later stages of development of the laser milling process. It is a flexible and universal machine design allowing high scanning speeds and increased productivity. The laser spot is moved in the slice plane by a pair of CNC controlled mirrors, thus scanning the area with high precision and speed. The workpiece, specifically the slice plane, is positioned in the laser focus plane by one of the machine axes (Lasertech, 1999). A disadvantage of this method is that the energy delivered to the workpiece depends on the angular deviation of the laser beam from the optical axis. This limits the effective machining area and requires repositioning of the workpiece for larger parts, which introduces additional errors.

The shape of the laser spot in the laser ablation process is most often circular with a Gaussian intensity distribution. More complex spot contours are achieved by the projection of different masks on the slice plane (Toenshoff et al, 1993). In the most complex designs the mask consists of CNC controlled blades (Toenshoff et al, 1997; Toenshoff et al, 1999). Additionally, a beam homogeniser can be used to equalise the intensity over the entire spot area. These techniques are employed when process optimisations such as draft angle reduction are applied. They are also used in micro- and nano-manufacturing where projection ablation is the only possible method for feature machining (Ihlemann et al, 2000). This method is very

similar to lithography technology and is applicable to the micromachining of materials that could not be etched in a conventional manner.

2.3.3 Laser sources utilized

Different laser sources are used in laser machining systems. Previously, CO_2 lasers were the most frequently employed (Eberl et al, 1991; Beyer et al, 1994; Haferkamp et al, 1994), but recently Nd:YAG lasers, excimer lasers and ultrashort pulsed lasers are preferred (Tönshoff et al, 1998; Fiebig et al, 1999; Liu et al, 2000). The best machining results are achieved when a pulsed laser beam is strongly absorbed near the surface of the substrate material. Although a continuous wave mode can be adopted, it is not suitable for laser ablation purposes. The general trend is for shorter pulses to be produced in order to achieve a better process quality. The pulse duration affects the laser power delivered on the substrate surface and the physical mechanism of the ablation process. The laser light wavelength combined with the pulse duration are important factors that determine the nature of the material-beam interaction and the final machining results (Petkov, Dimov et al, 2008, Petkov, Sholtz et al, 2008).

Several models have been proposed to reduce the time required for trial-and-error adjustments of the process parameters and to improve the overall process quality (Chen et al, 2000; Meiners et al, 1992; Dobrev et al, 2008).

2.4 System description

2.4.1 Machine description

This section presents a laser milling system that was first introduced in 1999 and is still one of the few commercially available machines of its type in the world. The system, shown in Figure 2.5, is of the scanning design and includes the following main components (Lasertech, 1999):

- Laser and laser scanning head
- Worktable
- Control panel
- Laser protection cabin.

Table 2.2 gives the technical specifications of the machine (Lasertech, 1999; Foba-las ,1999)] and Figure 2.6 shows the laser scanning head (Foba-las, 1999).

A Q-switch device controls the pulsed mode operation of the laser. It determines the pulse duration and frequency. The beam expander collimates the laser beam and provides a low energy distribution inside the machine. Two NC controlled galvanometer mirrors deflect the laser beam and provide slice scanning in the focal plane of the lens. This plane coincides with the uppermost surface of the substrate to be machined.

The system removes material in layers with a predefined thickness (Figure 2.7).

2.4.2 Process description

As mentioned previously, each single layer is machined by overlapping a sequence of micro-cavities. The 2D data obtained by slicing the volume to be removed is used to programme the movements of the laser beam. The contour of each layer is outlined with border cuts (four in the case of the example shown in Figure 2.7). Then, the material inside the inner most border cut is removed by hatching the area as depicted in Figure 2.7. Two hatching parameters, the track displacement and the distance between the end of the hatch line and the last border cut, are adjustable to tune the process. By increasing the scanning speed and making the track displacement larger than the laser spot diameter, the single pulse craters along the path of the laser beam can be separated from one another. In this way, clear photographs (Figures 2.8(a) and 2.8(b)) obtained by the author using the machine shown in Figure 2.5) can be obtained to

Figure 2.5 A commercially available laser milling system
1. Laser and laser scanning head
2. Worktable
3. Control panel
4. Laser protection cabin.

Table 2.2 Technical Specification

Machining area		
X axis	mm	400
Y axis	mm	300
Z axis	mm	550
Table size	mm	300x400
Laser working area	mm	Ø70
Max. machining depth	mm	10
Surface roughness	μm	1.0
Removal rate (steel)	mm^3/min	4-6
Beam spot diameter	mm	0.1
Laser characteristics		
type		Q-Switch Nd:YAG
output modes		Continuous wave operation (CW) Pulsed operation (QS) - 0.1-50 kHz
CW output power	W	100
QS output power	W	200 000/pulse at 1 kHz 40 000/pulse at 10 kHz
wavelength	nm	1064
energy density	J/m^2	up to $2x10^4$
average power density	W/m^2	up to 10^6
peak power density of a single pulse at 10 kHz	W/m^2	up to $5x10^{11}$
scanning speed	mm/s	Up to 5000

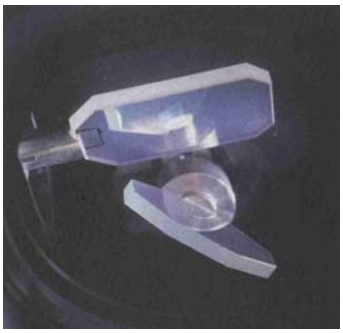

(a)

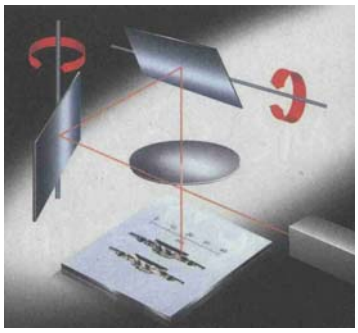

(b)

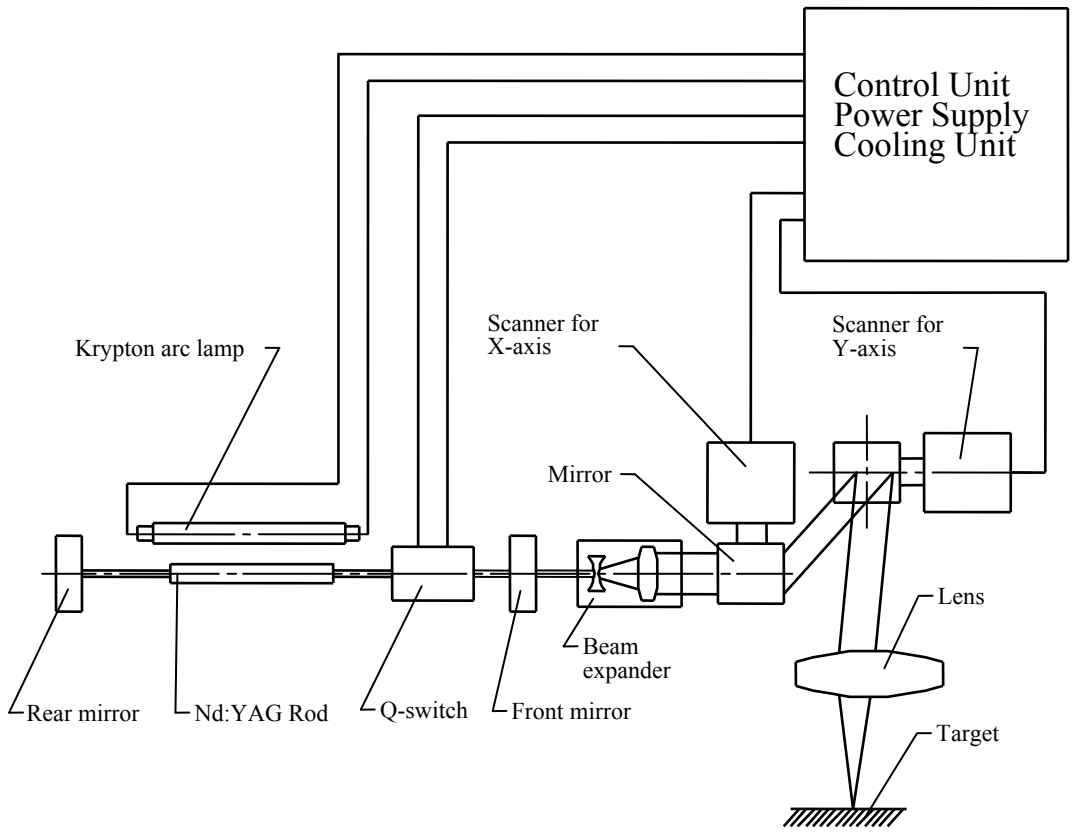

(c)

Figure 2.6 Scanning head (adapted from Lasertech)
(a- galvanometer mirrors; b- mirror axes; c - system diagram)

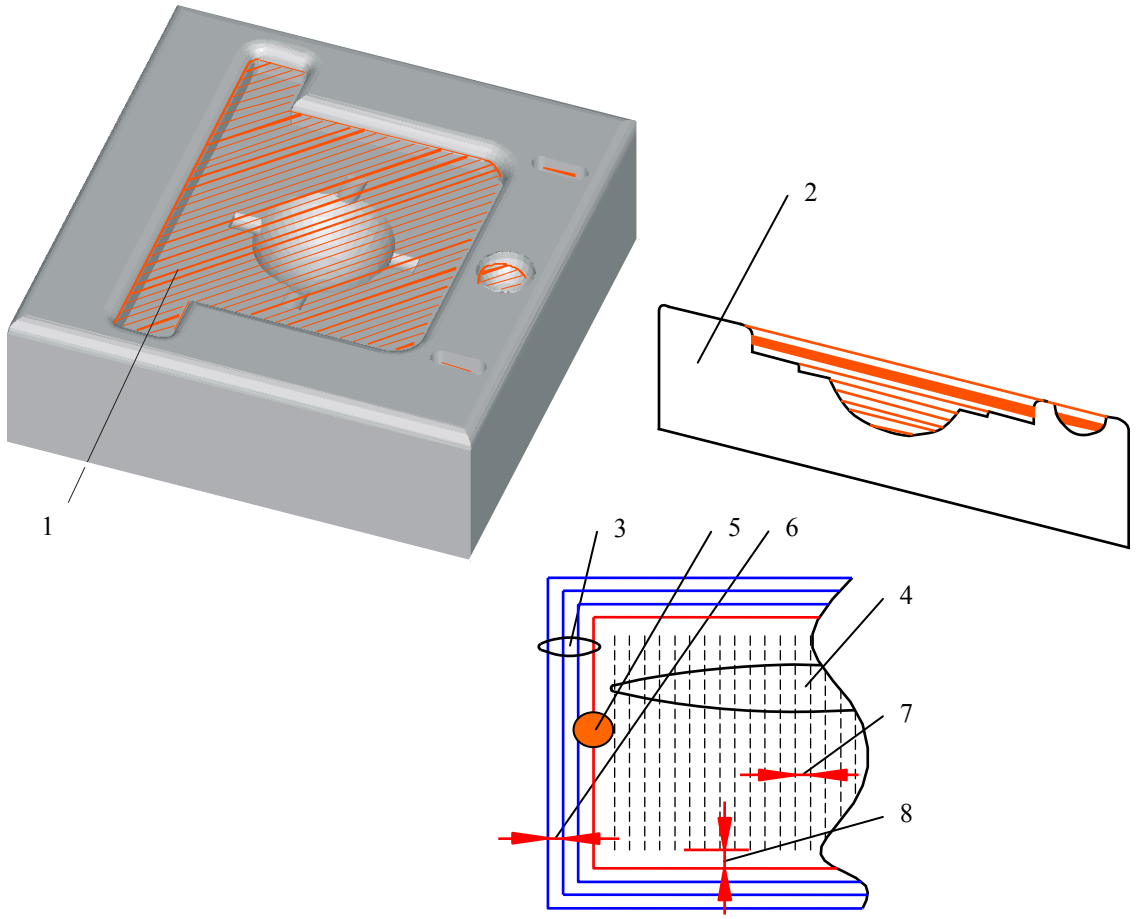

Figure 2.7 Material removal in the laser milling process

1. cavity with a hatched slice
2. cross-section of the cavity with slices
3. border cuts
4. hatching cuts
5. laser spot
6. border cut track displacement (step-over)
7. hatch track displacement (step-over)
8. distance between the end of the hatch line and the innermost border cut

illustrate the laser milling strategy adopted. It should be noted that such process parameter settings are not appropriate for real machining.

The surface finish of the machined area can be controlled by varying the scanning speed and track displacement. Figure 2.9, also obtained using the machine shown in Figure 2.5, illustrates the effect of these process parameters on surface finish. Empirically, it has been found that a substantial reduction of the surface roughness in multi-layer machining cycles can be achieved by changing the scanning direction from layer to layer. This is why the control software of the machine changes the scanning direction on each layer by 90°. Furthermore, the software allows the scanning angle at the start of each machining cycle to be defined by the operator. The surface finish is also influenced by the degree of overlapping of the craters. This influence has been studied in micromachining applications (Hellrung et al, 1999; Tönshoff et al, 2000).

Another important aspect not discussed above is the depth of the removed material per pulse (Figure2.10). It is a result of the material-laser beam interaction and is dominant in determining the layer thickness. Note, however, that the real layer thickness is a mean value and differs from the depth of a single crater.

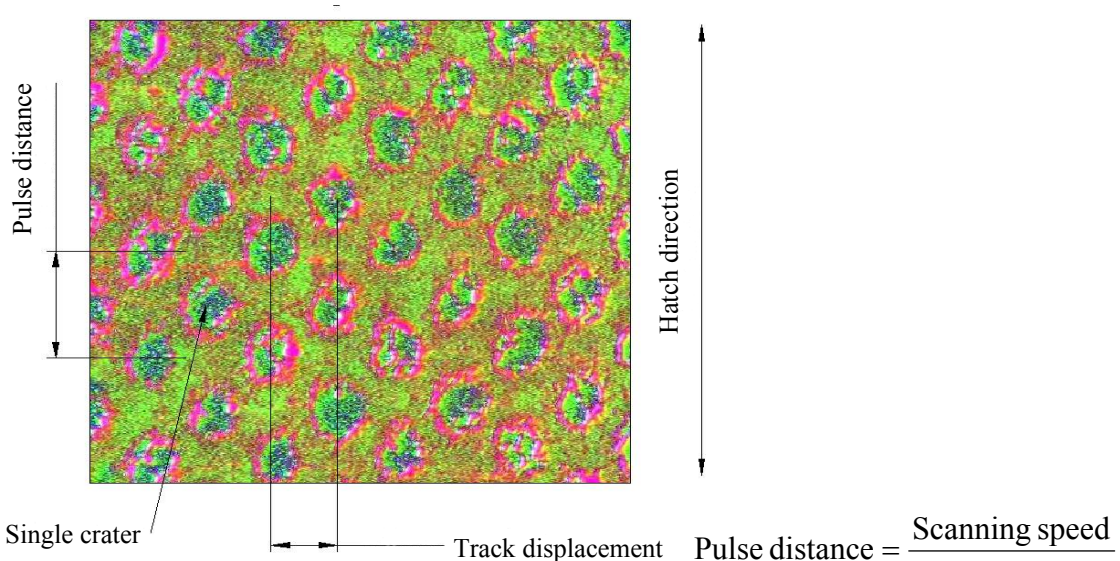

(a) Inner area hatching tracks

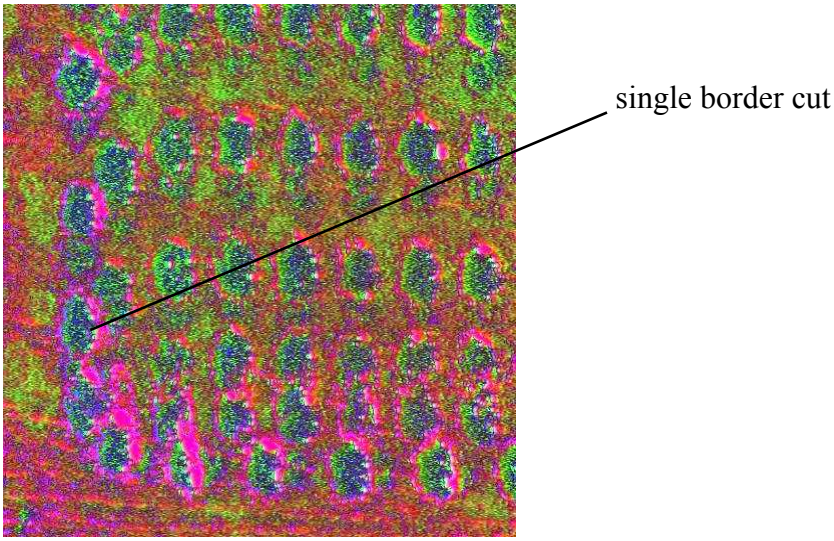

(b) border area track

Figure 2.8 Laser path descriptions

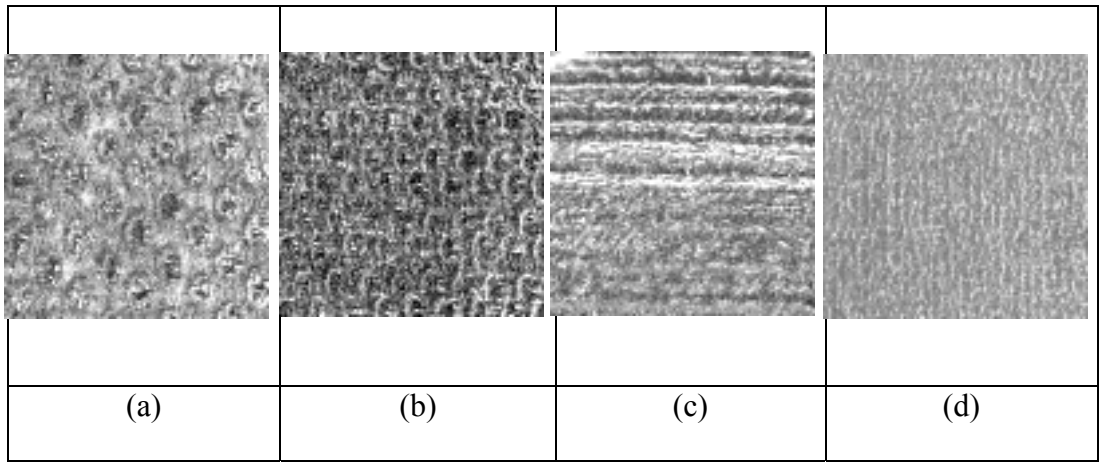

Figure 2.9 Effect of the scanning speed and track displacement on the surface finish

a) pulse distance 142μm and track displacement 100μm

b) pulse distance 142μm and track displacement 50μm

c) pulse distance 142μm and track displacement 15μm

d) pulse distance 17μm and track displacement 15μm

2.5 Advantages and disadvantages of the laser milling process

An analysis of the advantages and disadvantages of laser milling could assist users in identifying suitable application areas for it. This section gives an overview of the strengths of the process and also highlights some of the problems associated with it.

2.5.1 Advantages of the laser milling process

- *Optical-thermal process that can be easily integrated in CNC machines.* Laser milling is a flexible process which, when combined with a multi-axis positioning system, can support a wide range of applications with high precision. Laser milling does not require complex tool-workpiece kinematics and thus closed-loop control systems can easily be incorporated (Eberl et al, 1991; Beyer et al, 1994; Tönshoff et al, 1998).

- *Noncontact process*. There is no mechanical interaction between the laser beam and the workpiece. Therefore, there is no tool wear during the process. This gives high dimensional accuracy and repeatability and also eliminates the need for tool changes. Tool costs related to the life of the laser are low.

- *Direct method of machining*. Laser milling is a process in which part geometry is formed by direct removal of material from the workpiece. Intermediate stages and associated errors are therefore avoided. A typical example is the elimination of repositioning errors. The influence of the operator on the process is also limited, which ensures consistent machining results. Moreover, the NC program required by the process is generated from data

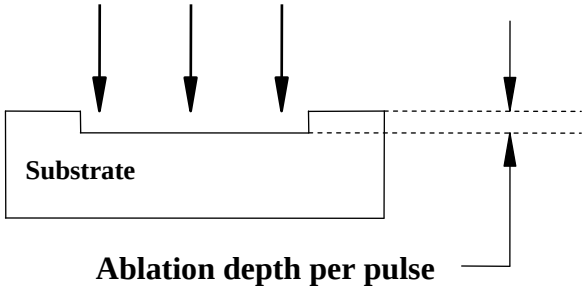

Figure 2.10 Depth per pulse

directly imported from 3D CAD models, which is a prerequisite for high accuracy and overall process automation.

- *Processing of a wide range of materials*. As an optical-thermal process that does not involve any mechanical tool-workpiece interactions, laser milling is applicable to any materials that absorb light in a spectrum covering the wavelength of the laser source adopted. Advanced engineering materials that are opaque to visible and infrared light, such as ceramics, hardened steel, titanium and nickel alloys, can all be machined using laser sources such as CO_2 and Nd:YAG (Tönshoff et al, 1998; Burck et al, 1995; Oliveira et al, 1998; Mendes et al, 2000; Pham et al, 2001). For optical materials, which are transparent in the visible spectrum and infrared band, excimer lasers with UV emission can be utilised (Yilbas et al, 1997; Toenshoff et al, 1997; Nantel et al, 2001; Lalev et al, 2008). Another strategy for machining materials with low radiation absorptivity is to reduce the laser pulse length to the femtosecond range and in this way to influence the mechanism of laser-induced material damage (Krüger et al, 1998; Pham et al, 2002).

- *Machining of intricate features*. The laser beam diameter can be as small as a dozen microns. This allows very small internal radii and fine details to be reproduced. Laser machining promises to extend the limits of current milling technology.

- *Micromachining ability.* The need for miniaturisation of features and even entire systems has opened up new application areas for laser milling. Features with dimensions ranging from several microns to nanometers can be produced through laser ablation (Beck, 2000; Pham et

al, 2004). This process is increasingly used for materials that cannot be machined with existing lithography technologies. Typical examples are microdrilling for micro-electronics, micro-lens machining for micro-optics, ablation of precision inductors and micro-actuators and production of micro-surgical devices (Toenshoff et al, 1998; Toenshoff et al, 1997). Laser micro-machining is an important element of developments in the area of nanotechnology.

- *Negligible cutting forces and simple fixturing of the workpiece.* With laser machining negligible cutting forces are applied to the workpiece, which means that there is no elastic deformation during the process. This leads to a further reduction of machining errors, simplifies fixture design and significantly decreases the cost of auxiliary equipment.

2.5.2 Disadvantages of the laser milling process

- *Low energy efficiency*. The energy losses associated with the process are due to the low efficiency of the lasers currently used (losses of up to 80%). Despite this, the operational costs for laser milling are still low for the reasons stated previously.

- *Slow processing*. The small layer thickness (2-5 μm) and spot dimensions make the entire machining cycle slow, although the scanning speed is significant. This problem worsens as the volume of material to be removed increases. Another factor that prolongs the machining cycle is the use of closed-loop control to enhance the accuracy of the process.

- *Large number of process parameters*. Laser milling is a complex process performed on CNC machining centres. A number of process parameters are controlled, the interdependency

and influence of which have yet to be fully studied. Process models have to be developed to ensure efficient use of the technologies.

- *Heat affected zones.* As already described, the main mechanism for laser material removal involves energy absorption, which leads to heat transfer and phase transitions. With some pulse regimes, heat transfer to the bulk of the material by thermal conductivity results in heat affected zones where changes in the material structure can be observed. These heat affected zones have a negative effect on material properties and introduce residual stresses. Cracks can occur due to these stresses. Additionally, shock waves during ablation can amplify the formation of microcracks.

- *Recast*. As mentioned earlier, a recast layer is formed as a result of the resolidification of molten material. The removal of this recast layer requires additional finishing efforts. For some applications, such as the micromachining of lenses, the formation of a recast layer is not acceptable. Layers of resolidified oxides accumulated during laser machining can also be observed on cavity walls and borders.

- *Draft angle*. After laser milling, nominally vertical walls have a draft angle. This is a serious limitation for applications that require the machining of vertical walls. It results from several factors occurring simultaneously. In particular, draft angles on vertical walls are due to reduced intensity in areas away from the optical axis, diffraction caused by the walls and thermal conductivity from the walls and the bottom of the workpiece.

- *Surface roughness.* As the removal mechanism is based on craters overlapping, there is always a distinctive pattern on the resulting surface. Though further laser polishing is possible, improvement is no better that 30 percent from the starting point. For some micro applications like tooling inserts higher roughness can affect the demoulding process.

2.6 Examples

2.6.1 Machining of small ceramic components

Laser milling is one of the few processes capable of machining ceramic parts. Other processes based on sintering technology require expensive tools and are not feasible for small quantities. Thus, laser milling offers an alternative for the rapid manufacturing ceramic parts directly from a CAD model.

The component chosen as an example here is part of a microsurgical tool. It acts as an insulator located between a tissue cutting electrode and a metal housing. As there is no relative movement between the insulator, electrode and housing, and the surface roughness of the insulator is not critical, the most important functional parameters of the ceramic component are its dimensional accuracy and insulation properties.

The geometry of the ceramic component is shown in Figure 2.11. Note that the part has cavities on both sides, as well as a hole and a slot. The material of the component is alumina 23. The overall dimensions of the component are 6 mm × 2.9 mm × 1.18 mm.

A batch of 24 components was manufactured. The machined component can be seen in Figure 2.12. The key dimensions of the components were measured. Most of the actual tolerances for the measured dimensions were between ISO Grade IT12 and IT14, which is within the prescribed tolerances for the component. For a small number of non-critical dimensions, the measured values were outside the specified limit, but this did not affect part functionality.

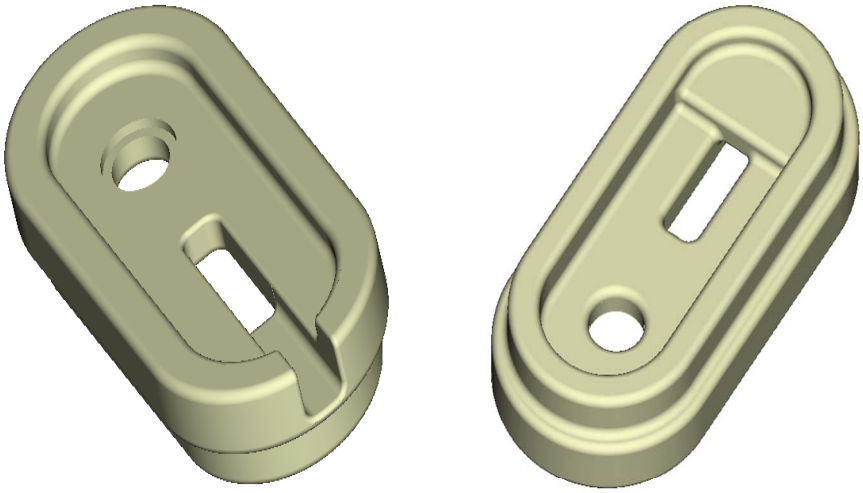

Figure 2.11 CAD model of the component

Figure 2.12 Machined component

2.6.2 Pro FIB mask

A mask for pro fib was manufactured (Figure 2.13) utilising both microsecond and nanosecond laser sources. The substrate was stainless steel 316 with a thickness of 250 micrometers. Feature sizes varyied from 50 micrometers up to 400 micrometers.

In this case it was very important to retain sharp edges; otherwise it would create problems during exposure to the beam of Ions. A few problems were encountered during the manufacture of this component:

- Producing a feature with a dimension close to the laser spot is always difficult, if not impossible. As the effective laser spot for the 1064nm Nd:Yag laser is around 45 micrometers, producing a wall of 50 micrometers near a groove of 100 micrometers proved to be challenging.
- Draft angles associated with laser milling have always been a problem, although there are some techniques to create 0^o wall angles. The main problem becomes width/depth ratio as the laser beam needs to be tilted in order to produce a vertical wall. Usually good results are achieved up to a ratio of 2. In this case with a groove 100 micrometers wide and 250 micrometers deep the ratio was 2.5 – so it required a lot of optimisation in order to achieve a stable process capable of manufacturing the component.

Results from both laser types can be compared – Figure 2.14(a) shows results from the microsecond laser where Figure 2.14(b) shows results from the nanosecond laser. It is noticeable that the nanosecond laser produced much sharper edges and smoother walls.

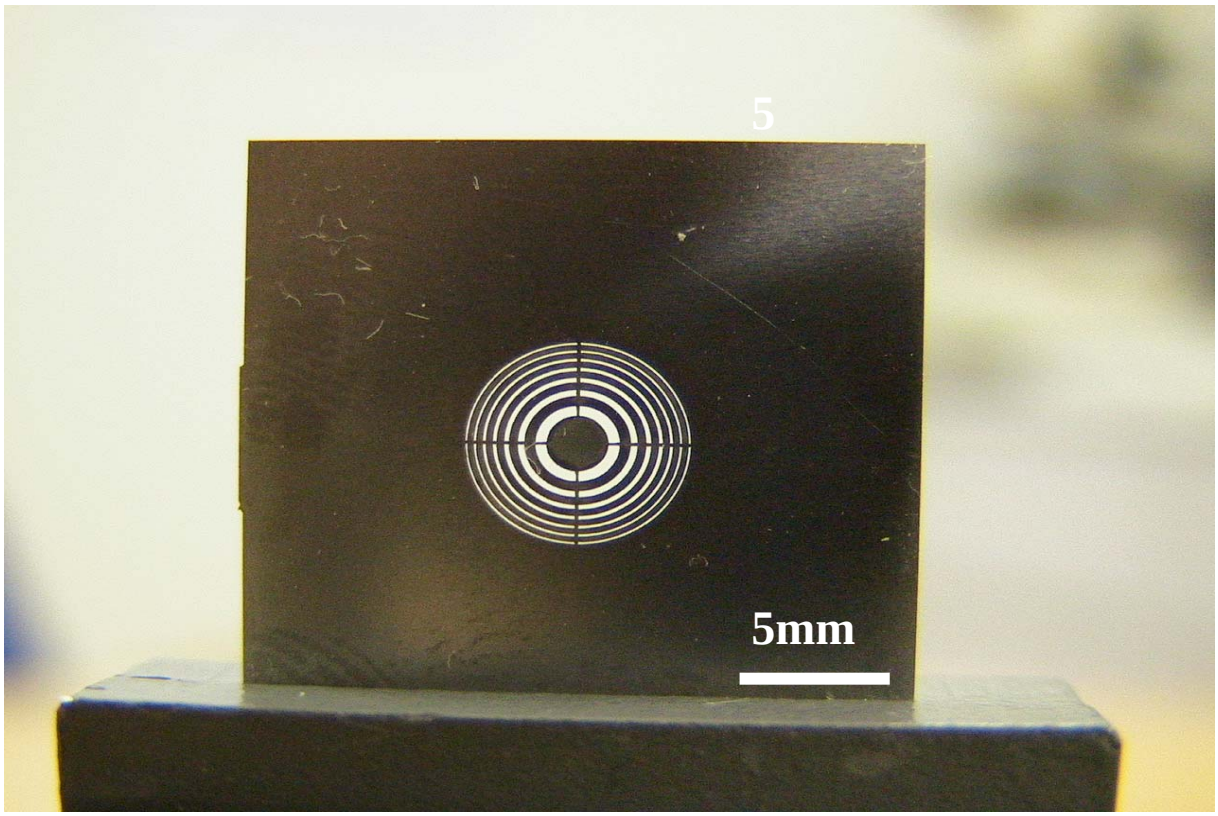

Figure 2.13 Pro FIB mask

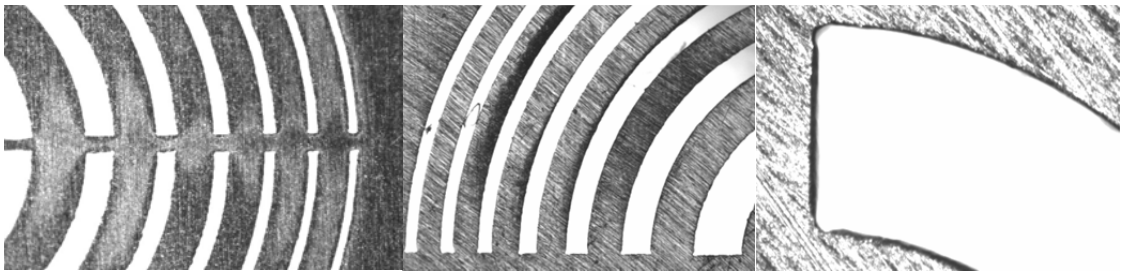

(a)Manufactured by μs laser

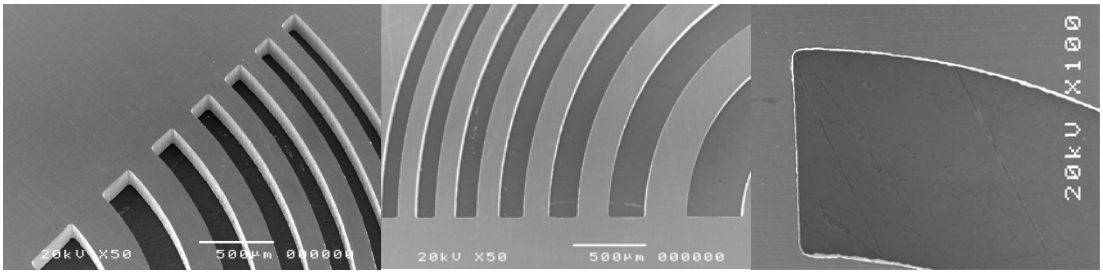

(b)Manufactured by ns laser

Figure 2.14 Pro FIB mask close up
(a) Manufactured by μs laser
(b) Manufactured by ns laser

2.7 Summary

Laser milling is capable of processing a large range of materials, which are not machinable with conventional manufacturing processes. It was demonstrated here that engineering ceramics can be machined without requiring expensive special tools and without any limitations on the 3D complexity of the component.

Nevertheless, laser milling is still in its infancy. Laser material interactions are not yet fully understood. Much effort in the research and development of the available laser sources is still needed. Ultrafast lasers are beginning to be applied. They can offer more precise machining without the thermal damage that accompanies long-pulse laser manufacturing.

Chapter 3 Pulse duration effects on surface integrity

Laser source characteristics such as pulse duration and wavelength are very important for the ablation process. Very important is also the material response to the wavelength of the laser light. Surface integrity of the processed area in terms of a heat affected zone and roughness is a crucial factor for some applications. Heat penetration needs to be studied in order to estimate the influence it will have on functionality of the component/feature as well as lifecycle. Micro cracks, redeposition and other secondary effects need to be controlled, but first there should be a reliable method for establishing the extent of the changes triggered by the heat transferred into the bulk of the material. In this chapter a novel methodology for a heat affected zone analysis is presented. The influence of the laser source and the substrate material on the heat penetration are discussed.

3.1 Laser Sources

There are three types of laser source: semiconductor-diode, solid-state and gas lasers. Table 3.1 lists the operating mode, wavelength, power and typical applications of commonly used lasers.

In manufacturing, the most widely employed lasers are the CO_2 laser, the Nd:YAG laser and the Excimer(EXCIted diMER) lasers.

The CO_2 laser is an example of a gas laser that employs a mixture of helium and nitrogen as the protective atmosphere, and carbon dioxide as the laser emitting material. The CO_2 laser produces a collimated coherent beam in the infrared region (10.6 μm), which is characteristic for the active material. The wavelength is strongly absorbed by glass or polymers, so either mirrors or ZnSe lenses with excellent infrared transparency are used to handle the beam (Haferkamp et al, 1994).

The Nd:YAG laser is a solid-state laser producing a collimated coherent beam in the near-infrared region of wavelength 1064 nm that can be either pulsed or continuous. In pulsed mode, peak-power pulses of up to 20 kW are now available. The shorter wavelength allows the adoption of optical glasses to control the beam position

There are three types of interactions between laser and material, as shown in Figure 3.1, the light can be reflected, transmitted or absorbed. In reality, all three occur to some degree. In order for laser milling to be possible, the material must absorb the laser light. Reflected and transmitted light represents energy that is lost to the manufacturing process. Only absorbed light is used to perform material removal.

Laser source characteristics such as wavelength and pulse duration are very important for the ablation process as well as the material response to the wavelength of the laser light. Material absorption varies in the different regions of the laser light – Infrared, Visible, UV and deep UV.

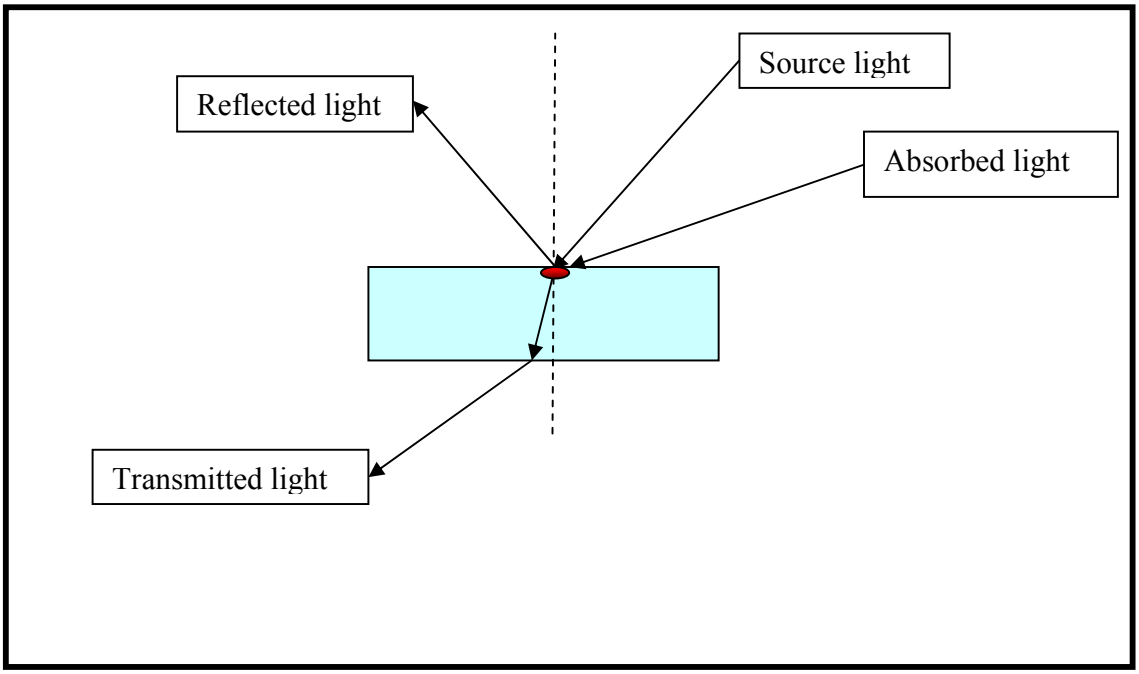

Figure 3.1 Laser light – material interactions

Chapter 3 Pulse duration effects on surface integrity

Depending on the pulse duration, there are three main groups of laser source:

- Ultrashort – femtosecond pulse duration,
- Short – picoseconds pulse duration,
- Long – nano and microsecond pulse duration.

In the case of ultra short pulse duration there is beam absorption by the material, energy is transferred to the lattice which breaks element bonds and leads to fast plasma expansion. No recast layer is formed because there is no melt phase. This material removal method is known as cold ablation. Although the cold ablation method looks very attractive, it is only achievable on very complex and expensive systems that generally have a low repetition rate (typically just a few kilohertz). The low removal rate and high cost makes those systems unsuitable for industrial work.

In the case of short pulse duration, the system is controllable so that a single pulse can remove only 10nm of material from the surface of a part. The short pulse means the energy is localized to a very small depth. The fact that there is no time for thermal conduction into the workpiece material makes the laser effective for machining metals such as steel, stainless steel, aluminium, molybdenum, brass and copper. This also enables the laser to machine non-metals such as Teflon, diamond, ceramics and glass without micro cracking or chipping to their surface. The minimal thermal and mechanical effects associated with short ablation allows for a high repetition rate, which translates to high ablation (material removal) rates.

The repetition rate could go as high as 640 kHz, which means ablation rates for steel can be as much as 1 mm^3/min for an 8 kW laser.

In the case of long pulse duration, there is enough time for the heat to propagate into the bulk of the material and cause thermal damage, as well as micro cracks and redeposition on the surface. The material undergoes solid-molten-vapour transformation. The melt/vapour proportion determines to what extent heat will propagate through the substrate.

Table 3.1 shows the most commonly used laser sources with their most important characteristics and possible applications (Fraunhofer, 2011).

3.2 Substrate Material

The response of the substrate to laser radiation is influenced by a number of material characteristics. Laser ablation occurs only at wavelengths for which the particular material is strongly absorptive. Hence, for optimal machining results a proper match of laser source and material must be achieved. Generally, higher absorption efficiency leads to a more effective laser milling process. A number of ways exist to increase laser absorptivity, in particular, by creating an appropriate surface finish prior to laser milling or by applying a suitable surface coating.

Table 3.1 Types of laser sources (Fraunhofer, 2011)

	Wavelength	**Power**	**Operating mode**	**Applications**
Semiconductor diode lasers				
Single diodes	Infrared to visible	1 mW - 100 mW	Continuous and pulsed modes	Optoelectronics
Diode laser bars	Infrared to visible	up to 100 W	Continuous and pulsed modes	Pumping light source for solid state lasers
Solid state lasers				
Nd:YAG laser	1.06 µm	1 W - 3 kW	Continuous and pulsed modes	Materials processing, dimensional metrology, medicine
Ruby laser	Red	Several MW	Pulsed mode	Dimensional metrology, pulse holography
Gas lasers				
CO2-Laser	10.6 µm	1 W – 40 kW (100 MW in pulsed mode)	Continuous and pulsed modes	Materials processing, medicine, isotope separation
Excimer laser	193 nm, 248 nm, 308 nm (and others)	1 kW - 100 MW	Pulsed mode, 10 ns - 100 ns	Micro-machining, laser chemistry, medicine
HeNe laser	632.8 nm (most prominent)	1 mW - 1 W	Continuous mode	Dimensional metrology, holography
Argon ion laser	515 & 458 nm (several)	1 mW - 150 W	Continuous and pulsed modes	Printing technology, pumping laser for dye laser stimulation, medicine
Dye laser	Continuous between infrared and ultraviolet (different dyes)	1 mw - 1 W	Continuous and pulsed modes	Dimensional metrology, spectroscopy, medicine

Chapter 3 Pulse duration effects on surface integrity

During laser ablation, the material passes through several phase transitions, depending on the process parameters. Thus, relevant material characteristics are transition energies such as evaporation energy and melting energy. This can be illustrated by the fact that, compared with ceramics, metals are easy to melt but are relatively more difficult to evaporate, which influences the laser ablation mechanism.

During interaction between the laser radiation and the material, electrons in the substrate are excited by the laser photons. As a result, the electron subsystem is heated to a high temperature and the absorbed energy is transferred to the atomic lattice. Energy losses are caused by heat transport via electrons into the bulk of the substrate. According to classical linear theory, light absorption is described by the Beer-Lambert law, which states that the absorption of a particular wavelength of light transmitted through a material is a function of the material path length and is independent of the incident intensity.

For the very high intensities which can be achieved in laser processing, non-linear phenomena take place and cause stronger energy absorption. According to the linear absorption model, electrons excited by photon absorption transfer heat energy to the lattice and cause melting or vaporisation. In the case of extreme intensities, as with ultrashort pulse ablation, the bound electrons of the material can be directly freed. Effects such as multiphoton absorption and avalanche ionisation can be observed. Thermal conduction in the material draws energy away from the focal spot and leads to heat affected zones.

For metals, laser light absorption is not a major problem, because the band structure of the material (Figure 3.2) allows the absorption of most low-to-moderate energy photons. Metals absorb laser radiation with their electrons in the conduction band and near to the Fermi level. For semiconductors and insulators, including ceramics and polymers, the Fermi level is between the valence and conduction bands (Figure 3.2). The requirement that an electron has to absorb enough energy to pass through the forbidden region between the valence and conduction bands sets a limit on the photon energies that can be absorbed by a linear process. There are two methods for non-linear absorption: an electron avalanche and a strong multiphoton absorption (Shirk et al, 1998).

In the case of an electron avalanche, some electrons with intermediate energies are excited into the conduction band by single photon absorption. The electrons in the conduction band can absorb single photons of the incident light, which will increase their energy. These electrons collide with bound electrons, which leads to avalanche ionisation.

Multiphoton absorption is another mechanism for non-linear absorption in which an electron transfers from the valence band to the conduction band by absorbing several photons.

In general, as material reaches a critical density of electrons they start absorbing sufficient photon energy to undergo ablation (Shirk et al, 1998). It is important to note that there is a material dependent ablation threshold fluence (Shirk et al, 1998), below which the laser

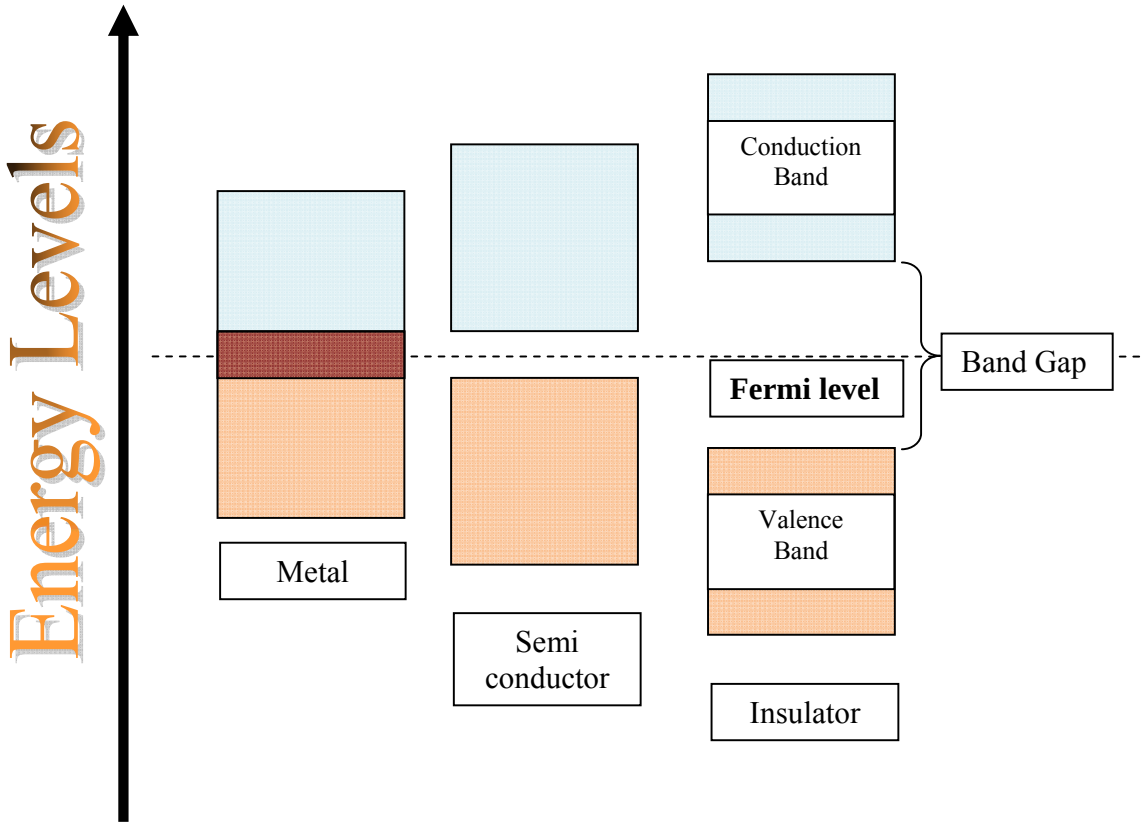

Figure 3.2 Band gaps

ablation cannot start and material removal is not possible. Best results are achieved when the energy applied is just above the ablation threshold – otherwise the excess energy will transform into heat and dissipate into the substrate, causing distinctive unnecessary thermal damage.

3.3 Ablation effects on the substrate

During laser milling, applying different ablation mechanisms, the material goes through several phase transitions (solid-liquid-vapour) that have a direct impact on the surface integrity of the processed area. Thus, the relevant material characteristics are the transition energies, such as evaporation energy and melting energy. In addition, thermal conductivity is a key material factor affecting the resulting surface integrity. In particular, this affects the dissipation of the absorbed energy into the bulk of the material and the energy losses, and hence determines the size of HAZ.

3.4 Method for Heat Affected Zone Investigation

The heat affected zones have significant importance as in many applications a knowledge of the resulting surface is required. Not only is the depth of penetration important, but also the quantity of the heat transferred into the bulk of material and the changes that are triggered by it. In publications/reports the usual practise is to look at a micrograph of the resulting surface

and, using a scale, to estimate optically the depth of the heat penetration. An example of such estimation is given in Figure 3.3.

Such estimates can be quite accurate for the depth penetration if done by an experienced person, but it is always dependant on the skills of the operator and does not give any further information.

With a broad range of laser sources available it would be difficult to choose the most suitable unless clear criteria are specified. Obvious characteristics such as removal rate and surface finish measured in micrometers R_a are most often used, but in some cases additional data is required. Structural changes beneath the surface can significantly change the properties of the substrate and subsequently affect the usability of the component/structure. In order to obtain comprehensive information about the structure and the changes resulting from laser ablation, a new method for analysis is proposed utilizing image processing. The new method not only independently identifies the zones affected by the heat transfer, but also provides quantitative information such as how much change took part at certain levels. The method is based on grains of material and grain size is used as the criteria. Figure 3.4 shows the sequence of operations for heat affected zone analysis.

3.4.1 Sample Preparation

This is a very important step of the process. The substrate needs to be sliced through the affected area, so later effects can be revealed. As the heat treatability of tool steels is a quality

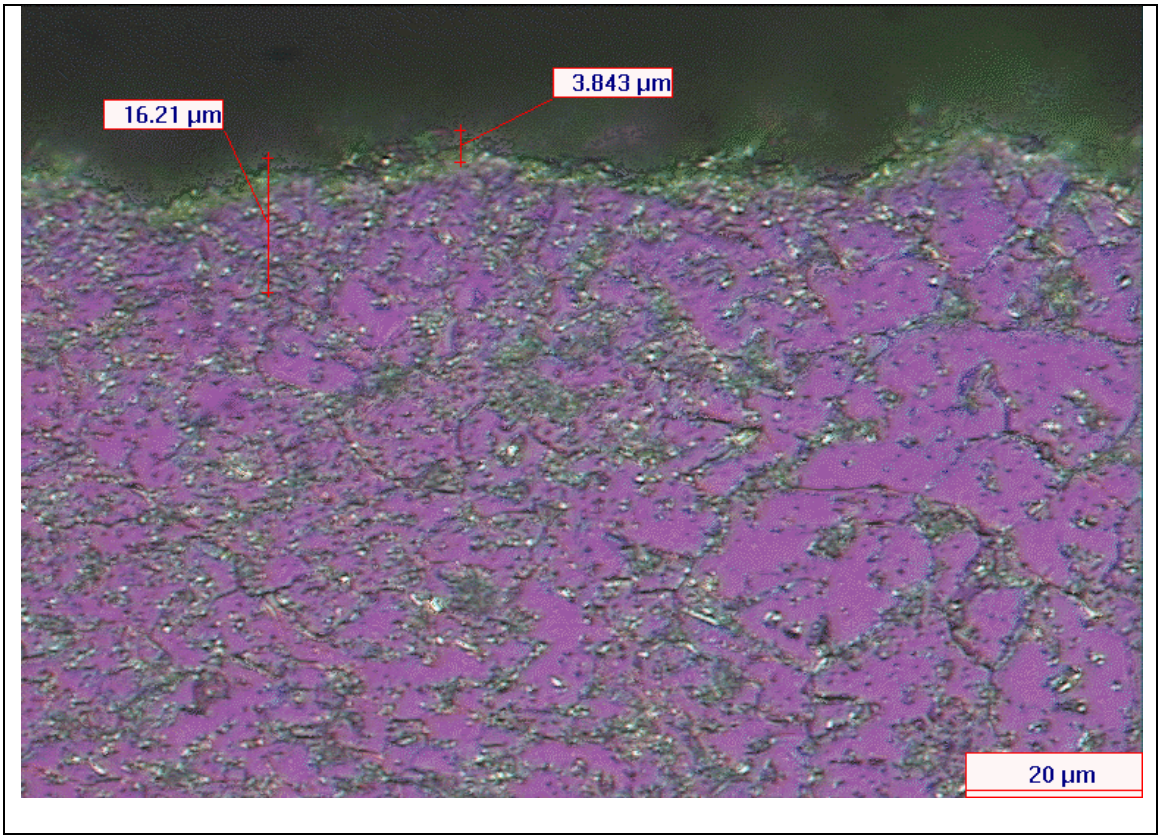

Figure 3.3 Heat affected zone estimation

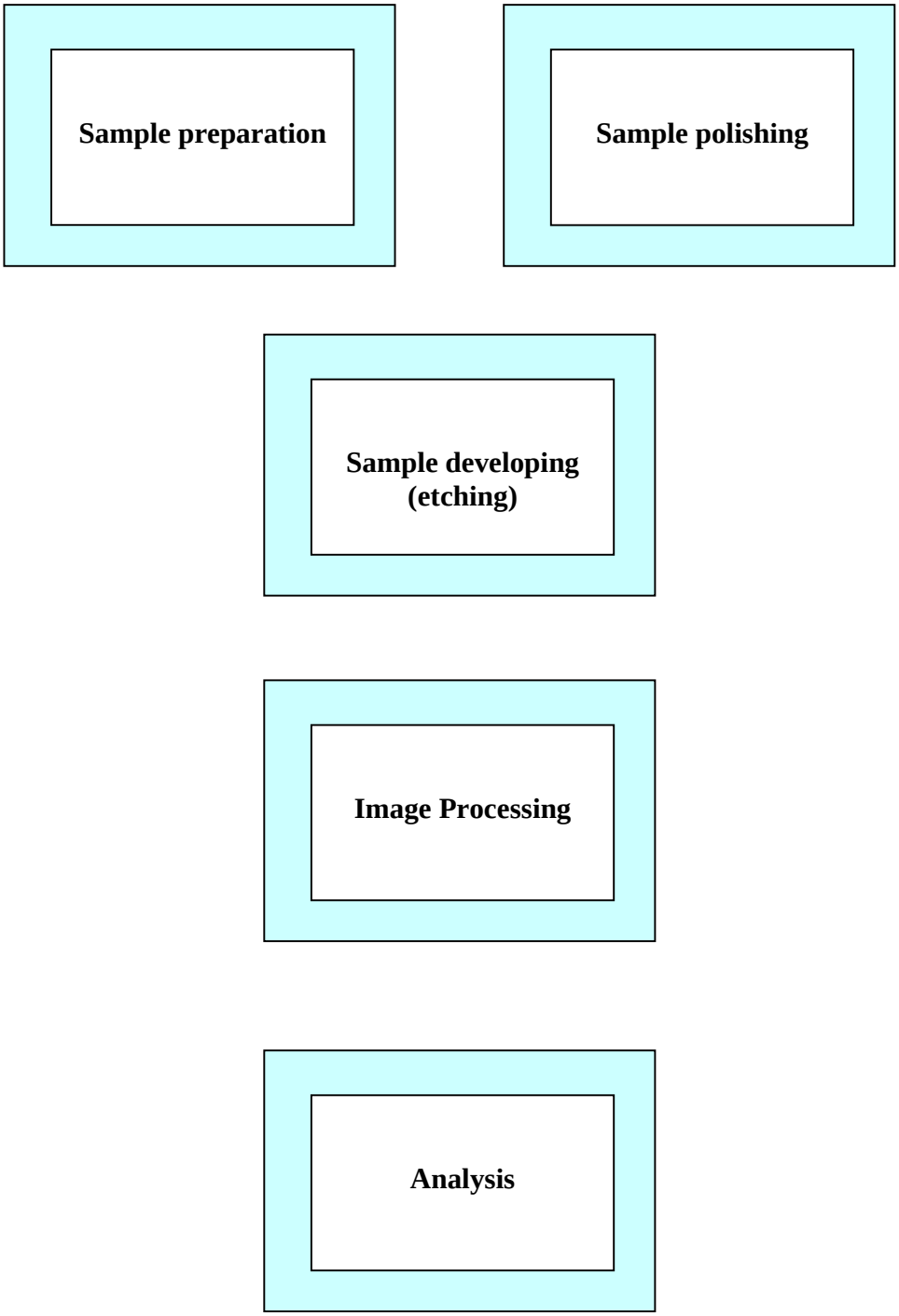

Figure 3.4 Typical sequence of operations for heat affected zone analysis

criterion, thermal influence during cutting has to be avoided in order to give a true representation of the actual structure. The danger at this stage is that a sample could be contaminated – either by introducing additional affected areas or mechanically destroying the structures.

When cutting larger sections and failure analysis samples this preparation step has to be carried out with great care. Wire EDM is usually a good choice as there is no force and the cut is done with minimal damage. Then, to ensure a better edge retention during the next step – polishing, the pieces are embedded in an epoxy based resin.

The main difficulty of grinding and polishing high alloyed tool steels is the retention of carbides and non metallic inclusions. In cold working tool steels primary carbides are very large and fracture easily during grinding. In fully annealed conditions, secondary carbides are very fine and can easily be pulled out from the softer matrix.

Any damage at this stage would invalidate the data collected later, so it is advisable to check carefully the specimen before further processing. If significant thermal damage is introduced or mechanical contamination has occurred, the procedure should be repeated again or an alternative solution found.

3.4.2 Sample Polishing

The main requirements on the preparation of high alloy tool steels are a true representation of form, amount and size of carbides, and the retention of non-metallic inclusions in a non deformed matrix. Large volumes of samples of high alloy steels are best processed on fully automatic grinding and polishing machines, which guarantee a fast and efficient workflow and reproducible results. As tool steels are hard, fine grinding with diamond is more efficient and economical than grinding with silicon carbide paper. Sometimes a final oxide polish after the diamond polishing step can be useful for contrasting and identifying carbides.

3.4.3 Sample developing

Usually samples of tool steel are first examined unetched to identify inclusions, carbide size and formation. To reveal the structure, either Nital or picric acid in various concentrations is used. For instance, to show the carbide distribution in cold work steel a 10% Nital colours the matrix dark while the white primary carbides stand out. For fine globular pearlite a brief submersion into picric acid followed by 2% Nital gives a good contrast and avoids staining.

3.4.4 Image processing

As a result of the development of the sample, grain structure is revealed. Typical results are shown in Figure 3.5. For better contrast polarized light was used as in this case colours are not really important – contrast is used to identify the grains boundaries.

A routine was developed to identify the grains and boundaries based on colour separation. Each image undergoes a series of processing filters in order to sharpen the contrast and adjust the sensitivity of the boundary recognition. Hence this makes this method applicable to

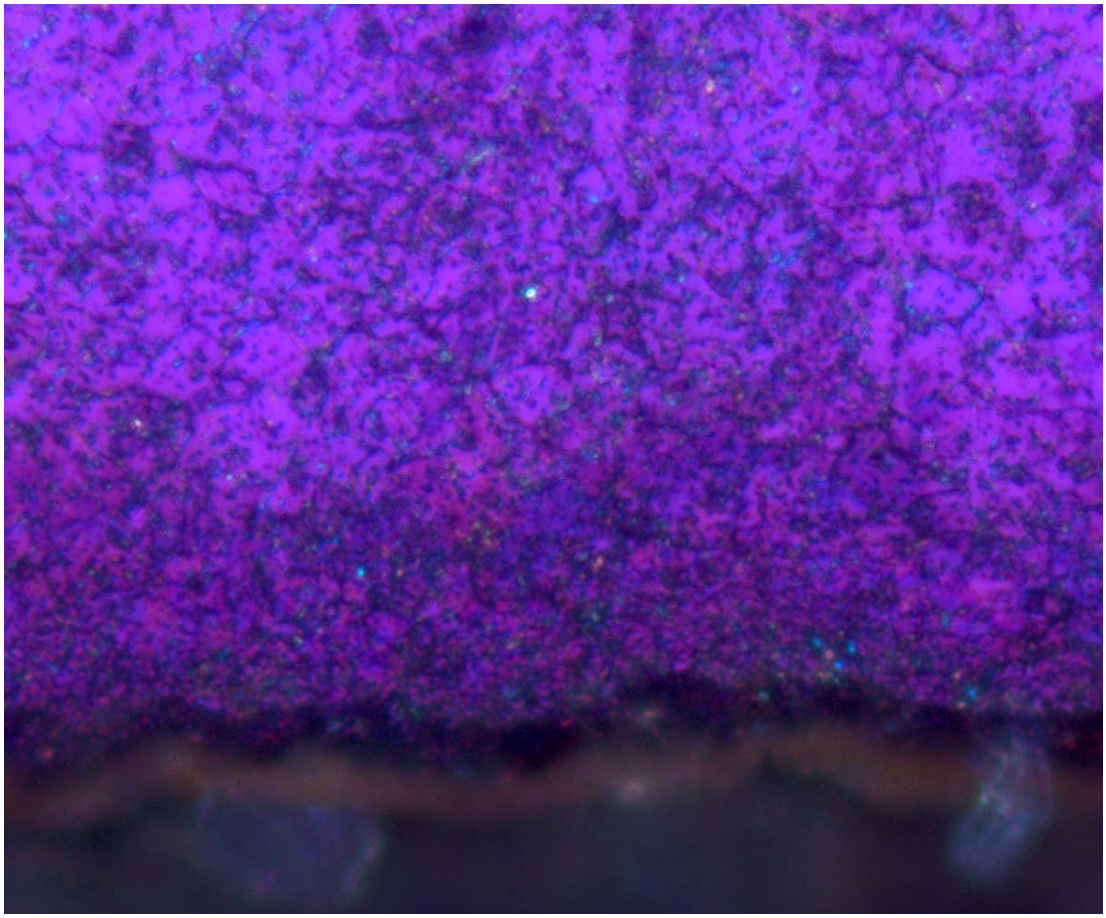

Figure 3.5 Typical result of grain structure

specimens with different contrast. When large volumes of samples are prepared, the procedure is usually automated and the results should be similar, but when preparation is done manually a variation in each specimen's properties can be expected.

The results of this routine can be seen in Figure 3.6. The yellow zones represent the grains detected. From there the perimeter of the grains is calculated, and the number of grains counted.

In order to validate the routine, a number of tests were done on the base substrate on 4 specimens in different locations. There was very little variation in the results obtained - comparable with the variations when the routine was applied to the same specimen in different locations.

3.4.5 Sample analysis

After completion of the previous steps, information is available for the number of grains identified in the specified area, as well as their perimeter. A statistical report is generated containing information about:

- field area ,
- object count,
- diameter – min. , max. and mean

- distribution chart.

An example is given in Figure 3.7.

3.5 Experimental set-ups and method

A series of experiments were conducted to assess the impact of the laser pulse duration on the surface integrity of a substrate. Two main effects were studied, in particular changes in material microstructure and surface quality by carrying out metallographic and surface profile analyses. In order to estimate the thermal load exercised on the substrate, the processed areas were analysed for phase transformations and changes in the grain structure.

Four different laser milling systems were employed having femto-, pico-, nano- and micro-second pulse durations, respectively, to ablate a field with dimensions 1 × 1 mm. The characteristics of the laser sources employed in this experimental study are shown in Table 3.2. The experiments were conducted at four different sites within a day on the same workpiece and included:

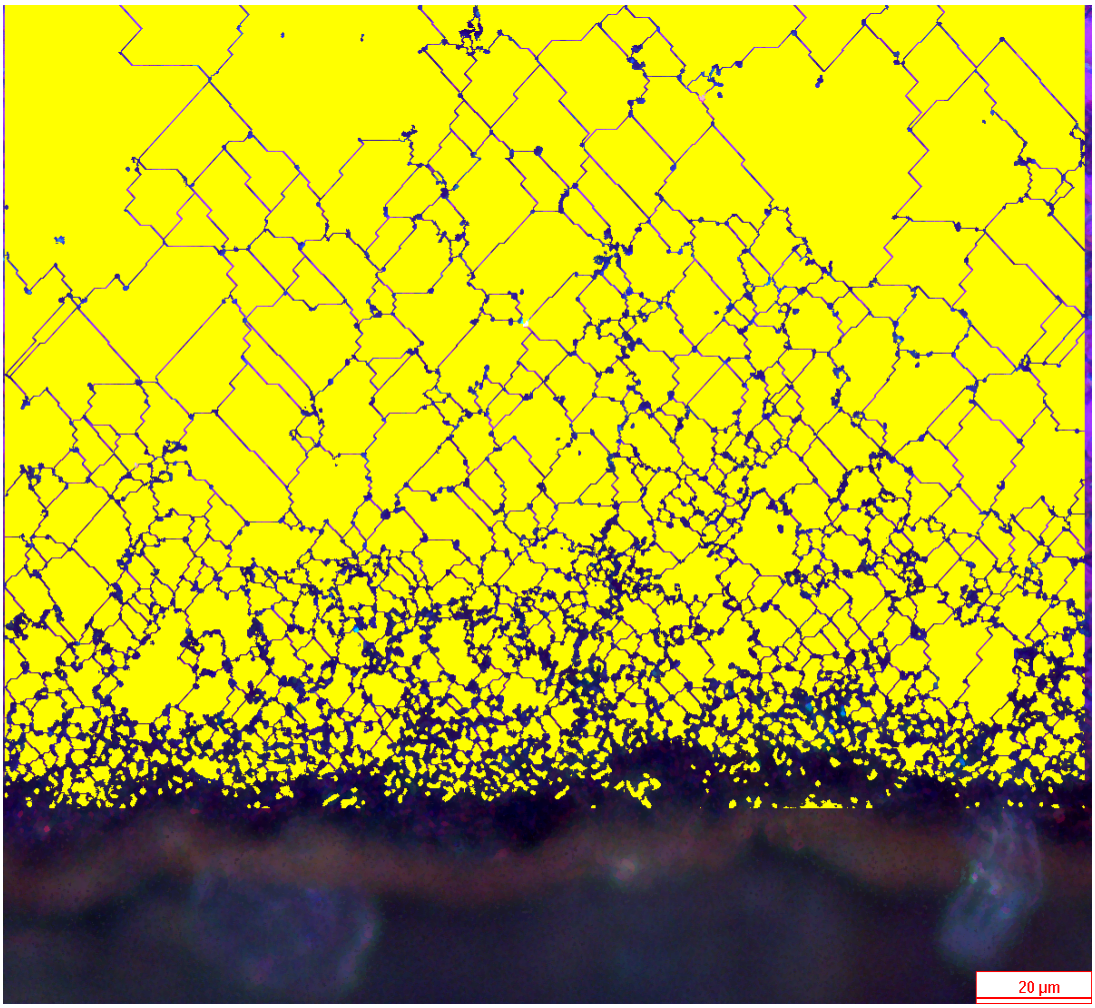

Figure 3.6 Grains structure identified

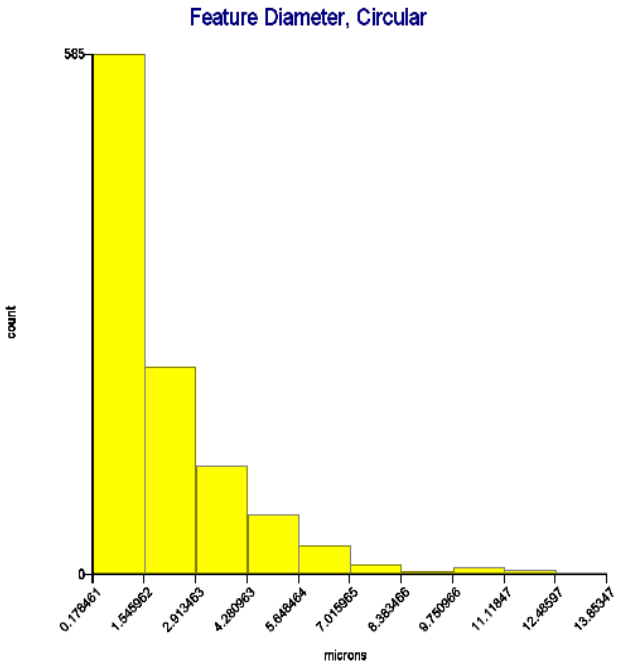

Field Summary

Bitplane(s):
Feature

Statistics:

Min:	0.178461 µm
Max:	13.85347 µm
Mean:	2.003536 µm
Std Dev:	1.941114 µm
95% CI:	0.119073 µm
% RA:	5.943158 %

Field Information:

Field Area:	30016.43 µm²
Total Area:	30016.43 µm²
Field Count:	1

Object Information:

Object Count:	1063
Data Points Over:	0
Data Points Under:	0
% Data Points Displayed:	100 %

Figure 3.7 Statistical report

- Familiarisation with the material. The four partner organisations involved in this study did not have experience with the selected material for the trials. Thus, some test features were produce to find the best processing window within the available time frame. It should be stressed that these may not be the optimal parameters; however the effects on the surface integrity of the substrate could be considered representative for performing ablation in these four different regimes.

- Machining of a series of 1 x 1 mm fields. A few test structures were produced on each system by varying laser milling parameters within the identified processing window. However, the time available did not allow the analysis of the machined surfaces to be carried out immediately after the tests. Therefore, as already indicated, the obtained surface roughness may not be the best achievable with these four laser sources.

For further analysis in this research, the fields with the best surface roughness for each of the four studied ablation regimes were selected.

The experiments were conducted on a BS EN ISO 4957 – X40CrMoV5-1 tool steel substrate (0.35%C, 1%Si, 5%Cr, 1.4%Mo, 1% V). This material was selected because it is commonly used to manufacture tooling inserts for micro injection moulding and hot embossing, and can endure many thermal cycles. The material properties of the X40CrMoV5-1 tool steel are provided in Table 3.3.

The workpiece used in this experimental study was polished before it was processed with the four different laser sources in succession. After completing the machining, all fields were cleaned in an ultrasonic bath with a gentle degreaser to preserve the topology of the resulting surfaces. The fields were inspected with a white light profiling microscope before dicing the substrate into pieces. Then, for a better edge retention the pieces were embedded in an epoxy based resin.

Finally, the specimens were polished and developed with picral (recommended for structures consisting of ferrite and carbides) and nital (the most common etchant for revealing alpha grain boundaries of Fe, carbon and alloy steels) reagents in order to analyse the material microstructure. In particular, this was done to highlight the boundaries of the ferrite grains (α-phase) and carbide sets.

An analysis of the material microstructure was carried out employing the Buehler-Omnimet software (Buehler-Omnimet, 2000).

Table 3.2 Laser sources characteristics

Laser type	**Laser Source**	**Laser process parameters**	**Roughness achieved,Ra (μm)**
A	Femtosecond Laser source SP Hurricane (amplified Ti:Sapphire) Wavelength = 800nm Rep. Rate = 5kHz Pulse = 130fs	Power = 20 mW Scanning Speed = 100 mm/min Number of passes = 4 Step = 0.01 mm Fluence = 0.25 J/cm^2	0.35
B	Picosecond laser source – Stacatto (Lumera) Wavelength = 1064 nm Rep. Rate = 50 kHz Pulse = 12 ps	Power = 100 mW Scanning Speed = 100 mm/s Number of passes = 10 Step = 0.002 mm Fluence = 1.13 J/cm^2	0.29
C	Nanosecond – CVL MOPA (Oxford lasers) Wavelength = 511 nm Rep. Rate = 10 KHz Pulse = 17 ns	Power = 10W Scanning Speed = 100 mm/s Number of passes = 10 Step = 0.01mm Fluence = 2 J/cm^2	0.86
D	Microsecond – Foba (Lasertech) Wavelength = 1064 nm Rep. Rate = 30.5 kHz Pulse = 10 μs	Power = 5.2W Scanning Speed = 305 mm/s Number of passes = 10 Step = 0.01 mm Fluence = 1.8 J/cm^2	2.18

The changes in the grain structure were the main criterion for estimating the heat affected zones. The material microstructure of the workpiece was uniform before performing any processing. After the ablation, a grain refinement was observed in the area surrounding the machined surface. Such changes are the result of the thermal wave propagation into the substrate, which is immediately followed by a quick cooling down at the end of the pulse. In particular, to analyse the affected regions in this experimental study, they were split into three zones taking into account the extent of these changes. Zone 1 covers the area where most of the heat was absorbed, and therefore the changes are clearly visible. In Zone 2, some changes can still be observed, but at the same time there is a steady decrease of the thermal impact. Finally, in Zone 3, the materials microstructure can be considered to be the same as in non-processed areas of the substrate.

Table 3.3 Material Properties of BH13

C.	Si.	Mn.	Cr.	Mo.	V.
0.38%	1.00%	0.40	5.00%	1.30%	1.00%

Physical Properties:	**At temperature:**		
	200°C	**400°C**	**600°C**
Density (Kg/dm³)	7.75	7.70	7.65
Coefficient of thermal expansion (per °C from 0°C)	11.9 x 10-6	12.4 x 10-6	12.8 x 10-6
Thermal conductivity (cal/cm.s °C)	60.0 x 10-3	62.4 x 10-3	63.6 x 10-3
Modulus of elasticity **(** N/mm²)	184 000	175 000	154 000

To make the comparison of microstructure changes easier it was assumed that these three characteristic zones cover the same area in depth for micro- and nano- second, and pico- and femto- second ablation regimes, respectively. In particular, the three zones were set to be equal for:

- Long pulsed lasers (micro- and nano- second regimes) – Zone 1 below 15 μm in depth, Zone 2 from 15 to 50 μm, and Zone 3 above 50 μm;
- Short pulsed lasers (pico- and femto- second regimes) – Zone 1 below 10 μm, Zone 2 from 10 to 30 μm, and Zone 3 above 30 μm.

A quantitative assessment of the microstructure changes was carried out by calculating the number of grains in each zone, and their maximum, minimum and mean diameters with the Buehler-Omnimet software (Buehler-Omnimet, 2000).

3.6 Results

3.6.1 Surface roughness

The surface maps of fields laser milled with four different pulse durations were studied in order to understand the effects of the four ablation mechanisms on the resulting surface roughness. The fields with the best surface roughness for each of the four studied ablation regimes were selected for further analysis.

In Figures 3.8 – 3.11, the 3D surface maps of the four studied fields are presented.

In addition, surface profiles were created to analyse the effects of pulse duration on the resulting surface topography. They are shown in Figures 3.12 -3.15.
All roughness measurements were taken using a white light profiling microscope. The size of the scanned areas was chosen according to ISO 4288:1996 and ISO 11562:1996 (http://www.predev.com/smg/standards.htm, 2011).

The parameter used to evaluate the surface roughness was the arithmetic mean roughness (Ra) because relative heights in micro topographies are more representative, especially when measuring flat surfaces.

The best results were obtained from the picosecond pulsed laser ablated specimen – showing a roughness of only R_a 0.29µm, followed by the femtosecond – R_a0.35µm, nanosecond – R_a 0.86 µm and microsecond – R_a 2.18 µm.

As expected the longest (microsecond) pulse laser source produced the worst roughness, but the best roughness was achieved by the picosend pulsed laser - not by the shortest pulsed laser (femtosecond).

In figure 3.16 surface profiles of ps and fs lasers are superimposed for direct comparison and in figure 3.17 the ps and µs surface profiles are compared.

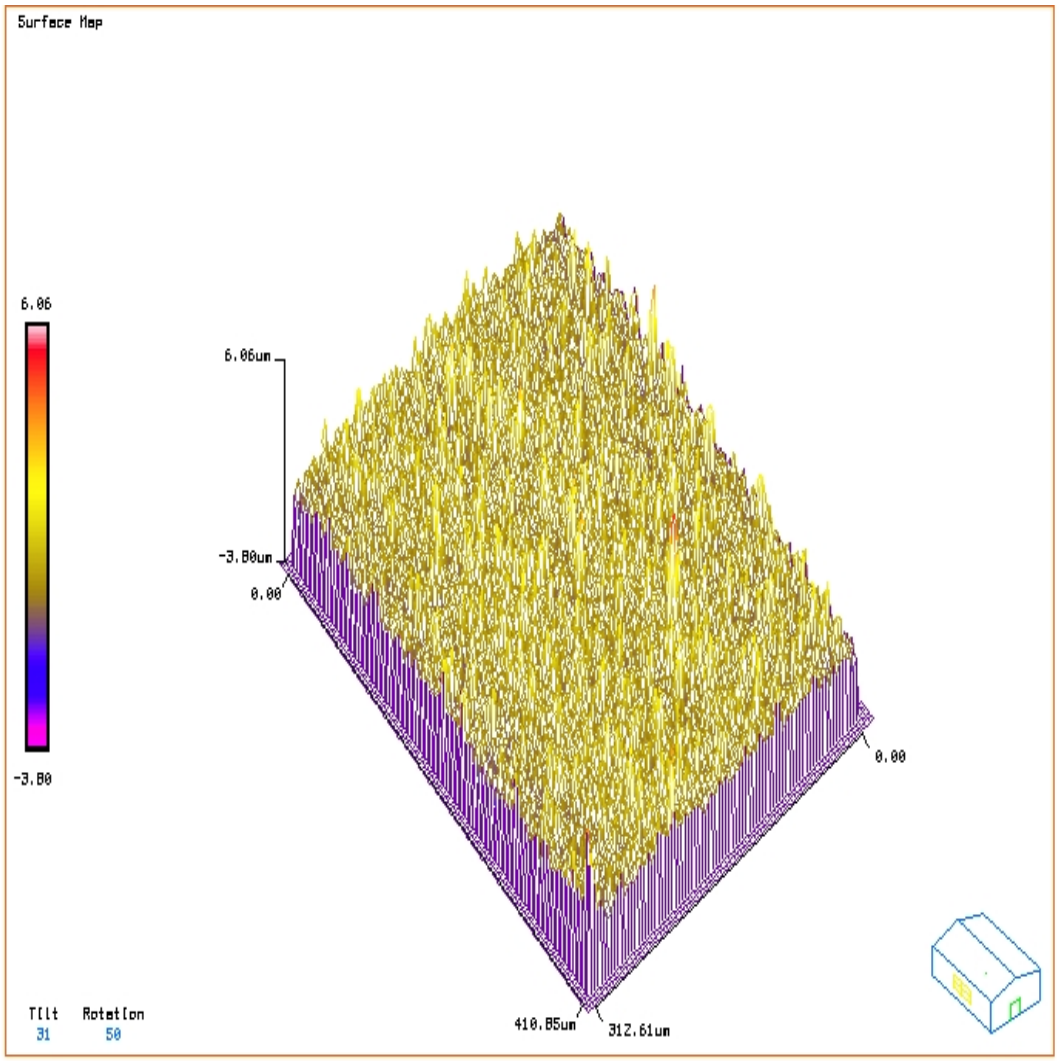

Figure 3.8 fs pulse duration specimen map

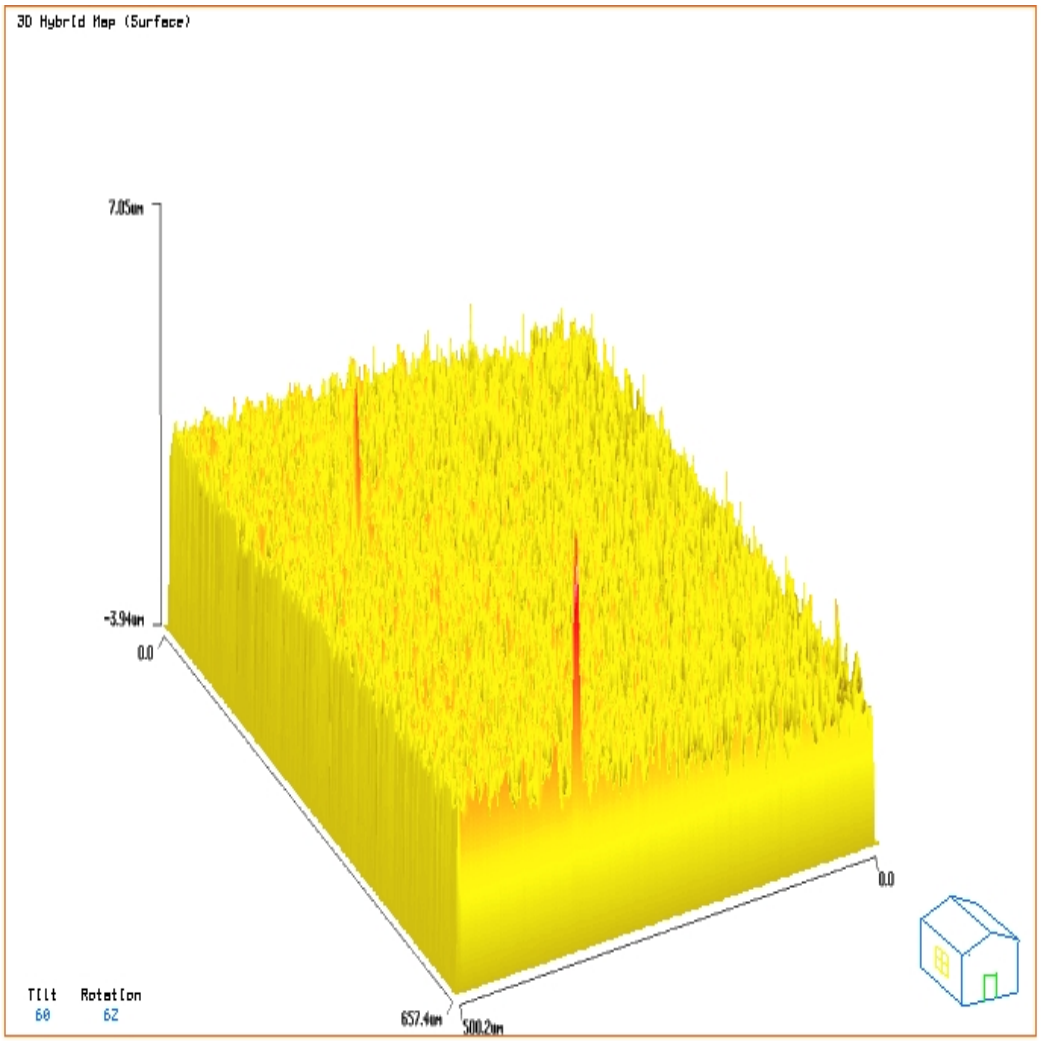

Figure 3.9 ps pulse duration specimen map

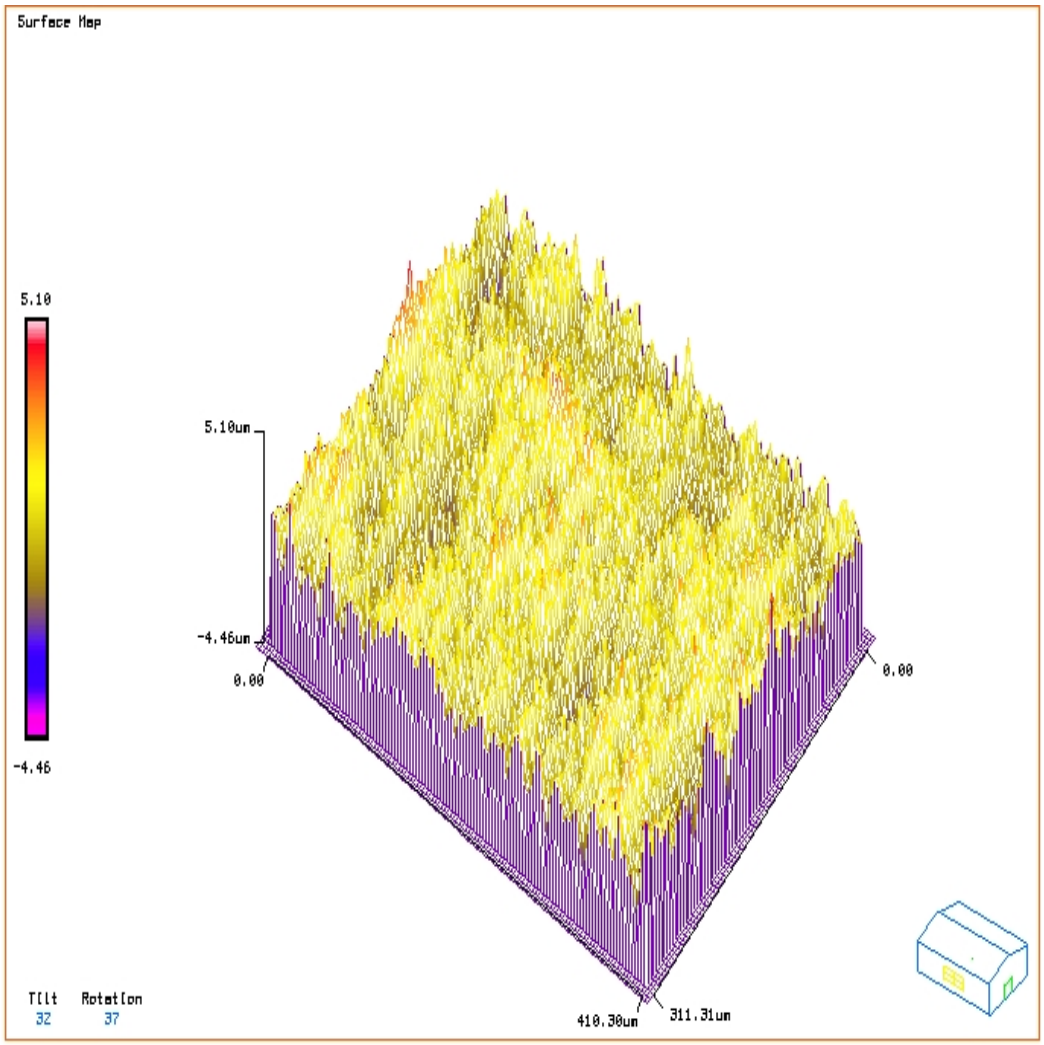

Figure 3.10 ns pulse duration specimen map

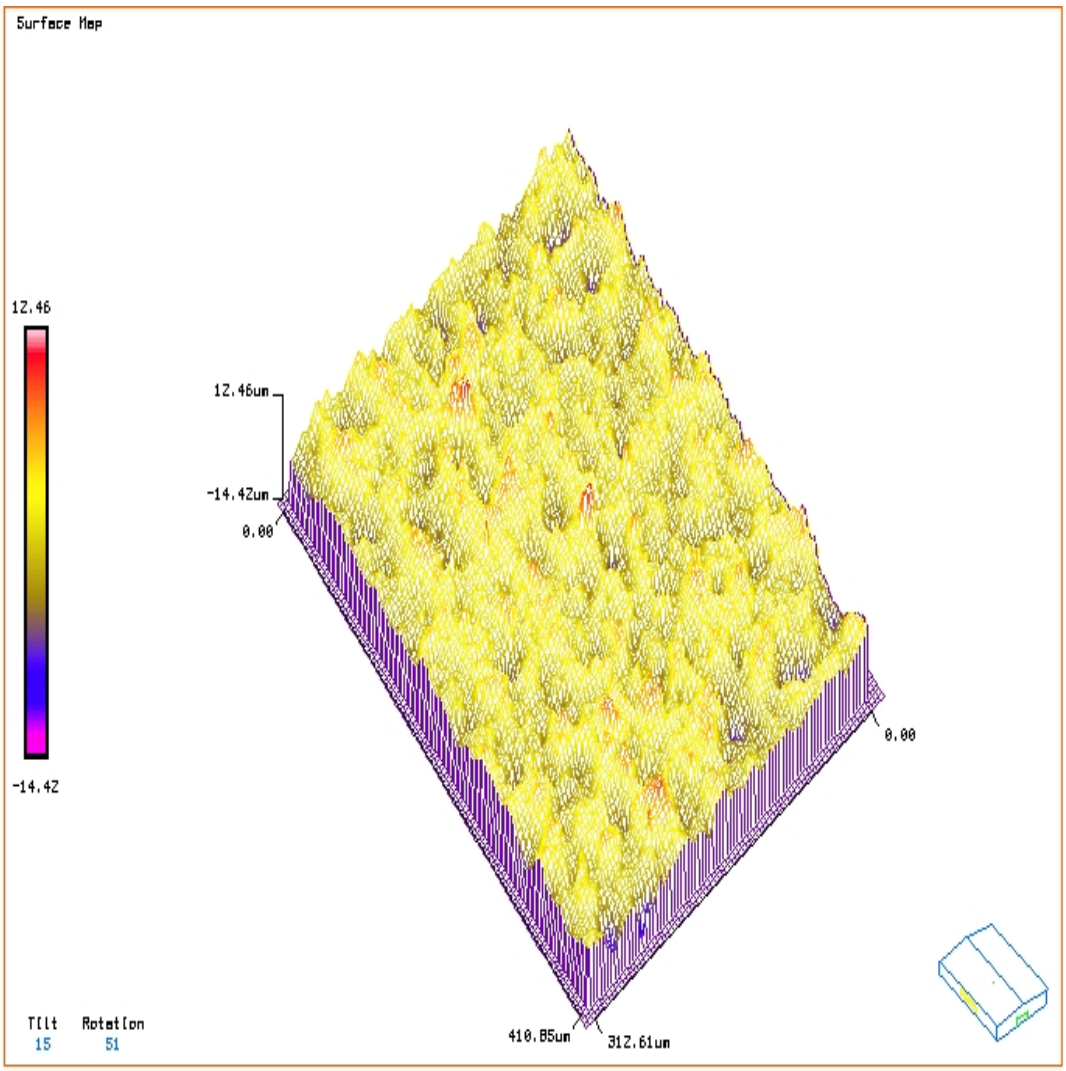

Figure 3.11 μs pulse duration specimen map

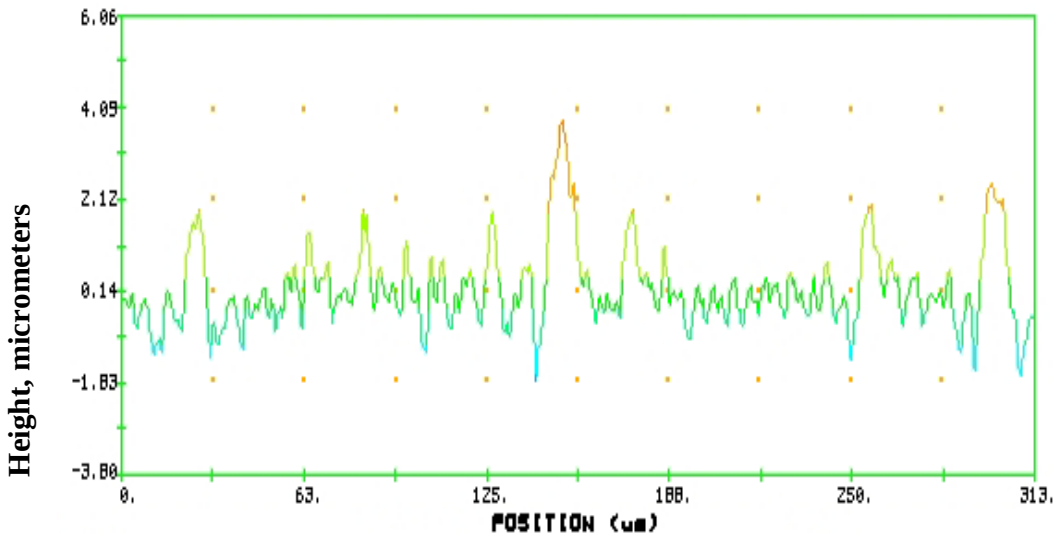

Figure 3.12 fs pulse duration surface profile

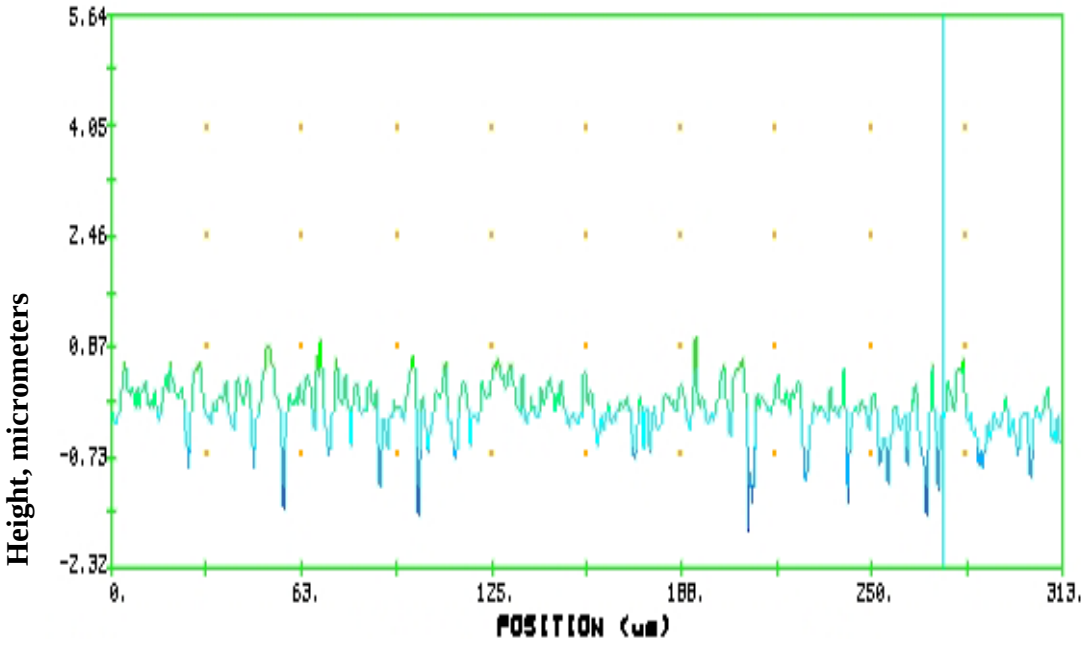

Figure 3.13 ps pulse duration surface profile

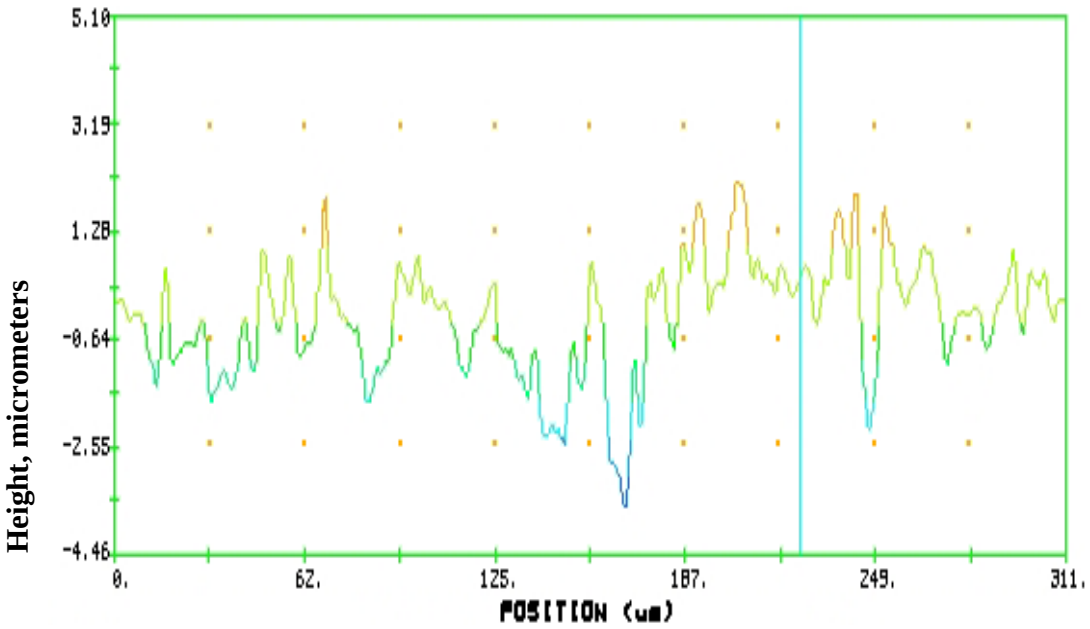

Figure 3.14 ns pulse duration surface profile

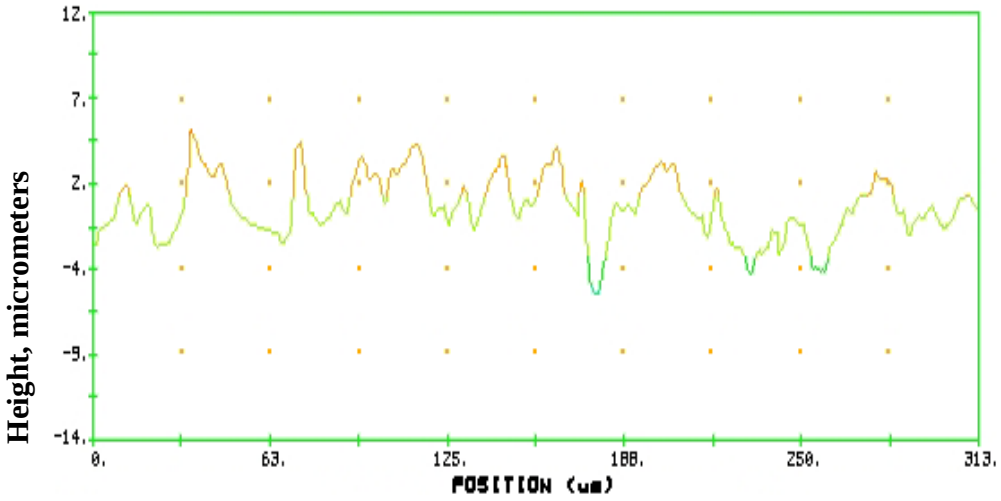

Figure 3.15 μs pulse duration surface profile

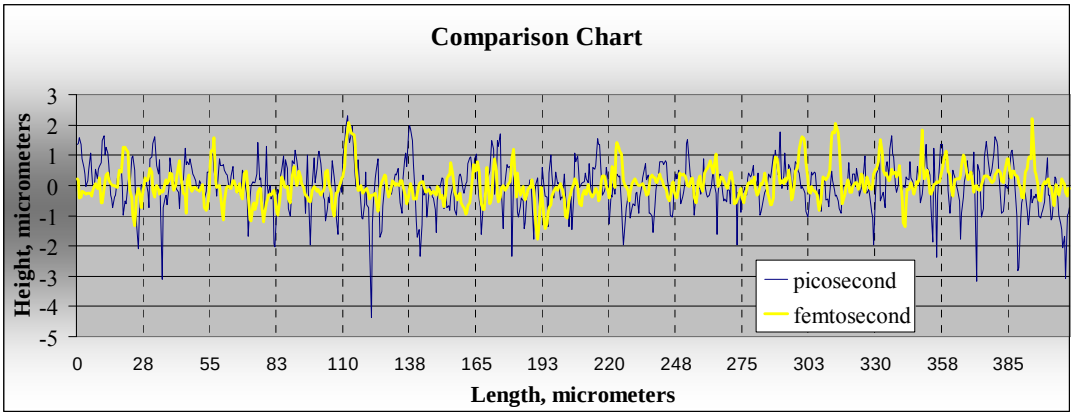

.

Figure 3.16 A direct comparison of the surface profiles of the fields machined with the ps and fs laser sources

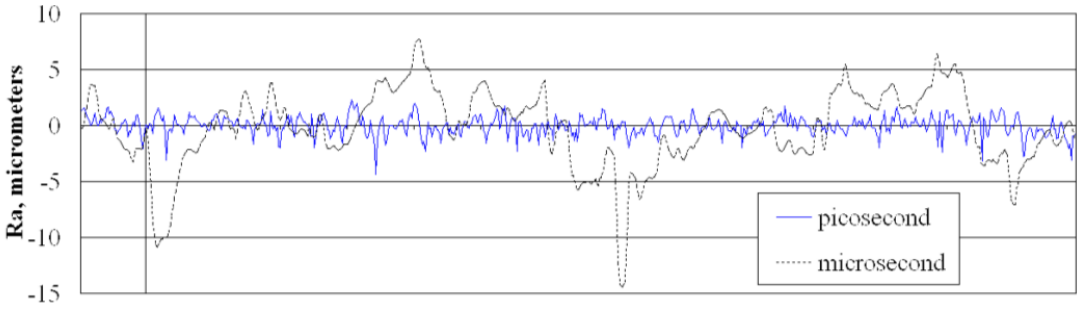

Figure 3.17 A direct comparison of the surface profiles of the fields machined with the ps and μs laser sources

3.6.2 Material microstructure

Micrographic pictures were obtained in polarised light in order to enhance the appearance of the crystallographically identical ferrite grains. The area and equivalent circular diameter of each individual grain were calculated using the Buehler-Omnimet software as explained previously. Based on this data, it was possible to estimate the average grain sizes, and thus to have a quantitative measure for assessing the thermal effects on the processed surfaces, and ultimately to judge the thermal load exercised on the substrate in each ablation regime.

A qualitative analysis of the resulting grain structure after performing laser milling with long pulsed lasers is provided in Figure 3.18 and for short pulsed lasers is provided in Figure 3.19.

The changes of the material microstructures in the three characteristic zones after processing in different ablation regimes can be summarised as follows:

- *Microsecond pulse duration.* Figure 3.20 shows the studied three characteristic zones. In Zone 1 (0-15 μm) the mean diameter of the grains was estimated to be approximately 1.3 μm, and the maximum diameter measured was 7.5 μm. In Zone 2 (15-50 μm) the mean diameter was equal to 2.5 μm while the maximum diameter was 11.5 μm. Finally, above 50 μm no changes in the grain structure were identified. The mean and maximum diameters were 7.9 and 36 μm, respectively, the same as in unprocessed areas on the substrate.

- *Nanosecond pulse duration.* The three studied zones in the micrograph are shown in Figure 3.21. In Zone 1 the estimated mean diameter of the grains was approximately 1.45 μm while the maximum diameter measured was 9.8 μm. In Zone 2, from 15 to 50 μm, the mean and maximum diameters were 2.8 μm and 15.5 μm, respectively. Again, above 50 μm there were no more changes in the grain structure. The mean and maximum diameters were 7.8 and 33 μm.

    - *Picosecond pulse duration.* In Figure 3.22, a micrograph depicting the three characteristic zones used for analysing the thermal load of short pulsed lasers is provided. The results obtained showed that mean and maximum diameters of the grains in Zones 1 and 2 were 2.3 μm and 4.1 μm, and 9.3 μm and 21.5 μm, correspondingly. No changes in the grain sizes were observed in Zone 3, above 30 μm. In particular, the measured mean and maximum diameters were equal to 8.2 μm and 31 μm, which were the same as those for unprocessed areas of the substrate.

- *Femtosecond pulse duration.* The analysis of the material microstructure was carried out again by splitting the micrograph in three zones as shown in Figure 3.23. In Zone 1 the estimated mean diameter of the grains was approximately 1.6 μm while the maximum diameter measured was 8.2 μm. In Zone 2, from 10 to 30 μm, the mean and maximum diameters were 4 μm and 17.5 μm, respectively. Again, above 30 μm from the ablated surface there were no changes in the grain structure, and the mean and maximum diameters were 8.2 and 31 μm, correspondingly.

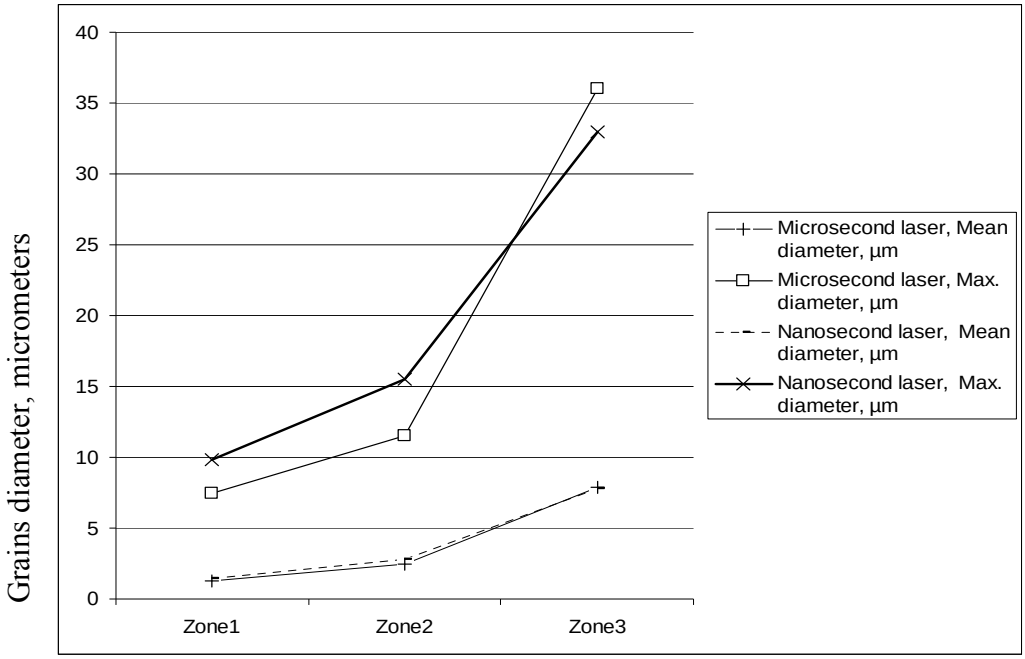

Figure 3.18 The changes of maximum and mean grain diameters in the three studied zones after processing with long pulsed lasers

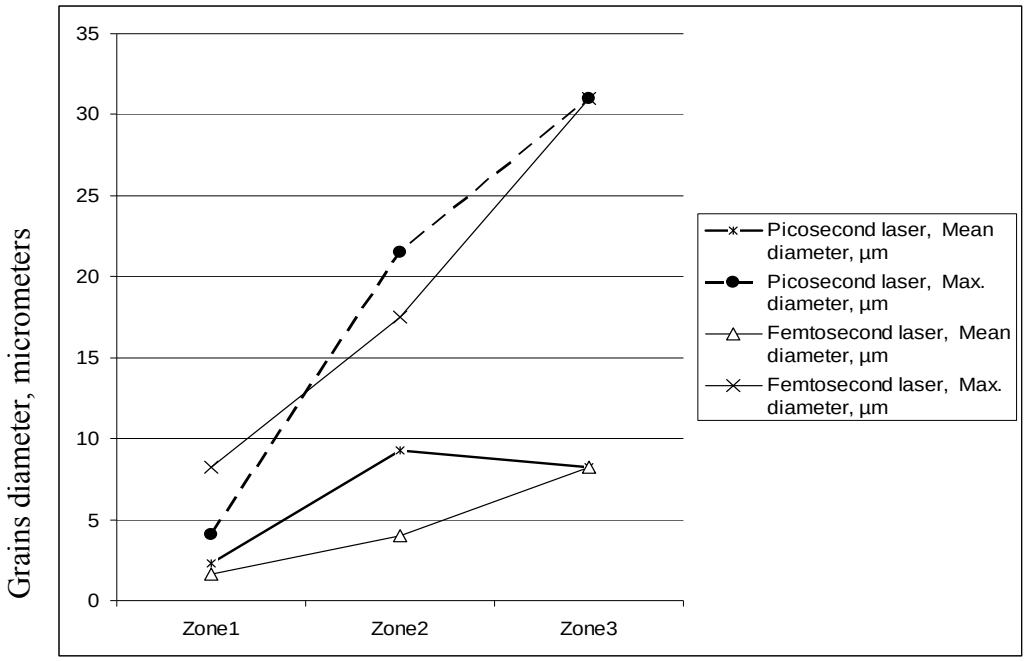

Figure 3.19 The changes of maximum and mean grain diameters in the three studied zones after processing with short pulsed lasers

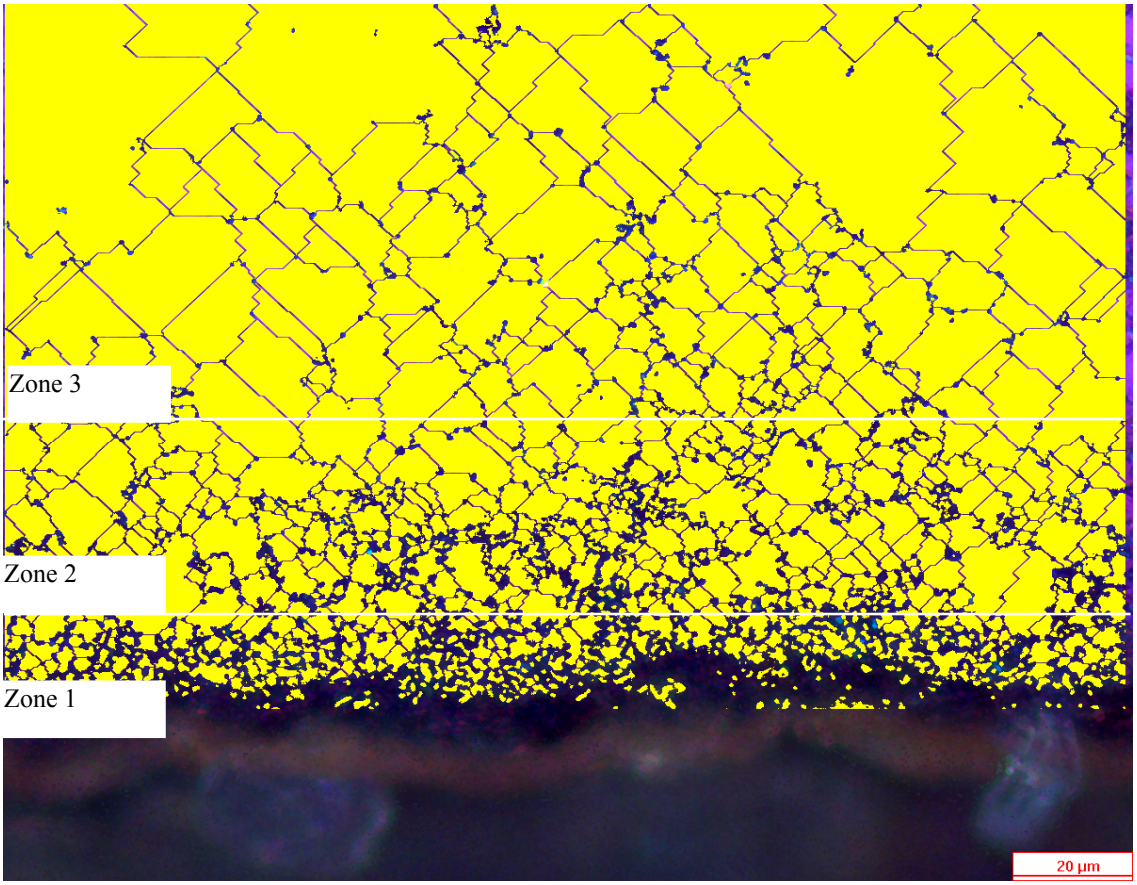

Figure 3.20 A micrograph depicting the three characteristic zones after machining with µs laser

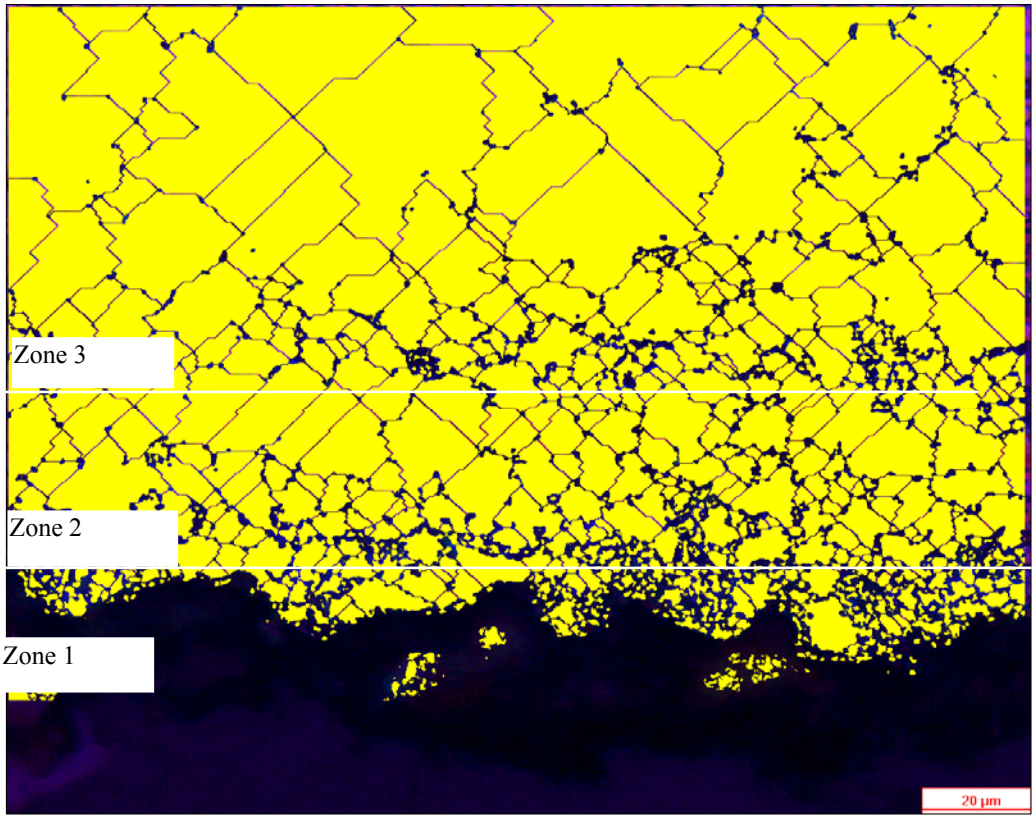

Figure 3.21 A micrograph depicting the three characteristic zones after machining with ns laser

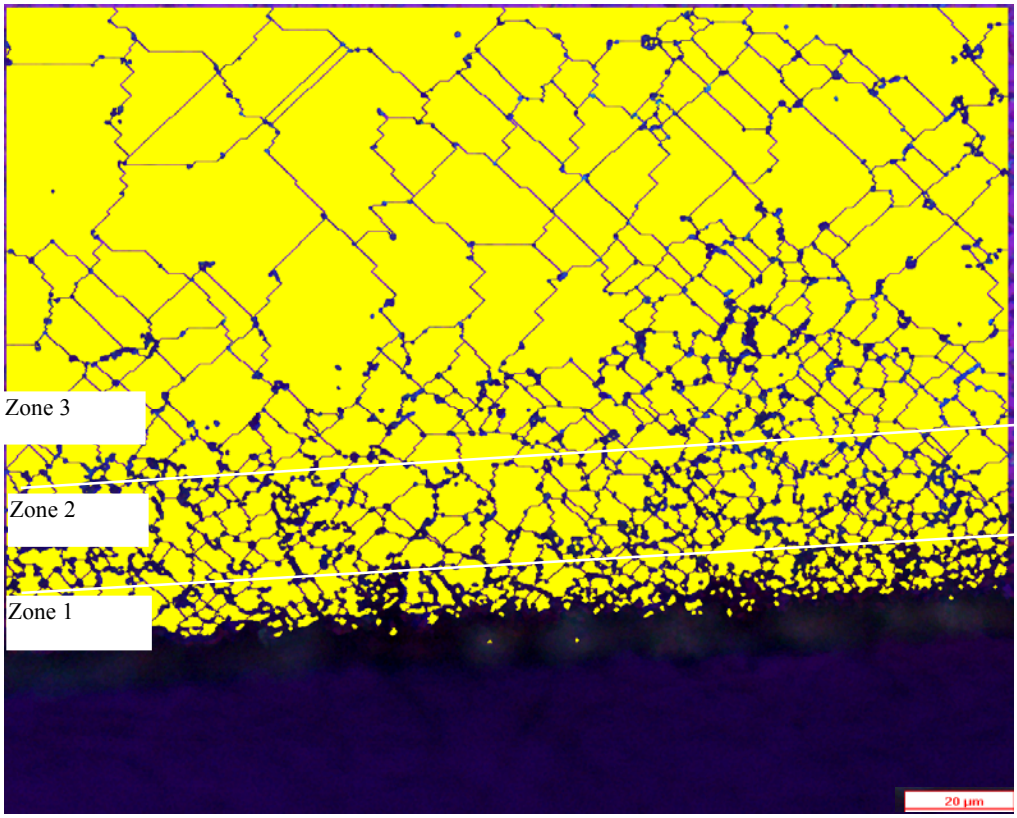

Figure 3.22 A micrograph depicting the three characteristic zones after machining with ps laser

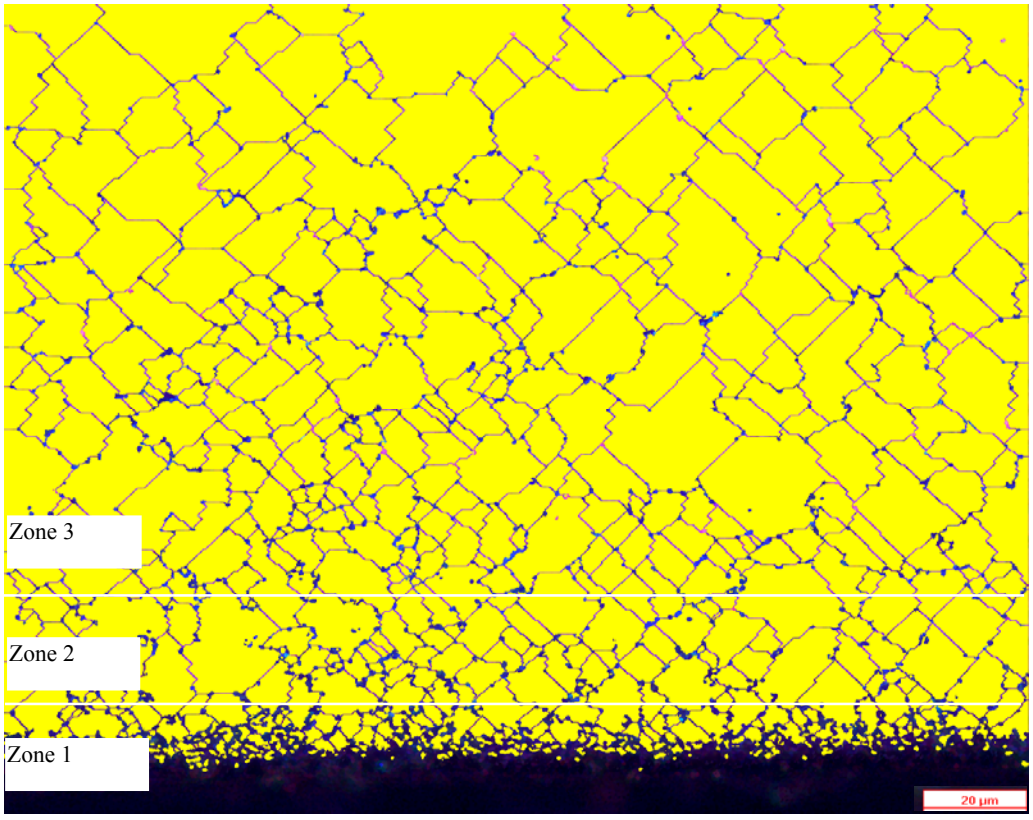

Figure 3.23 A micrograph depicting the three characteristic zones after machining with fs laser

3.7 Discussion

3.7.1 Surface roughness

As expected the roughness of the field processed with the µs laser was the highest, Ra 2.18 µm. The surface profile after machining with the ns laser source was significantly better; in particular, the roughness was reduced to Ra 0.86 µm. However, the results produced working in ps and fs regimes were not expected. Initially, it was anticipated that in these two ablation regimes a shortening of the pulse duration would lead to a better machining response, in particular surface finish. The surface roughness measured on the surface ablated with the fs laser was Ra 0.35 µm compared to Ra 0.29 µm achieved with the ps one. This could be explained with nonlinear effects that are typical when processing materials at this regime, and also with the specific machining response of the tooling steel to the selected processing parameters.

3.7.2 Material microstructure

Pulse duration is a major factor affecting the surface integrity of processed areas. In particular, it is important to understand the effects of heat dissipation into the regions nearest to the machined surface. In this research, these effects were studied by analysing the changes in material grain structure, and thus indirectly to make a judgement about the specific thermal load of each ablation regime.

Based on the grain size refinement observed in the areas processed with μs and ns lasers, it was estimated that the temperature in the affected Zones 1 and 2 reached more than 800-900 ^{o}C before the heat started to dissipate into the substrate. Thus, the temperature was sufficiently high to initiate an austenite (γ) transformation, which was followed by $\gamma \rightarrow \alpha$ transformation with cooling rates much higher than those in a conventional heat treatment. This resulted in the creation of a non-equilibrium microstructure in the material, in particular a higher stress level, smaller α grain sizes and with carbides precipitated within the α grains. At the same time the cooling rate was not high enough to initiate a martensite transformation. Martensite transformations were observed only in some areas exposed to extreme conditions, where a significant deterioration of surface integrity was observed together with formation of large torch-like recast zones as shown in Figure 3.24. The microhardness measurements carried out in these areas resulted in values around 550 MHV (see Figure 3.25) that are typical for quenched structures. Although, in this case the martensite structures were an undesired effect, the trials demonstrated that laser systems could be used for performing controlled surface modifications.

As expected, the material microstructures formed after processing with ultra-short laser pulses showed less phase transformations than those created by performing ablation with longer pulses. This can be easily explained with the specific characteristics of these two distinctive ablation regimes. In particular, the material undergoes a direct solid-vapour transition, in the case of ps and fs laser pulses, compared to the solid-melt-vapour transitions when exposed to longer pulses. The melt/vapour proportion determines the amount of heat which is dissipated

into the substrate, and eventually causes secondary effects such as microcracks, phase transformations and grain size changes.

As reported by Breitlung D. et al, 1998, the melt/vapour ratio depends on pulse duration and fluence, and decreases with the reduction of the interaction time. The presence of melt instigates more intensive heat transfer to the substrate, and subsequently to a larger HAZ.

In ps and fs laser ablation regimes, the overall energy transfer is very small, and thus the changes of the microstructure are almost negligible. A direct de-sublimation of the atoms occurs and the energy is taken immediately away from the substrate. In spite of that, some changes in material microstructure can still be observed in the micrographs for both ablation regimes. In case of ps laser ablation they are more evident (see Figure 3.22), while for the fs regime if there are any changes they are only within 1 to 2 μm in depth (Figure 3.23).

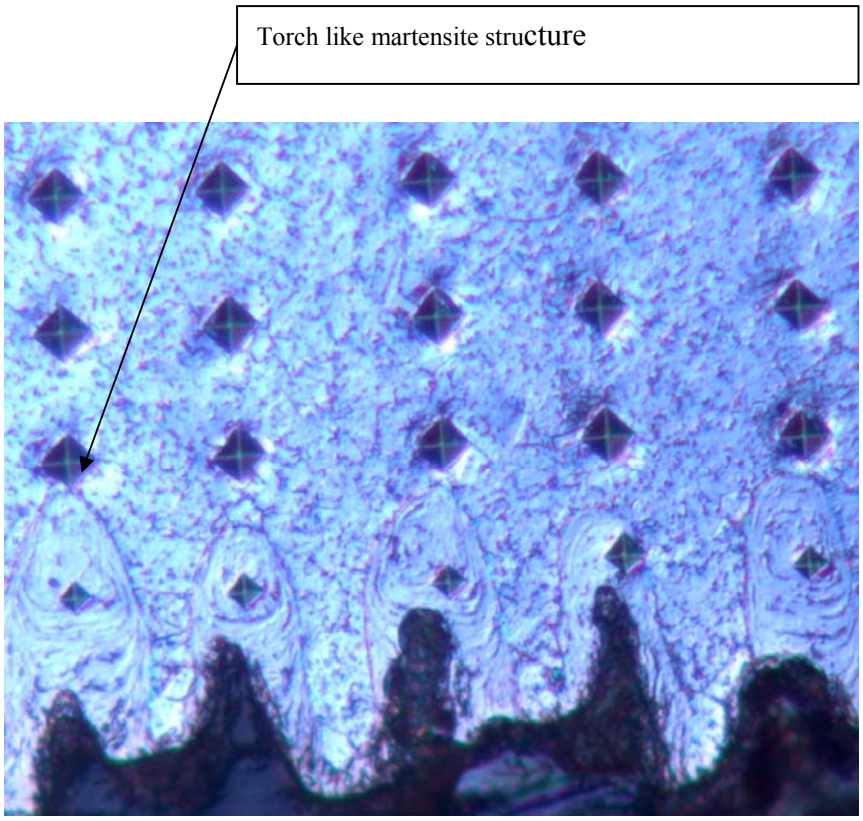

Figure 3.24 Martensite structure

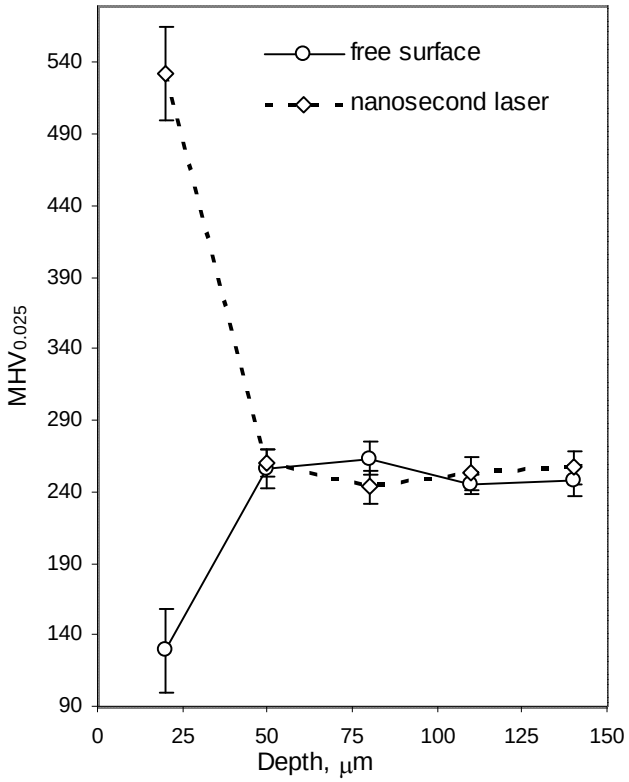

Figure 3.25 Microhardness test results

3.8 Summary

In this research, the effects of pulse duration of four different laser sources on surface integrity were investigated. In particular, an attempt was made to assess the impact of four different laser regimes on surface quality and material microstructure. These are the issues that have to be taken into account when considering the tradeoffs between high removal rates and the resulting surface integrity. This is a particular dilemma when selecting the most appropriate ablation regime for performing micro structuring.

During laser milling applying different ablation mechanisms, the material goes through several phase transitions that have a direct impact on surface integrity of the processed area. Thus, the relevant material characteristics are the transition energies, such as evaporation energy and melting energy. In addition, thermal conductivity is a key material factor affecting the resulting surface integrity. In particular, this affects the dissipation of the absorbed energy into the bulk of the material and the energy losses, and hence determines the size of any HAZ.

The results presented in this study are grouped into three distinctive groups for visual representation. The affected area could be fully charted and a profile of the changes could be created, containing information for the count and sizes of the grains at any point.

The following generic conclusions can be drawn from this study:

- For both ms and ns laser milling, the HAZ on the ablated surface is estimated to be within 50 μm. However, there were some differences in grain size refinements when comparing the resulting microstructures. The melt phase during μs laser processing was bigger, and more heat was transferred into the substrate, leading to the formation of a finer grain structure.
- When performing ultra short pulsed laser ablation, the effects of heat transfer are not evident as was the case with longer laser pulse durations. Although some heat is transferred into the bulk, it is not sufficient enough to trigger significant structural changes. Heat penetration is much smaller and grain refinement is minimal. The effects of pulse duration on the resulting material microstructure are more evident in the micrograph of the field exposed to ps laser ablation than that of the area which underwent processing with fs laser pulses.
- Due to the ablation mechanism that is in place when applying ultra-short pulses, significant improvements of surface roughness can be achieved by applying ps and fs pulse lasers. In this research, a marginally better surface quality was achieved when performing laser milling with a ps laser source. This could be explained by nonlinear effects that are typical for processing materials at fs regimes, and also by the specific machining response of the tooling steel to the selected processing parameters, in particular the lasers' wavelength.

These generic conclusions again underline the existing tradeoffs between the resulting surface integrity and removal rates. Therefore, it is necessary to look for the best compromise when selecting the optimum laser source for each specific application. Taking into account the specific requirements of micro tooling applications, in particular the best possible surface quality, and relatively small volumes of material that have to be removed, ultra-short pulsed laser ablation regimes present a viable solution. Furthermore, this research suggests that ps pulse lasers offer some advantages over fs laser sources when they are utilised for machining micro cavities in tooling steel. Taking into account that the fluence of the ps laser source is four times higher than that of the fs laser, it can be expected that through further process optimisation an even better surface quality could be achieved.

Chapter 4 Strategies for material removal

The laser milling of diverse engineering materials has been demonstrated with long and short pulse lasers ranging from microsecond to femtosecond pulse durations, and with wavelengths from the far infrared to vacuum ultra-violet. In all cases a balance between quality, throughput, cost of ownership and running cost must be found in order to determine commercial relevance. The latest generation of Q-switched Diode Pumped Solid State Lasers offers the potential for the industrial uptake of laser milling for a wide variety of materials including aerospace alloys, tool steels, ceramics, diamond and fused silica. Laser milling is a complex process (see process chain in Figure 4.1) which involves 3D CAD data preparation, toolpath generation which incorporates material removal strategies and ablation process optimization followed by post processing/cleaning.

Combining the accuracy and mature development of existing CNC technology with the latest developments in laser sources, laser milling is becoming a viable alternative for micro manufacturing. Utilizing a laser beam as a removal tool solves some of the fundamental problems associated with the micro milling – tool wear and tool breakage. Material hardness is no longer a problem – the removal mechanism is not influenced by the hardness as much as with the milling process.

After completion of the process, further steps are required in order to clean oxides deposited on or around the machined surface. In most cases mechanical cleaning is not possible, so alternative solutions need to be implemented.

Selecting the most suitable strategy for processing will, in most cases, leave less post processing required due to an optimal use of the energy supplied in the working zone. This

improves the process efficiency and reduces the time for completion, hence it reduces the cost of the components.

4.1 Factors influencing laser milling process

Laser milling is a complex manufacturing chain influenced by a number of factors. Laser source characteristics govern the ablation process but the laser-material interaction is triggered and controlled by the machine controller. CAD data is the initial source of information but the actual CNC program is created with certain tolerances. Furthermore the strategy embedded into the CNC program influences the material removal process.

4.1.1 CAD model

As the first component in the accuracy chain for laser milling, the CAD model is a key factor for achieving good results. The accuracy of the whole system is usually associated with the least accurate chain. There are two approaches when handling CAD data:

- Already available software for slicing models. As in rapid prototyping, for

3D structures - .STL files are utilised. They offer a few advantages like watertight surface representation and neutral platform, but this comes with the inconvenience of handling a huge amount of data and an inability to work with native file formats. The .STL files consist of sets of triangles representing the surfaces of the model with a given tolerances. Hence triangulation should provide sufficient quality of the surfaces represented in .STL format. On the other hand too many details could lead to a very large file and makes toolpath generation time consuming without any real benefits. Figure 4.2(a) shows a model with excessively loose tolerances, whereas in Figure 4.2(b) there are too many details which make the model

difficult to handle. Figure 4.2(c) represents an acceptable level of tolerances for surface representation. Applying excessively loose tolerances could lead to data loss and cause some features to disappear completely. Ideally tolerances should be set one order higher than the expected final tolerances, but this is not always possible.

- Custom made software for 3D CAD data handling. The main advantage in this approach is the flexibility to handle all supported exchange data formats like .IGS , .STP, parasolid, etc and working with the native format for the system. In this case there is no need to transfer the data in the .STL file format. Calculations are faster and accuracy is better.

4.1.2 Toolpath

Toolpath is the information, supplied to the machine in order to govern the material removal process. Generally toolpath consists of a few components: Process data, laser spot positions (tracks) and some additional information.

.

4.1.2.1 Process data/initial set up

During the toolpath generation, process data is entered in a similar fashion as in the classical milling process, but controlled process parameters are different. Usually laser power, firing distance, Rapid and feed moves, and co-ordinate positions are specified. Information is given for the stage positions, if synchronisation is available then data is supplied on how to synchronise the stages and firing mechanism.

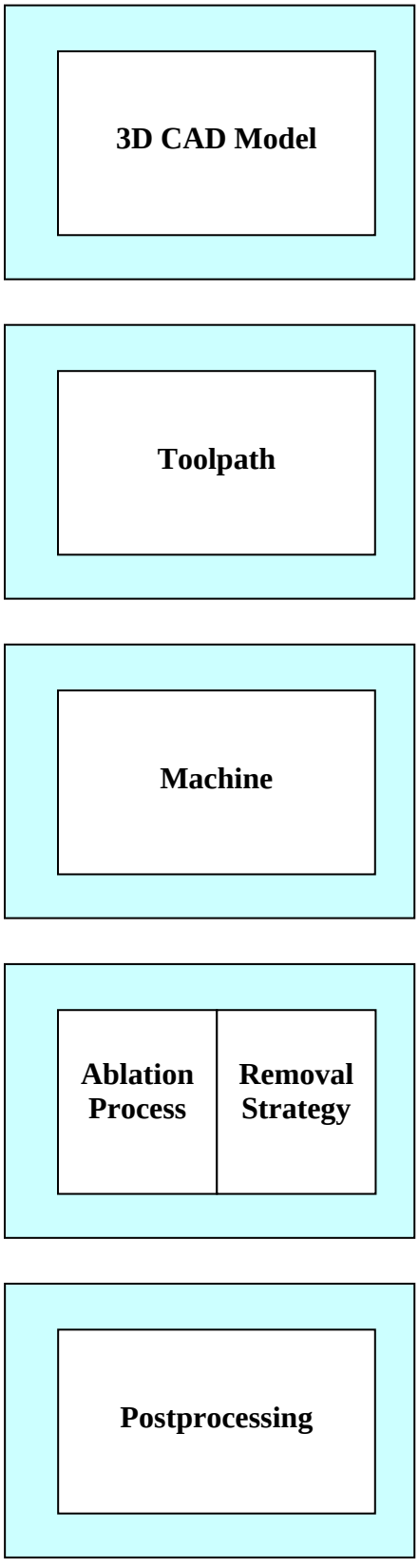

Figure 4.1 Manufacturing process chain

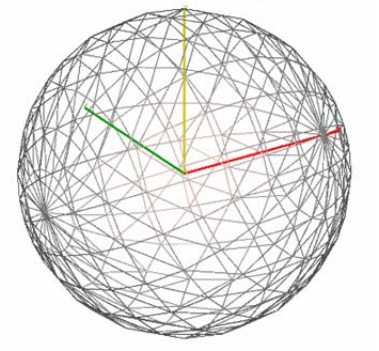

(a) Too loose tolerance

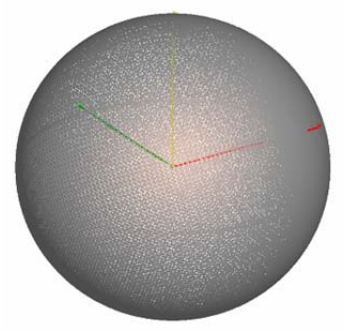

(b) Too many details.

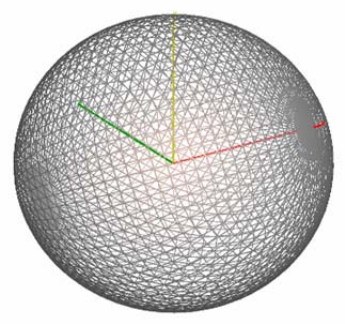

(c) Correct tolerance.

Figure 4.2 Triangulation of the model surfaces

(a) Too loose a tolerance

(b) Too many details.

(c) Correct tolerance.

That is not always the case, as it depends on the machine controller. All data could be transferred trough the toolpath file, or additional data can be requested throughout the milling process. All this depends on the type of NC controller utilised.

4.1.2.2 Laser spot positions/movements

Positions are achieved through movement of the galvo mirrors or stages. Depending on the system configuration, there could be 2, 3 or more axes, allowing either translations or rotations. Speeds are defined and transferred through the toolpath file.

In other words, the toolpath is the link between the 3D CAD data and the actual machine.
Laser milling is not so common a process yet, although there is already a need for such technology. If compared to traditional milling- where development of CAM software started more than 30 years ago - laser milling is still in its infancy.

A few research groups are working in this area as well as commercial ventures (Lasertech, 1999), but because the focus is on their existing systems and they are not really widely applicable.

In order to benefit from the latest development in this area and to be able to control the process better, the author has developed a special system for toolpath generation. The system is based on a commercially available PowerMill CAM system from DELCAM. For traditional milling this solution is very powerful and delivers excellent results. Unfortunately, being a

milling software, the package does not take into account the specifics of the laser milling process.

As a solution, a customization (add on features) has been developed to reflect the needs of the laser milling process. Through the macro interface of the software, a special macro command file is generated and when executed, result in a toolpath specially generated for optimum results during the laser milling process. The interface is really simple. Please see Figure 4.3 . Some of the data needs to be predetermined – laser spot, steps between the tracks and step-down, speeds of the moves, etc. These are usually optimised for the performance required – removal rate, resulting roughness, heat affected zones.

There are some advantages and some disadvantages to this method, which will be discussed below:

- **Advantages**

— CAD data independent – through an exchange interface a wide variety of CAD data files can be imported into the system

— Machine independent - post processors are flexible and support most known NC controller types. Custom command definitions are also possible

— Flexible removal strategy selection – there are more removal strategies available than in standard milling software

— Easy integration of new strategies, additional features

- **Disadvantages**

— Slow calculation sometimes

— Difficult visualisation

— Here is a typical sequence:

  - Process parameters discovery – based on previous experience, requirements for the resulting surface quality –surface roughness, heat affected zone and material removal rate optimum laser parameters-machine parameters are established.
  - Toolpath generation – already set in the previous step parameters are entered into the software and appropriate strategy is selected in order to create the required geometry.

— Post processing/Cleaning – very important step. Especially for the features in micrometers range – mechanical finishing is not possible, chemical is to some extent, depending on the material. Laser cleaning is also possible, but with improvement not better than 30 % in terms of resulting roughness.

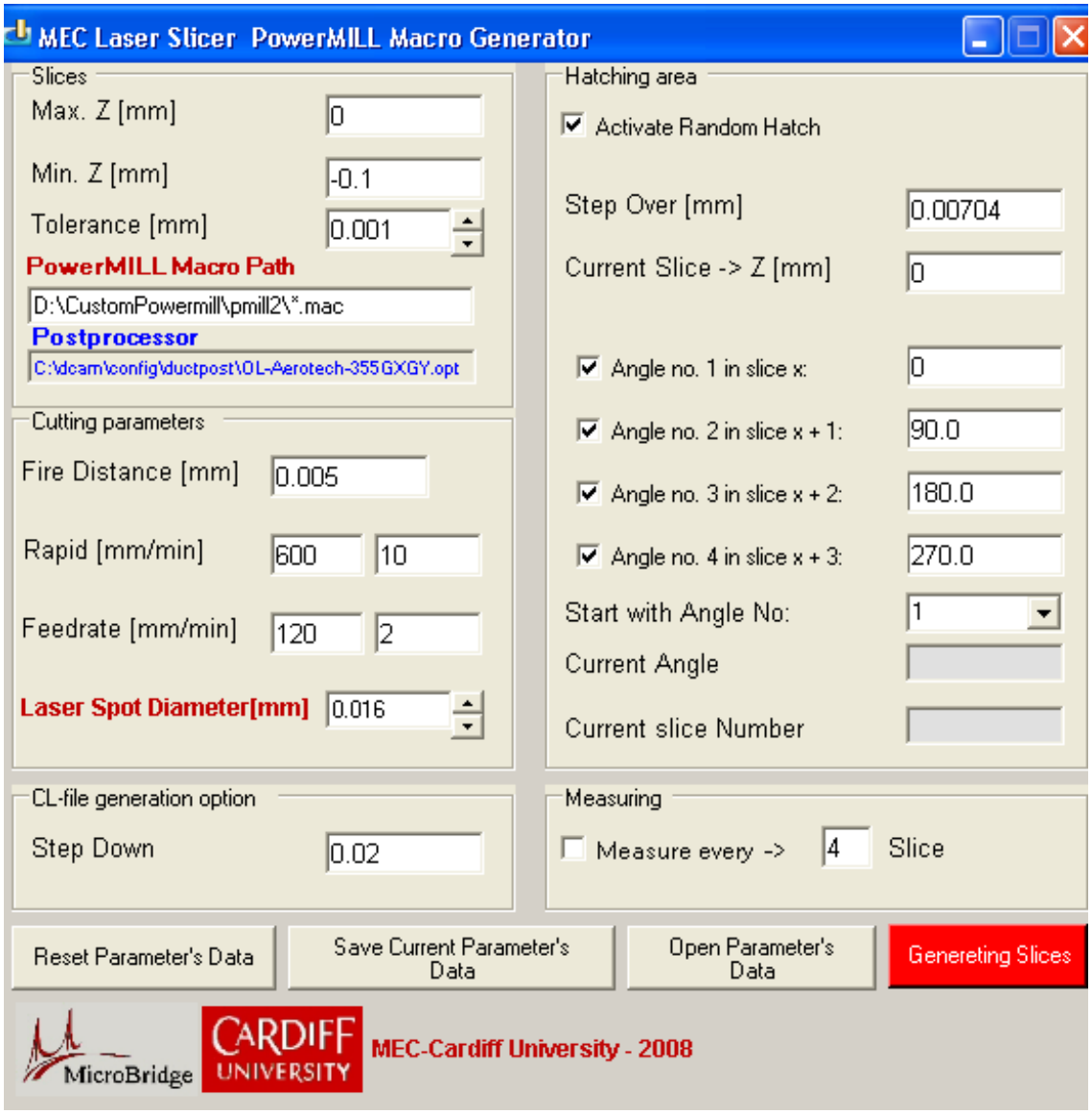

Figure 4.3 Entry form for the slicer

Example of macro program is given in the Appendix A and resulting NC program is given below:

```
%
O0001
; PROGRAM NAME  : 2
; PART NAME     : 2
; PROGRAM DATE  : 12.08.08 - 11:19:05
; PROGRAMMED BY : SCEPVP
; POWERMILL CB  : 1098016
; DP VERSION    : 1490
; OPTION FILE   : PVP_GXGY_NEW
; OUTPUT WORKPLANE : WORLD
;
; ESTIMATED CUTTING TIME :  1 TOOLPATHS = 00:13:29
;
#define FireDistance $global1
FireDistance = 00.00100
MSGCLEAR -1
BEAMOFF
:UseCurrentFireDistance
MSGDISPLAY 1, " 2: Program Started"
MSGDISPLAY 1, "{#F3 #F}" "Time is #TM"
MSGDISPLAY 1, "Using Fire Distance ", FireDistance
G71
```

```
G76
G90
DRIVECMD GX 67 3 1 0 0 0 0 0
DRIVECMD GY 67 3 1 0 0 0 0 0
A0 B0
; =========
; TOOLPATH  : 2
; =========
G1 G98 E83 F83
GX11.75 GY-8.5
Z0.002
GX19.475 GY-5.239
GXGYTRACKON l(FireDistance)
GX19.431 GY-5.173 E45 F45
BEAMOFF
......
......
GX6.429 GY-5.674
GX6.449 GY-5.707
GX6.454 GY-5.716
BEAMOFF
MSGDISPLAY 1, "{#F3 #F}" "Time is #TM"
MSGDISPLAY 1, "Program Finished"
M2
```

In this case NC code was generated for the Aerotech 3200 controller (Aerotech, 2005), utilising control of the beam through the galvo mirrors (GX GY Commands) but can be easily be post processed for any other controller.

4.1.3 Machine

A laser machine is a complete solution, incorporating different components – laser source, stages, bodywork, conditioning system, control system , protection etc. The machine acceptability will depend on the choice of each component and the most influential will be discussed below.

4.1.3.1 Laser source and optics

The laser source is the heart of the milling machine. There are many types of laser sources, based on medium (solid state, gas), wavelength (Deep UV, UV, Visible, IR), repetition frequencies (from a few Hz to a MHz), pulse energy, average power (from mW to KW), operational mode (continuous or pulsed), pulse duration (microsecond to femtosecond).

For material processing two main characteristics of the laser sources are considered – length of the pulse and working wavelength. Output power is a consideration as well, but is mostly associated with productivity, whereas the other two criteria have a more direct influence on the outcome of the laser-material interaction.

There are a few types of optical delivery system adopted in current laser systems. Figure 4.4 illustrates beam delivery by galvo scanner and normal optics, where Figure 4.5 illustrates

beam delivery by galvo scanner and a telecentric lens. The main difference between these two types of optics is the shape of the optical working envelope. The simplest optical delivery system utilises a focusing lense without position control (galvo mirrors). In this case movement is delivered by the stage, but the speed and velocity are much lower than those delivered by the galvo scanners.

4.1.3.2 CNC control and stages

CNC – control unit that manages machine axis motion.

NC machines were first developed soon after World War II and made it possible for large quantities of the desired components to be very precisely and efficiently produced (machined) in a reliable repetitive manner. Numerical Control (NC) was the forerunner of today's Computer Numerical Control (CNC), which controls the automation of machine tools and the inherent tool processes for which they are designed.

The CNC controller incorporates complete motion capabilities and includes point-to-point, linear, circular, helical, and spherical interpolation; velocity profiling; electronic gearing; on-the-fly trajectory modification; high speed I/O; camming 1 to 32 axes of scalable, synchronized motion. It uses commercially available IEEE-1394's (FireWire™) determinism for communications between drives and controller. It is programmable in native RS-274 G-code, AeroBASIC™ command set, C, C++, .NET, VisualBASIC®, or LabVIEW® for flexibility 20 kHz servo update rate for 1 to 32 axes provides consistent performance regardless of axis count. It incorporates digital current loops for improved control and stability. It also features integrated high-speed Position Synchronized Output (PSO) for laser firing or position latching.

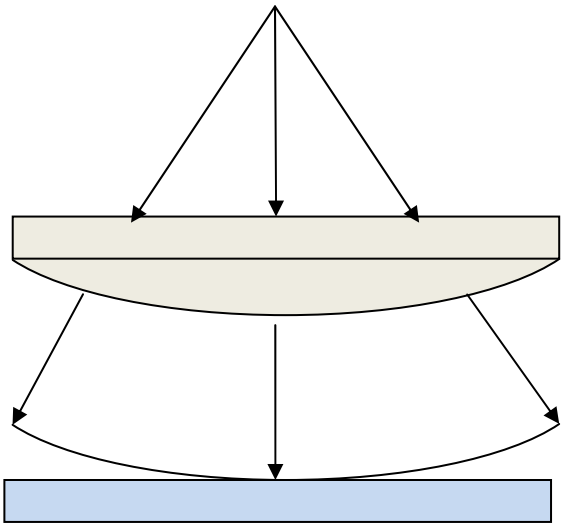

Figure 4.4 Galvo scanner and normal optic

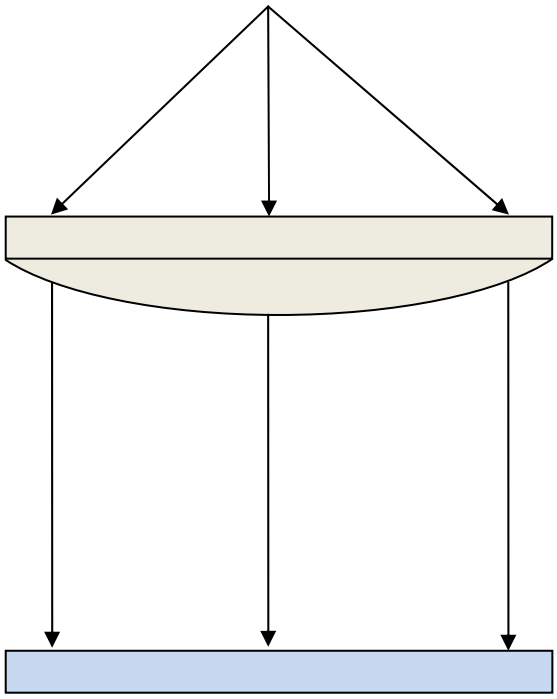

Figure 4.5 Galvo scanner and telecentric lens

The integration of multiple common automation tools into a single platform provides users the ability to integrate, develop, and maintain the system faster, with lower costs than ever before. For instance, coupling the vision module with the motion system that coordinates a cutting process (laser, drill, mill, etc.) provides the ability to identify the workpiece and its position, and to adjust the position and signal to the cutter all within one system. This integration dramatically reduces wiring and the necessary components, which not only lowers the integration and setup cost but also increases reliability. No Degradation of Performance as Axis Count Increases is evident.

The NC controllers utilize a distributed control architecture that enables it to maintain performance independent of the number of axes being controlled. It accomplishes this by avoiding the processing bottleneck caused by today's common single processor control architecture. Position, velocity, and current loop closure are handled by the NC's Intelligent Network Drive. Trajectory generation is done on the PC using a real-time operating system that runs with higher priority than Windows®. The PC executes programs and sends the position commands to the Ndrive via the IEEE-1394 (FireWire®) high-speed serial bus.

Typical characteristics of CNC stages are given in the Table 4.1 below:

Table 4.1 Typical characteristics of the stages

Axis	Travel (mm) Max	Velocity (mm/s)	Linear Accuracy per axis(μm)	Resolution (μm)	Repeatability (μm)
X	600	200	+/-1	0.05	+/- 0.5
Y	300	200	+/-1	0.05	+/- 0.5
Z	100	50	+/-1	0.1	+/- 0.5

4.1.4 Ablation process

Laser milling means material removal is accomplished by the laser-material interaction in succession. Laser material interaction is localized, non–contact machining and is almost reaction–force free. Photon energy is absorbed by the target material in the form of thermal or photochemical energy. In case of pico- and femtosecond laser pulses, material is removed by direct vaporization/sublimation.

In general, optimal laser micromachining is achieved when photons are strongly absorbed by the substrate. Furthermore, if these photons are delivered in a short duration pulse, a miniexplosion is created ejecting solid and gaseous particulates from the irradiated target without significant thermal damage (melting, spatter, recrystalization, etc.) occurring in the surrounding area.

4.1.4.1 Laser pulse energy

The pulse energy Ep is simply the total optical energy content of a pulse. For single pulses, e.g. from a Q-switched laser, the pulse energy may be measured e.g. with a pyroelectric device.

For regular pulse trains, the pulse energy is often calculated by dividing the average power (measured e.g. with a powermeter) by the pulse repetition rate. However, this is a valid procedure only if the energy emitted between the pulses is negligible. There are cases where, e.g., a mode-locked laser emits a pulse train together with a low-level background emission. Even if the background power level is far below the peak power, the background can significantly contribute to the average power. If, e.g., a photo detector has an insufficient

dynamic range for testing this, it can be useful to test the conversion efficiency of a frequency doubler in a carefully controlled situation in the low-conversion regime.

The pulse energy together with the pulse duration is often used to estimate the peak power of pulses. Conversely, temporal integration of the optical power results in the pulse energy.

Typical pulse energies from Q-switched lasers range from microjoules to millijoules, and for large systems to multiple joules or even kilojoules. Mode-locked lasers achieve much lower pulse energies (picojoules, nanojoules or at most a few microjoules) due to their high pulse repetition rates and sometimes due to limiting nonlinear effects in the laser resonator. Much higher energies of ultrashort pulses can be achieved by amplifying pulses at a lower repetition rate, as obtained e.g. with a pulse picker or a regenerative amplifier.

It is very easy to obtain the average laser power P, which enables the calculation of the laser pulse energy by:

$$E_p = \frac{P}{V}$$

Where V is the laser pulse repetition rate.

4.1.4.2 Peak power

The peak power of an optical pulse is the maximum occurring optical power. Due to the short pulse durations which are possible with optical pulses, peak powers can become very high

even for moderately energetic pulses. For example, a pulse energy of 1 mJ in a 10-fs pulse, as can be generated with a mode-locked laser and a regenerative amplifier of moderate size, already leads to a peak power of the order of 100 GW, which is approximately the combined power of a hundred large nuclear power stations. Focusing such a pulse to a spot with e.g. 4 μm radius leads to enormous peak intensities of the order of 4×10^{21} W/m^2 = 4×10^{17} W/cm^2. Peak powers in the terawatt range can be generated with devices of still moderate size (fitting into a 20-m^2 room). Large facilities based on multi-stage chirped-pulse amplifiers can even generate pulses with petawatt peak powers.

For handling the large numbers associated with high peak powers, the following prefixes are often used:

1 kW (kilowatt) = 10^3 W

1 MW (megawatt) = 10^6 W

1 GW (gigawatt) = 10^9 W

1 TW (terawatt) = 10^{12} W

1 PW (petawatt) = 10^{15} W

Measurement of Peak Power:

For relatively long pulses, the peak power can be measured directly e.g. with a photodiode which monitors the optical power versus time. For pulse durations below a few tens of picoseconds, this method is no longer viable. The peak power is then often calculated from the (full width at half-maximum, FWHM) pulse duration (measured e.g. with an optical

autocorrelator) and the pulse energy. The conversion depends on the temporal shape of the pulse. For example, for a Gaussian beam the peak power is:

$$P_p \approx \frac{0.94E_p}{\tau}$$

If pulses are subject to strong nonlinear pulse distortions or similar effects, a significant part of their pulse energy may be contained in their temporal wings, and the relation between peak power and pulse energy may be substantially modified.

4.1.4.3 Laser spot

The removal mechanism in laser milling is based on a single shot being repeated in succession. Therefore the size of the laser spot becomes a very important parameter . There are many factors affecting the laser spot – Laser source characteristics, optical components, etc.

Basically, the laser spot is given by the following equation (Madou, 2001):

$$2w_o = \frac{4M^2\lambda f}{\pi D}$$

Where: λ is the wavelength of the laser source,

f is the focal length of the lens,

D is the input beam diameter,

M^2 is the beam quality factor

The M^2 factor, also called beam quality factor or beam propagation factor, is a common measure of the beam quality of a laser beam. According to ISO Standard 11146 (International Organisation for Standards, 2011), it is defined as the beam parameter product divided by λ / π, the latter being the beam parameter product for a diffraction-limited Gaussian beam with the same wavelength. In other words, the beam divergence is

$$\theta = \frac{M^2 \lambda}{\pi w_o}$$

where w_0 is the beam radius at the beam waist and λ the wavelength. A laser beam is often said to be "M^2 times diffraction-limited". A diffraction-limited beam has an M^2 factor of 1, and is a Gaussian beam. Smaller values of M^2 are physically not possible. A Hermite–Gaussian beam, related to a TEM_{nm} resonator mode, has an M^2 factor of $(2n + 1)$ in the x direction, and $(2m + 1)$ in the y direction.

The M^2 factor of a laser beam limits the degree to which the beam can be focused for a given beam divergence angle, which is often limited by the numerical aperture of the focusing lens. Together with the optical power, the beam quality factor determines the brightness (more precisely, the radiance) of a laser beam.

For non circularly symmetric beams, the M^2 factor can be different for two directions orthogonal to the beam axis and to each other. This is particularly the case for the output of diode bars, where the M^2 factor is fairly low for the fast axis and much higher for the slow axis.

According to ISO Standard 11146 (International Organisation for Standards , 2011), the M^2 factor can be calculated from the measured evolution of the beam radius along the propagation direction (i.e. from the so-called caustic). A number of rules have to be observed, e.g. concerning the exact definition of the beam radius and details of the fitting procedure. Alternative methods are based on wavefront sensors, e.g. Shack–Hartmann sensors, which require the characterization of the beam only in a single plane.

Note that the M^2 factor, being a single number, cannot be considered as a complete characterization of beam quality. The actual quality of a beam for a certain application can depend on details which are not captured with such a single number.

The concept of the M^2 factor not only allows one to quantify the beam quality with a single number, but also to predict the evolution of the beam radius with a technically very simple extension of the Gaussian beam analysis: one simply has to replace the wavelength with M^2 times the wavelength in all equations. This is very convenient for, e.g., designing the pump optics of diode-pumped lasers. Note, however, that this method works only when a certain definition of beam radius is used which is also suitable for non-Gaussian beam shapes; see again ISO Standard 11146 (International Organisation for Standards ,2011) for details.

4.1.5 Removal strategy

Material removal strategy selection is based on the results of the ablation process. While ablation parameters affect the laser-material interaction on the low level, the macro strategy implemented governs the whole process. Very much simplified it would be split as follows:

- Ablation process deals with a single crater
- Macro strategy deals with 3D material removal (overlapping the craters in succession)

There are two main aspects of the material removal strategy – crater overlapping distance and toolpath trajectory.

4.1.5.1 Crater overlapping

As previously discussed, the laser milling process removes material in a layer-by-layer fashion. This is the main difference between laser milling and laser cutting. While in laser cutting, the main target is to cut through the material, in laser milling material removal is achieved layer by layer. A stable process – with equal removal depth for each slice and with adequate surface roughness - is absolutely necessary to perform a successful removal process. In other words – the process needs to be under control at each level.

While for the depth alone, the most influential parameter of the laser would be the power delivered, for the roughness the most influential parameter is the overlapping of the individual craters. Figure 4.6 shows the shape of a crater (single shot).

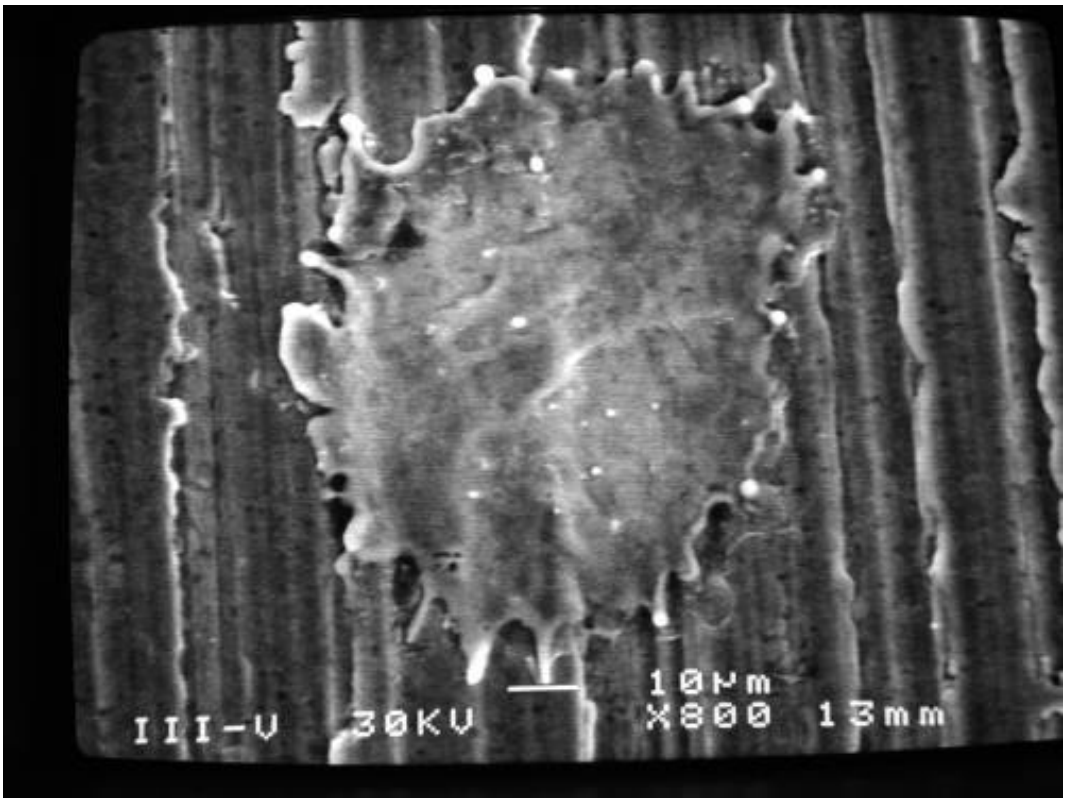

Figure 4.6 Single crater

4.1.5.2 Toolpath trajectory

There are six basic strategies for tool path generation for material removal:

- one way hatch as shown in Figure 4.7 (a)
- cross hatch as shown in Figure 4.7 (b)
- random angle hatch as shown in Figure 4.7 (c)
- hatch and border as shown in Figure 4.7 (d)
- profile offsets as shown in Figure 4.7 (e)
- special strategies Figure 4.7 (f)

The material removal strategy should be selected depending on the feature type and size. The geometry of the feature to a large extent determines the strategy required for adequate processing. Based on orientation, three main types of geometry could be considered:

- Flat (surface normal equal or very close to the vertical axis of the machine)
- Vertical (surface normal perpendicular to the vertical axis of the machine)

- Tilted (angle between surface normal and vertical axis of the machine bigger than 0^o and smaller than 90^o)

The ratio of depth to width should be considered, as in many cases, it has a direct influence on the removal process. Focusing the beam in a spot creates a cone and this cannot be ignored, as the side walls are created because of the interaction between beam cone and substrate.

- Flat Surfaces

For flat relatively big surfaces, the best results are achieved employing the strategy shown in Figure 4.7(c) – random angle hatch. This could be explained by the way material is removed. As the laser is in pulse modeevery pulse creates a crater. Hence the best results would be achieved by the strategy that ensures the best overlapping due to irregularity in the shape of a single crater.

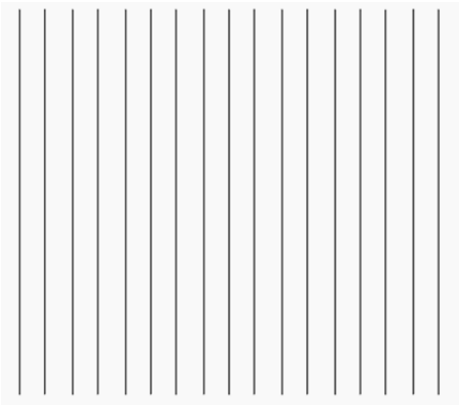

(a) One way hatch

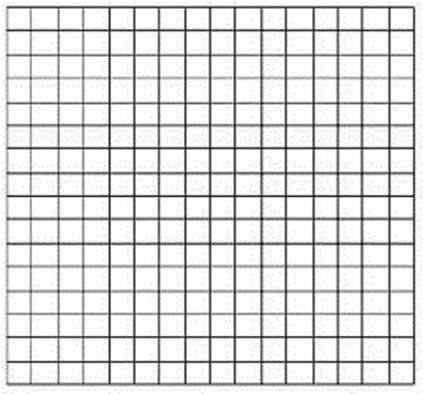

(b) Cross hatch

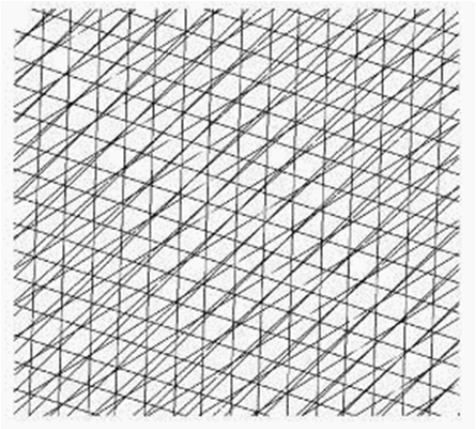

(a) Random angle hatch

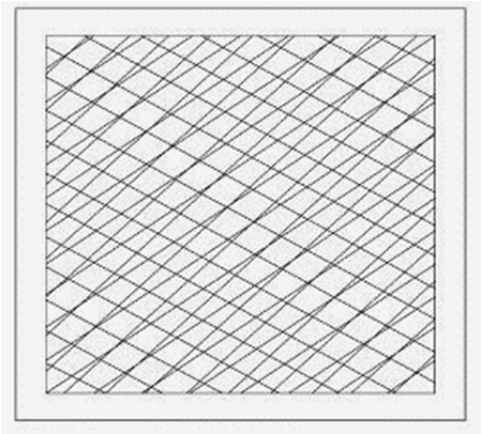

(d) Hatch and border

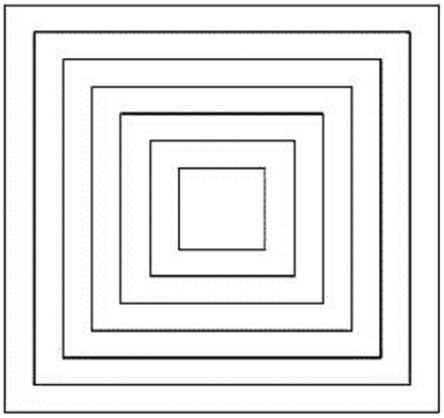

(e) Profile offsets

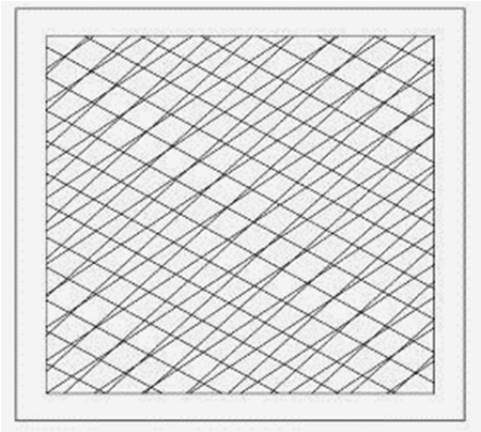

(f) Vertical walls

Figure 4.7 Six basic strategies for tool path generation

It is completely different when the feature is very small. In this case, because of the close proximity of the laser path there is not enough time for the heat to dissipate into the surrounding bulk of material. Heat is building up in the working area. This changes the initial state of the substrate and in this area, more material is going to be removed. Subsequently the heat released into the surrounding substrate is in larger quantities which leads to a bigger heat affected zone and more developed secondary effects such as cracks and redeposition .

This case is illustrated in Figure 4.8 Heater structure. The same structure is created using three different strategies, but keeping the same laser parameters.

(a)

(b)

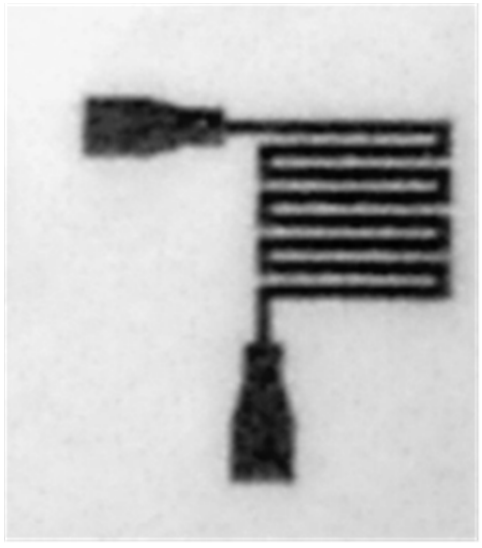

(c)

Figure 4.8 Heater structure

The structure shown in Figure 4.8(a) was created utilizing the strategy as shown in Figure 4.7(c), the structure shown in Figure 4.8(b) was created utilizing a strategy as the one in Figure 4.7(d) and the final Figure 4.8(c) utilizes a profile offsets strategy as shown in Figure 4.7(e).

The difference in the results is purely dependant on the strategy employed. In this case the last strategy gives more time between subsequent processing passes, so the heat dissipates better and presents the same processing conditions for each individual pass.

- Vertical surfaces

Vertical surfaces are usually considered the surfaces parallel to the vertical axis of the machine or the ones tilted at an angle close to 0 degrees. For laser material processing this angle is very important. The beam is conical, ending with the working focal spot. When material is removed a natural angle is created, dependant on the beam-material interaction – laser power, absorbance, focal distance. To a large extent this angle could be controlled by the laser power applied, but for the ultimate vertical wall machining, with 0 degree angle, an additional strategy needs to be adopted to overcome the problem created by the beam geometry.

A few solutions exist to tackle this problem:

— Utilising normal lenses. The beam is tilted by the galvo mirrors to approach the substrate at an angle and position is corrected by the stages. An additional lens is required to compensate for focus distortion.

— Utilising telecentric lenses. The beam is governed by the galvo mirrors, and directed straight down by the lens. In this case rotation and position

compensation are executed by the stages (rotation by gonio stages + translation by base XYZ stages).

Depending on the machine concept, one of these solutions could be implemented. Which one depends on the machine construction, NC control and intended application. In the first case the substrate is only translated, where in the second case rotation is required as well. In the first case the beam is deflected away from the ideal focal plane and so an additional lens for compensation is required, whereas in the second case the beam spot is in the ideal position.

4.1.5.3 Post processing

Initially all data is stored in a neutral format – CL (cutter location) data. Due to the differences in the NC controllers – additional processing of the data is required. Basically this is a translation to the command language of the NC controller. During the translation a lot of modifications can be done including manipulations of the integer formats, Axis sign conversions, etc.

Usually there is a basic format for almost all types of controller, but in order to customize it – the new features are described in a separate file. An example of such a file is given in Appendix B- Postprocessor. In the postprocessor some very important changes are required – due to the nature of the laser removal process – new ways of triggering the laser are employed, rather than just switch on and switch off. Advanced features such as PSO (pulse synchronization output) can be defined as well. Additionally limits for the

rotations/translations are specified – so if the input data does not comply – a warning will be issued.

4.2 Experimental set-ups

Material removal strategy is a key factor for an accurate and efficient process. As the removal mechanism is based on the single crater formation, the overlapping of the craters is studied in order to identify the most suitable overlapping in terms of resulting surface quality and removal rate.

4.2.1 Experimental set-up one

4.2.1.1 Experimental procedure

In order to investigate the influence crater overlap on removal depth and surface quality – an experiment was conducted. Typical laser parameters were selected – details given below:

Power 70% (9.55 W)

Pulse length 10μs

Repetition rate 30 kHz

Scanning speed 300 mm/s

The material selected for this experiment was stainless steel BS316.

In order to eliminate the influence of the scanning direction – 5 layers were ablated, rotating the angle in a random fashion.

The following cleaning procedure was followed:

- Gentle ultrasonic cleaning
- Chemical cleaning (Savan 200).
- Gentle ultrasonic cleaning.

All these steps were taken in order to clean the specimens, whilst preserving the topology for further measurements.

All measurements were taken using a white light profiling microscope. The size of the scanned areas was chosen according to ISO 4288:1996 and ISO 11562:1996 (http://www.predev.com/smg/standards.htm). The parameter used to evaluate the surface roughness was the arithmetic mean roughness (Ra) because relative heights in micro topographies are more representative, especially when measuring flat surfaces.

4.2.1.2 Results

The results are shown in Figure 4.9. Figure 4.10 shows depth as a result of the overlapping distance, where Figure 4.11 shows roughness as a result of the overlapping distance Figure 4.12 shows the overlapping of the spot area in percentage.

4.2.1.3 Discussion

The best results in terms of roughness were achieved with 10 micrometers overlapping, or ~72 % overlapping, of the craters. When establishing laser parameters this should be taken into account as sometimes results are close, but for the ultimate result –the optimal values have to be selected.

Overlapping distance µm	Roughness achieved Ra µm	Depth achieved µm	Overlapping %
0.5	3.5	52	97.5
1	3.1	51.26	97.2
5	3.29	20.88	85.9
10	1.62	12.16	71.9
15	1.94	7.42	58.4
20	1.7	5.21	45.3
25	1.84	4.98	33.1
30	1.8	3.14	21.9
35	2.42	3.57	12.1
40	2.6	2.59	4.4

Figure 4.9 Results of the (overlapping) experiment

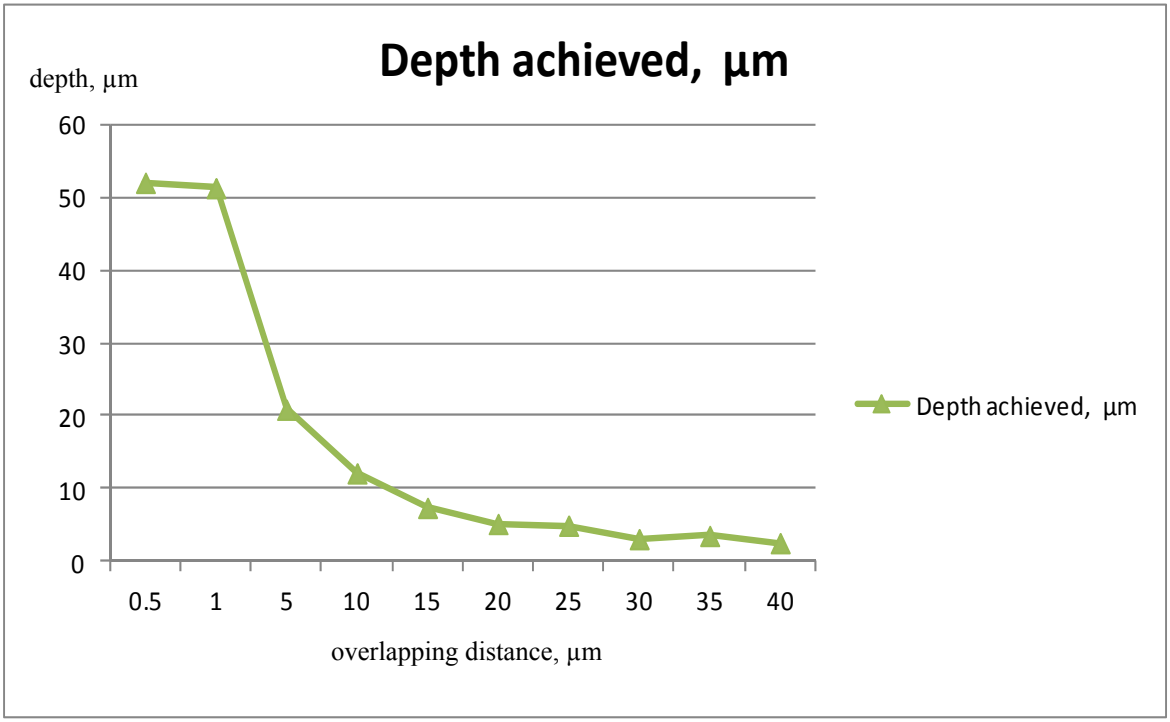

Figure 4.10 Depth as a result of the overlapping distance

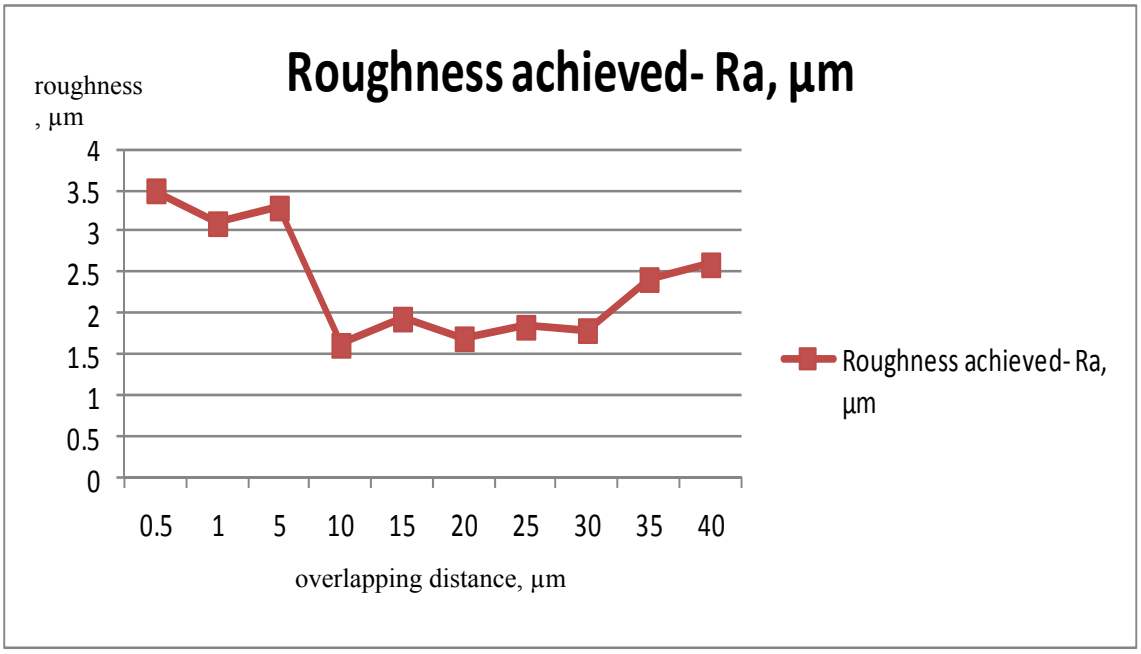

Figure 4.11 Roughness as a result of the overlapping distance

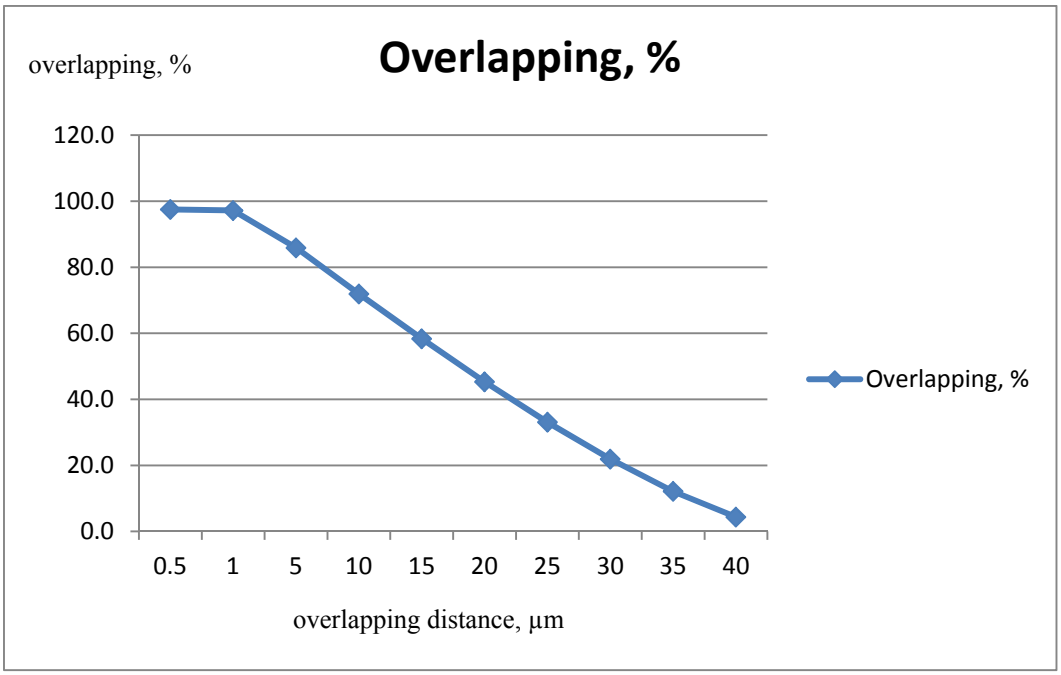

Figure 4.12 Overlapping, percentage

4.2.2 Experimental set- up two

4.2.2.1 Experimental procedure

A test structure as shown in Figure 4.13 was designed to investigate the influence of the material removal strategy on final part quality. The structure is comprised of 36 radially repeating 8.7 mm long segments, with a variable width between 40μm up to 800μm. The depth is kept constant at 150μm. Four different removal strategies as shown on Figure 4.7 were applied using the same processing parameters as given in Table 4.2. In particular, the strategies investigated in this research were:

(1)Random "hatching" inside together with a cut along the border as shown in Figure 4.7(c);

(2) Profile cuts only, Figure 4.7(e);

(3) Hatching only, Figure 4.7(c)

(4) The cuts have the same configuration as those for strategy (1), and the only difference is in the profile cut along the border where the beam is tilted in order to produce vertical walls, Figure 4.7 (f).

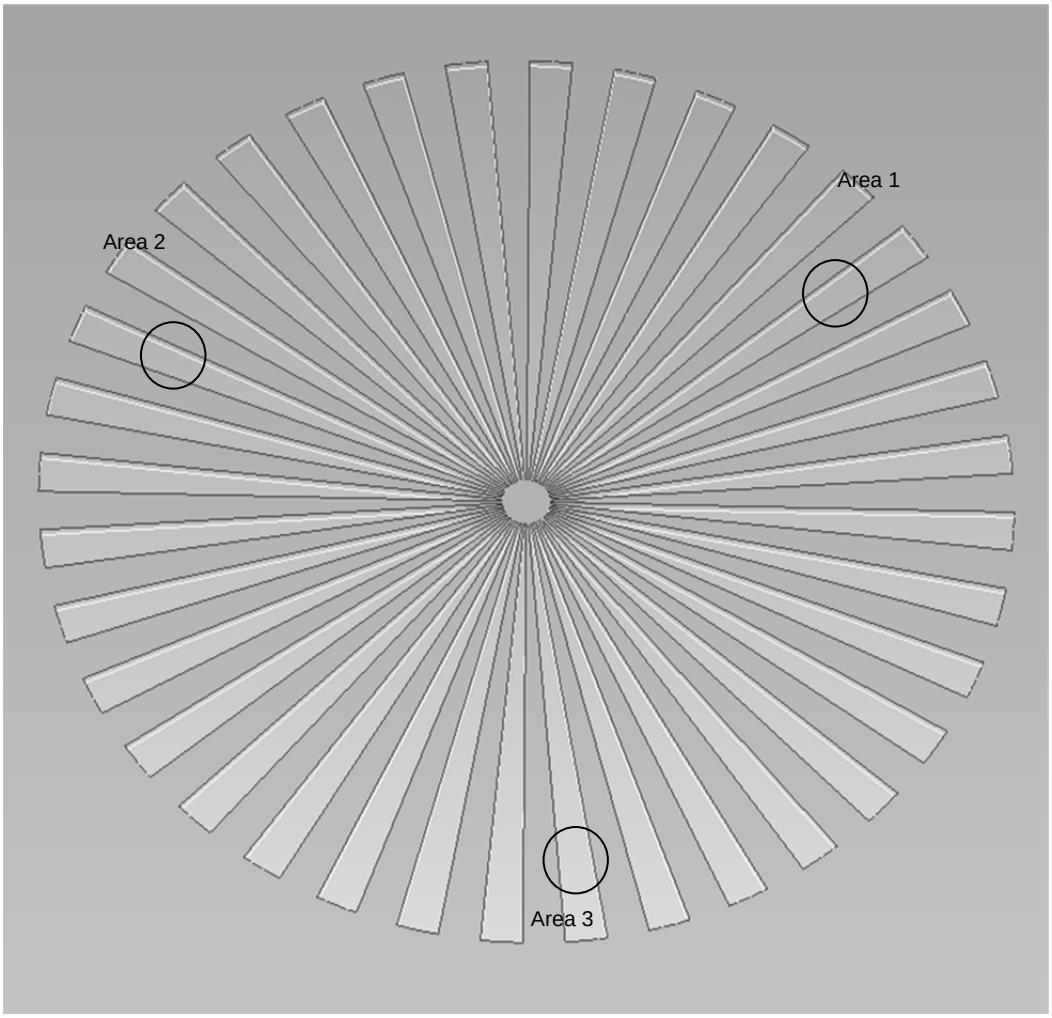

Figure 4.13 Test structure and measurement zones

Table 4.2 Laser parameters

	SS BS316	BrassBS2874 CZ121
Power	71.04%(9.5W)	56%(1.2W)
Frequency	40 kHz	15 kHz
Scanning speed	400 mm/s	150 mm/s
Wavelength	1064 nm	1064 nm
Pulse duration	10μs	10μs

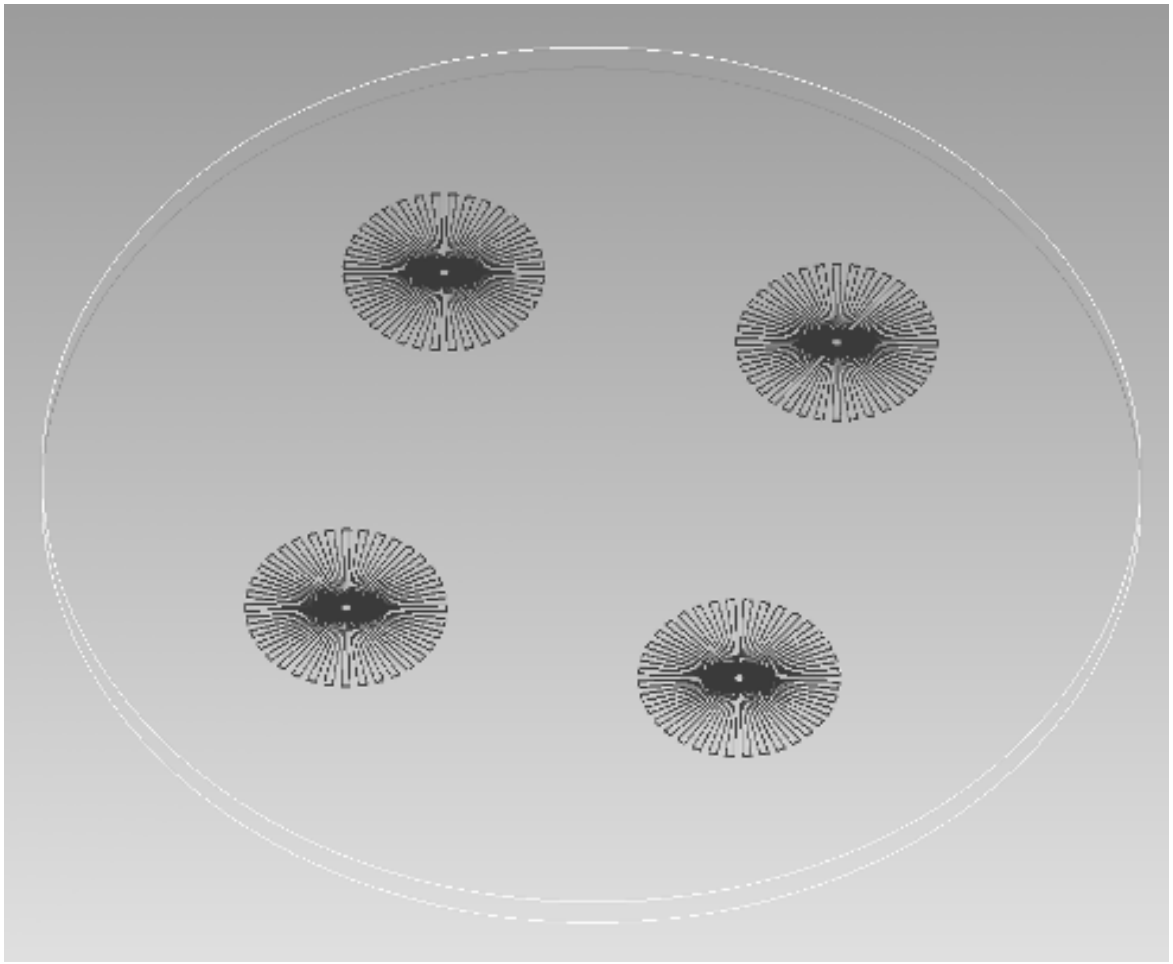

Figure 4.14 Test structures outline

Two test pieces were produced (stainless steel BS316 and brass BS2874 CZ121, later referred to as stainless steel or steel and brass respectively), each containing four structures (with relevant strategies) as shown on Figure 4.14. These two materials were selected because they have different ablation thresholds and thermal conductivity.

Based on previous investigations better results were expected for the stainless steel sample. The active control of the removal rate per layer available on the microsecond laser milling system used in this research was disabled in order to compare solely the effects of the four removal strategies.

After the milling operation, the samples were cleaned in an ultrasonic bath with a light degreaser to remove the debris from the ablation process without affecting the resulting surface roughness. Then, the roughness of different machined areas was measured by employing a white light interferometer, MicroXAM-100-HR(MicroXAM, 2003), and scanning a patch 250μmX330μm. The depth results were obtained on an optical system, MITUTOYO Quick Vision Accel(QuickVision, 2001), by performing 3 measurements in each area (all areas shown on Figure 4.13), and then the average was used in the experimental study.

4.2.2.2 Results

The roughness and the depth of the milled structures, four on the SS316 and brass substrates, were measured in three places as shown in Figure 4.13, and the results are provided in Table 4.3.

Table 4.3 Depth and Roughness results

	Zone	SS316		Brass	
		Ra, µm	Depth, µm	Ra, µm	Depth, µm
Strategy 1 Random hatch And border	1	1.84	202	3.5	164
	2	3.46	207	3.3	175
	3	3.32	209	3.5	167
Strategy 2 Profile cuts	1	13.37	204	3.5	201
	2	15.45	212	3.9	213
	3	12.47	209	na	210
Strategy 3 Hatching only	1	3.83	190	3.8	127
	2	3.04	207	3.9	139
	3	3.61	202	3.4	131
Strategy 4 Vertical walls	1	2.16	195	na	156
	2	2.63	206	6.36	164
	3	2.29	204	6.7	161

Additionally, scanning electron microscope (Carl Zeiss, 2005) images of the milled areas were taken in order to compare the resulting surface topography and border profiles after applying each of the four investigated machining strategies.

Figures 4.15-4.18 show SEM pictures taken from the steel sample near the centre, middle sector and at the end of the test segments. As can be seen from these figures the selected milling strategy has a significant effect on the resulting surface topography and border profile.

Since the CAD model and tolerances used to generate the laser path programmes and all laser parameters were exactly the same any differences in the machining results have to be attributed solely to the employed material removal strategies. The best average and most consistent surface roughness (see Table 4.3) and edge definition were achieved when the strategy vertical walls was applied, Figure 4.7(f). Only in Area 1 was the resulting roughness better on the sample machined with strategy random hatch and border (Figure 4.7(d)).

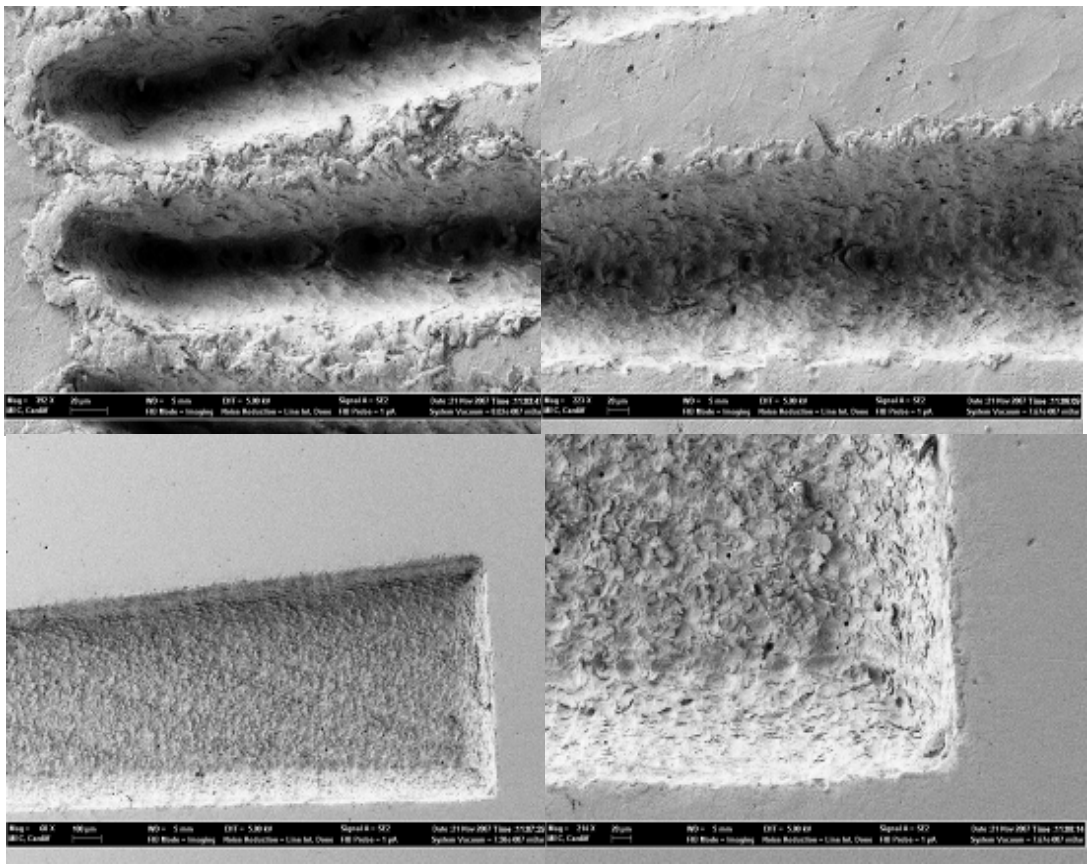

Figure 4.15 Resulting geometry in steel – strategy random hatch and border

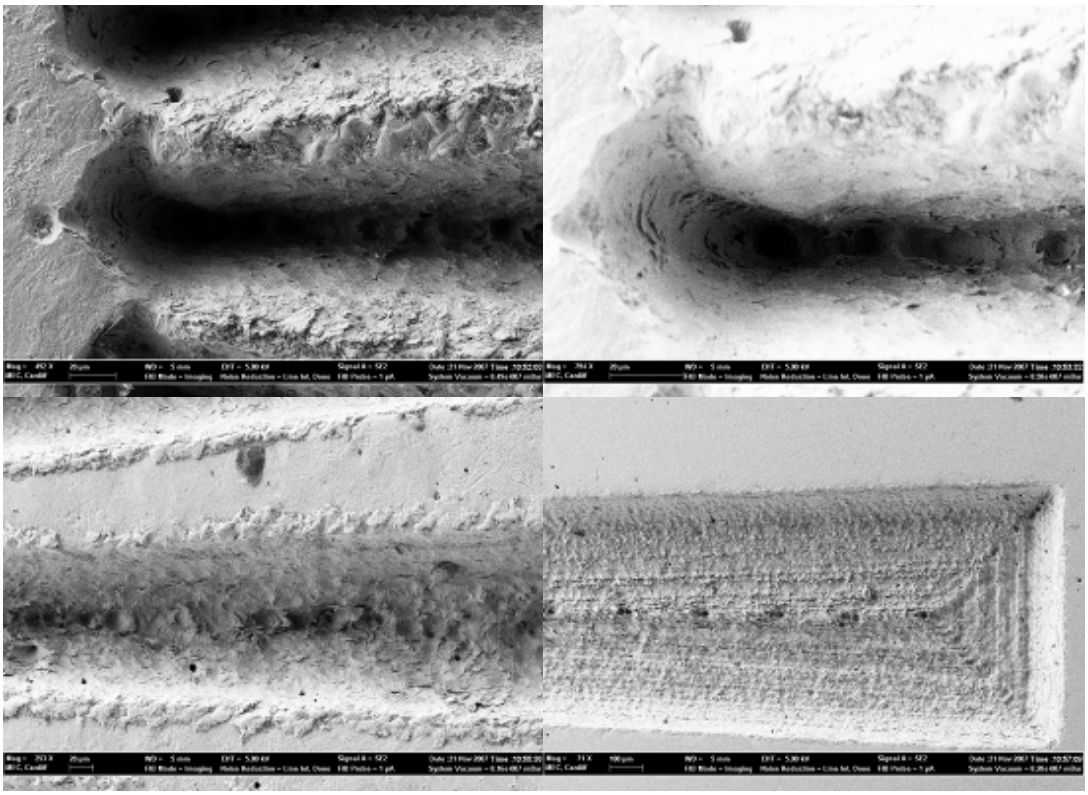

Figure 4.16 Resulting geometry in steel – strategy profile cuts

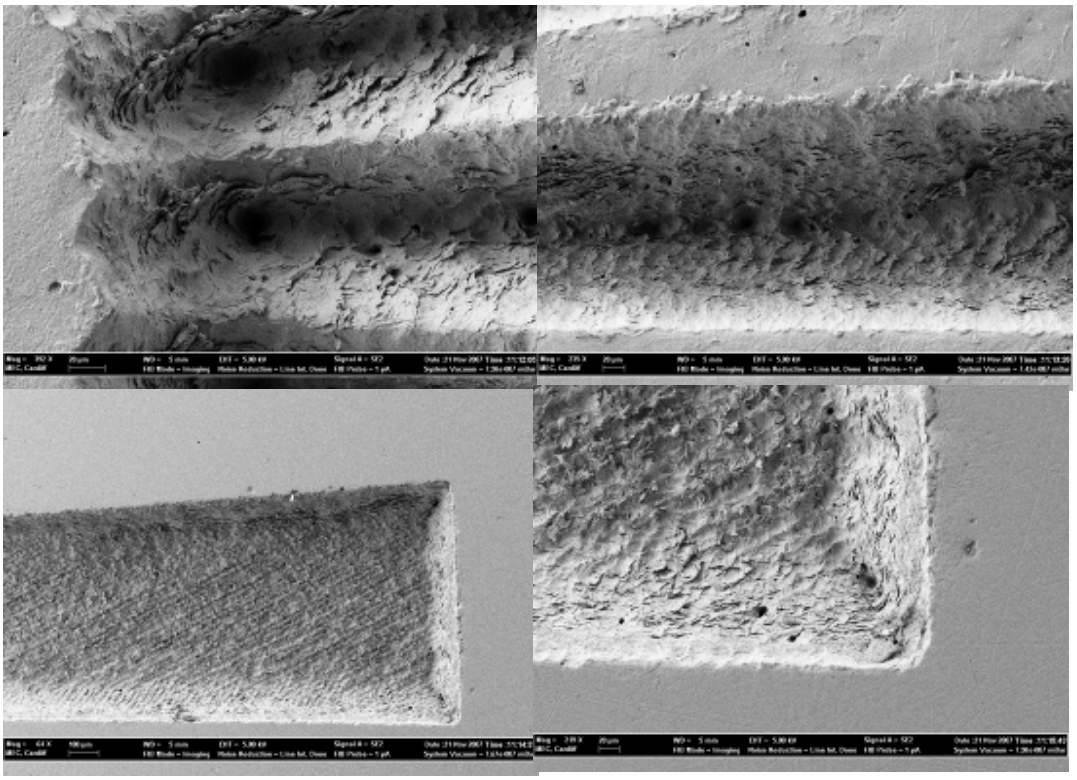

Figure 4.17 Resulting geometry in steel – strategy hatch cuts only

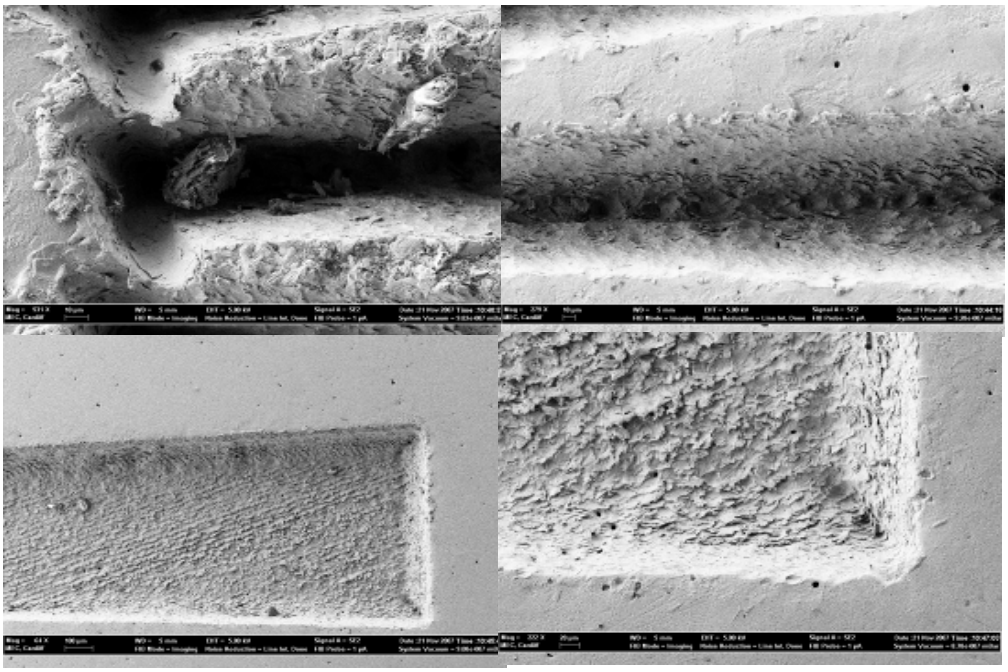

Figure 4.18 Resulting geometry in steel – strategy vertical walls

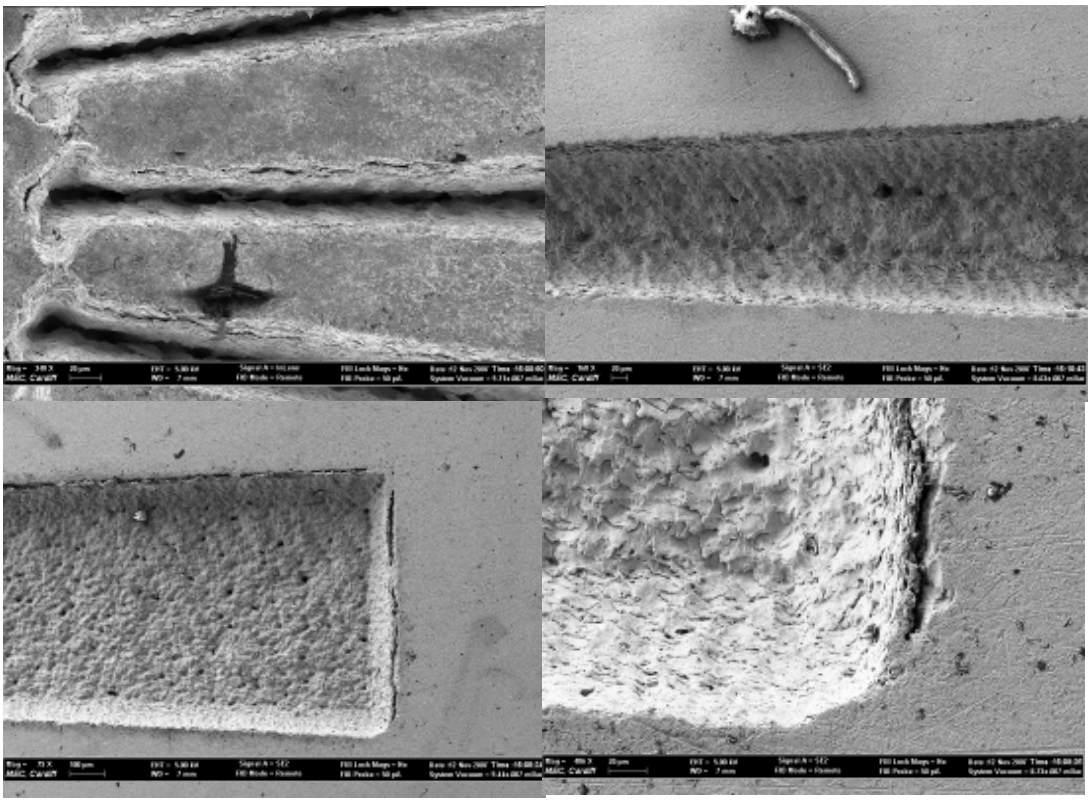

Figure 4.19 Resulting geometry in brass – strategy random hatch and border

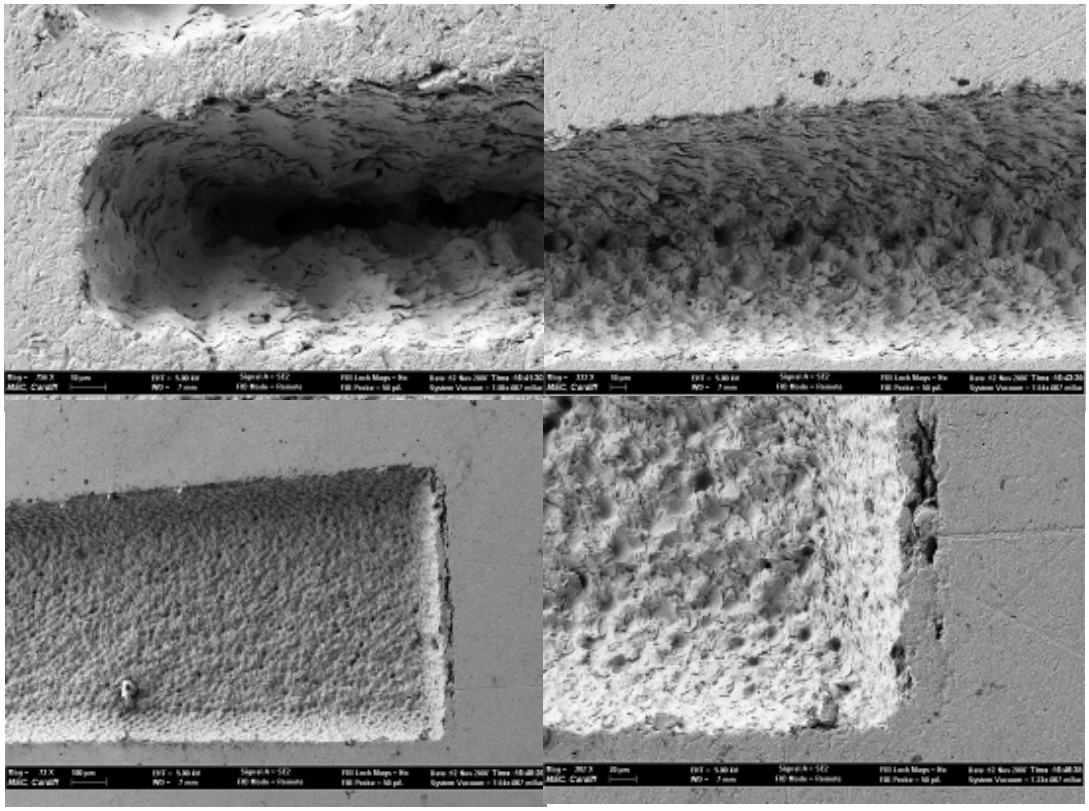

Figure 4.20 Resulting geometry in brass – strategy profile cuts

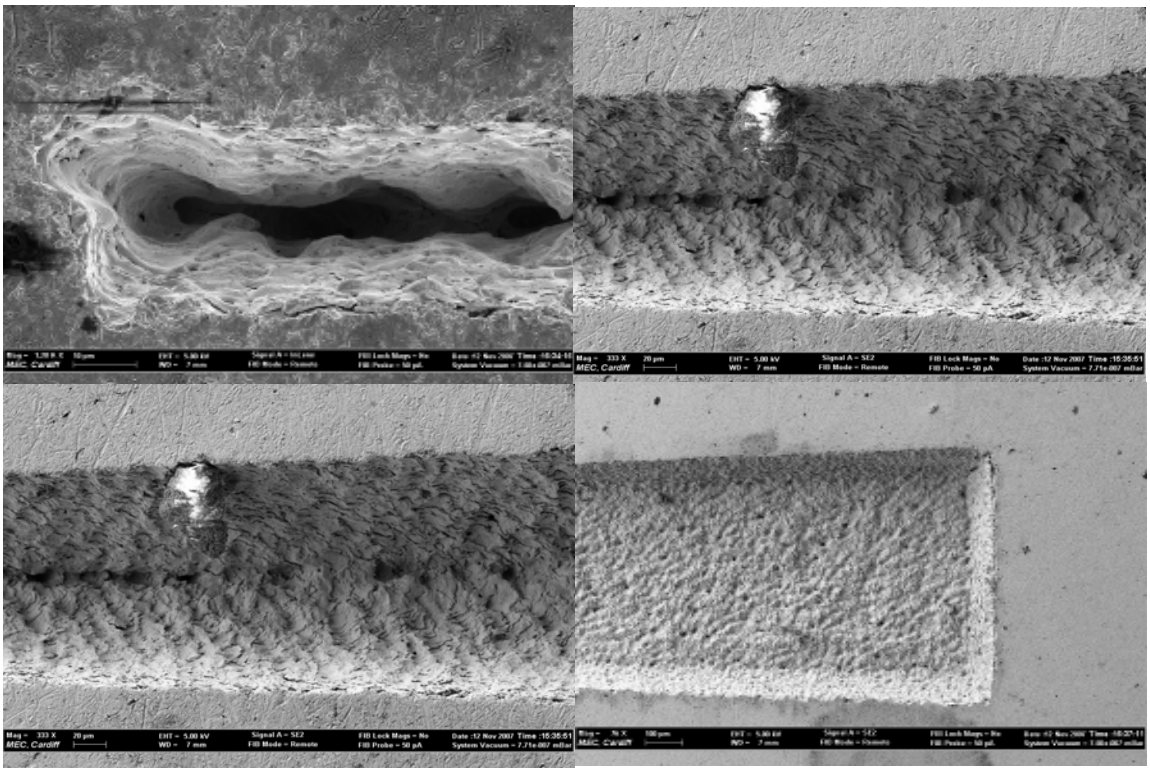

Figure 4.21 Resulting geometry in steel – strategy hatch cuts only

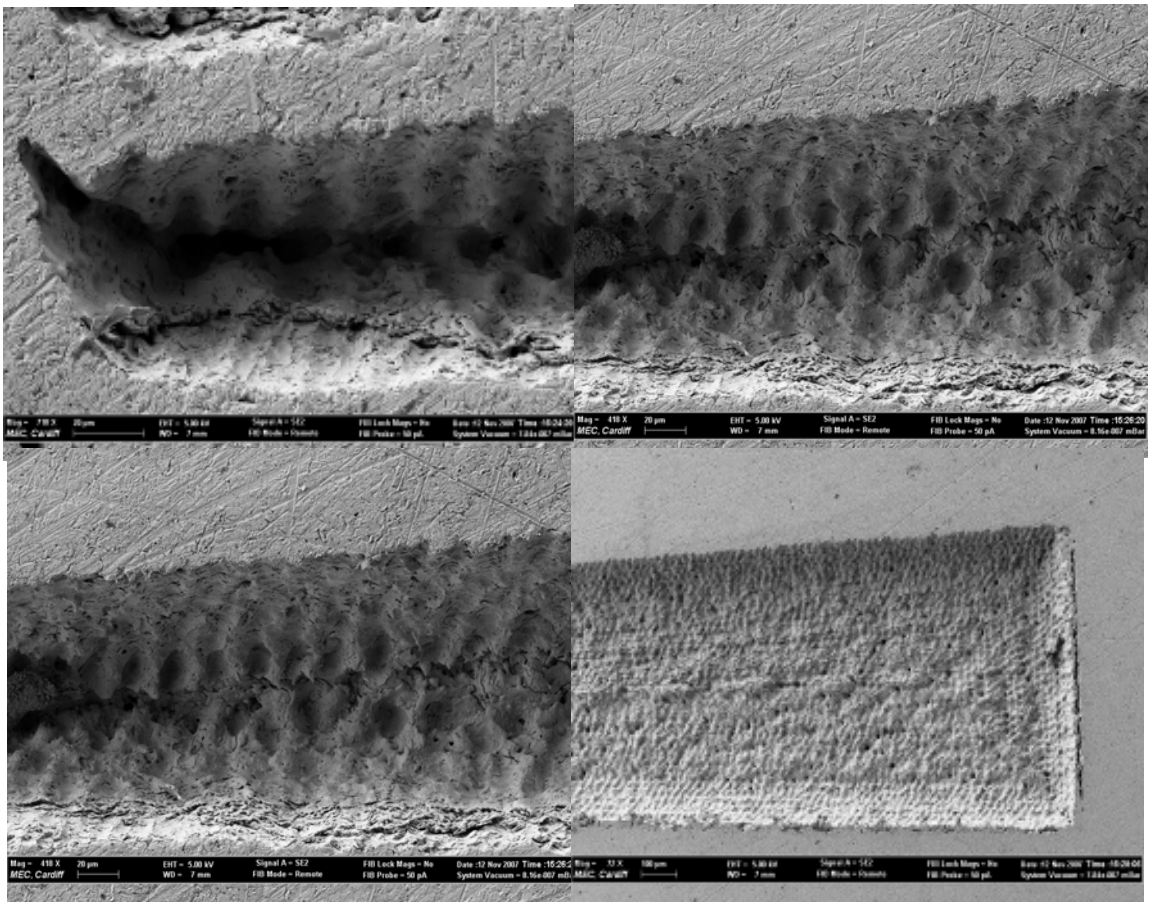

Figure 4.22 Resulting geometry in brass – strategy vertical walls

The results for the brass substrate are provided in Figures 4.19 to 4.22. The effects of milling strategies on the resulting surface roughness and segments' depth are different from those observed on the SS316 sample.

4.2.2.3 Discussion

A very high variation of machined depth was observed when comparing the results for the segments milled with different strategies. And this in spite of the fact that the laser parameters used during the machining of the brass sample were kept exactly the same as for the machining of the four stainless steel structures.

This can be explained by the dissimilar melting temperatures and thermal conductivities of the two investigated materials that result in different heat build up after the machining. While for the brass thermal conductivity is 115 W/mK, for steel it is only 13.4 W/mK(Weaver et al., 1981). However, in spite of the better heat dissipation in brass, surface defects, and especially the re-cast layer, are noticeably higher in comparison with the stainless steel sample due to its relatively low melting temperature of 885 ºC compared with 1371 ºC for the steel.

The results from roughness and depth measurements are provided again in Table 4.3. Please note that it was not possible to measure the surface roughness in some areas of Structures 2 and 4. The best result in terms of roughness and surface consistency was achieved by applying Strategy 1. Although, in the inner sector the machining results for Strategy 3 look the same as those for Strategy 1, there is a significant difference in the way these two strategies are applied. In order to produce vertical walls synchronised movements of both the stage and the galvo mirrors are necessary. Hence, additional error is introduced.

The best results would be achieved by applying strategies that do not require any stage movement, e.g. Strategies 1 and 3 compared with Strategy 4, and ensure the most consistent coverage of the ablated surface with single craters that exhibit some irregularities in their shape. At the start of the each segment where their width is only 40μm due to the close proximity of the neighbouring laser paths, there is not sufficient time for the heat to dissipate into the bulk of the material, and therefore heat builds up in the milled area. As a result of this, more material is removed and the edge definition is relatively poor. The other negative effects in these narrow areas are an increase in the HAZ and in general more pronounced secondary effects such as cracks and material re-deposition. These effects can be easily seen when comparing the SEM images in the top left corner in Figures 4.15 to 4.22.

Looking at the depth results in Table 4.3, it is easy to see the interdependence between measurement results and the applied milling strategies. In both materials, SS316 and brass, the mean depth achieved exhibits the same trend – in descending order - strategy 2, strategy 1, strategy 4, strategy 3. Variations in depth measurements could be attributed to material inconsistencies.

With respect to edge definition, as expected, the machined contours are sharper when the milling strategies include border cuts instead of laser passes normal to the side walls.

4.3 Summary

A very important, but commonly ignored, aspect of laser material removal is discussed in this chapter. In particular, the effects of tool path optimisation and material removal strategies on the resultant surface quality and edge definition were investigated. The conducted

experimental study shows clearly that the applied milling strategies have a significant effect on the resulting surface topography and the edge definition.

Careful process planning could dramatically change the outcome of the process.

Taking into account specifics of the geometrical features, machine controller and stages as well as laser parameters and laser-material interaction would improve the quality of the overall process and reduce the time required for processing.

Also, the research has demonstrated that, by optimising the laser path and material removal strategies, it is possible to reduce significantly the thermal load when milling micro features, and thus to minimise the HAZ and other secondary effects.

Chapter 5 Accuracy of the laser milling process

Many factors influence the accuracy of the laser milling process. Depending on the laser source, material to be processed, machine set up, optical components, beam quality, tool path and environment, different results can be obtained.

As already discussed in previous chapters the laser source-material coupling is the most influential factor. If this interaction is simplified to a single shot – then there are a few factors which directly affect the process of crater formation. Laser milling (again very much simplified) could be considered as overlapping the craters achieved by single shots.

5.1 Factors influencing accuracy

In order to understand better the material removal process, factors directly affecting the process are investigated. Beam characteristics and machine specifics contribute towards the efficiency and quality of the interaction between the laser and the substrate.

5.1.1 Beam quality

Beam quality directly influences the results of the material removal process. The resulting cavity is directly related to the spatial power distribution within the beam. Depending on the material it might have different effects. Usually, materials with higher ablation thresholds are less sensitive to such imperfections, where low ablation threshold materials like plastics are really vulnerable. Although in all calculations/representations the spot size is given as a circle with a certain diameter, sometimes the geometry of the spot is far from circular as shown in

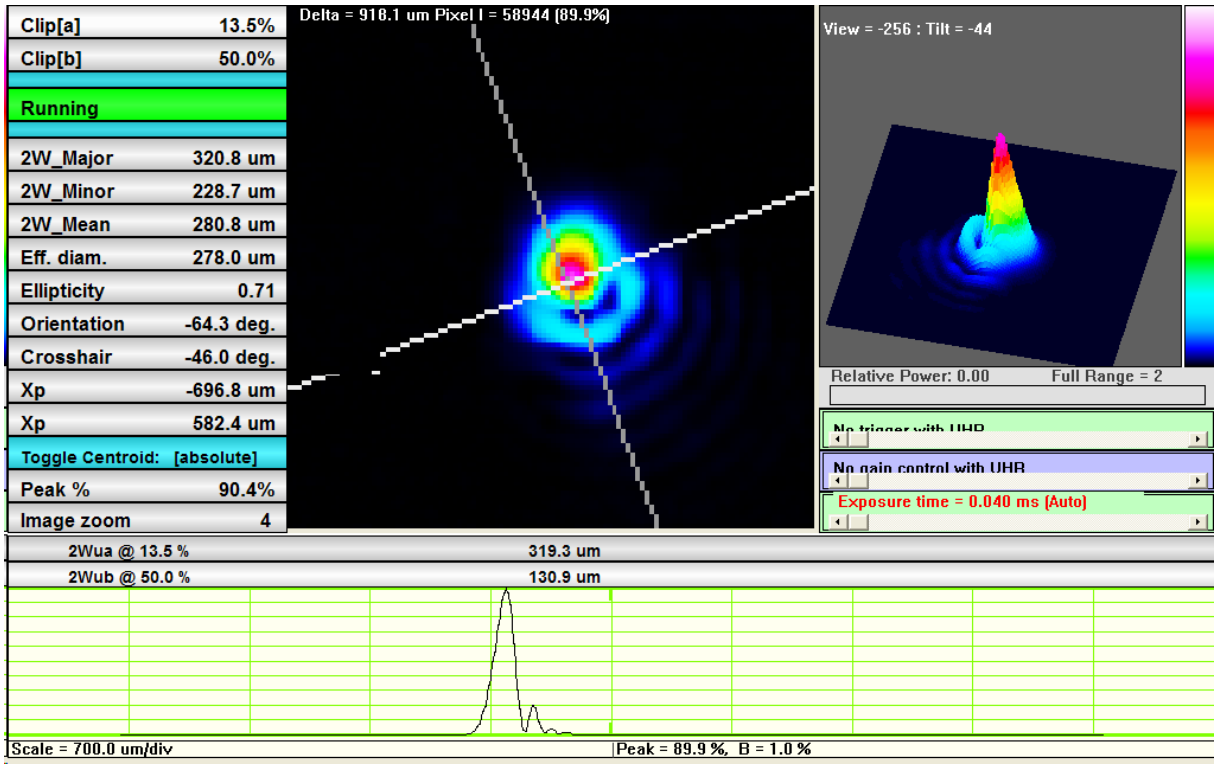

Figure 5.1 Beam profile with ellipticity 0.71

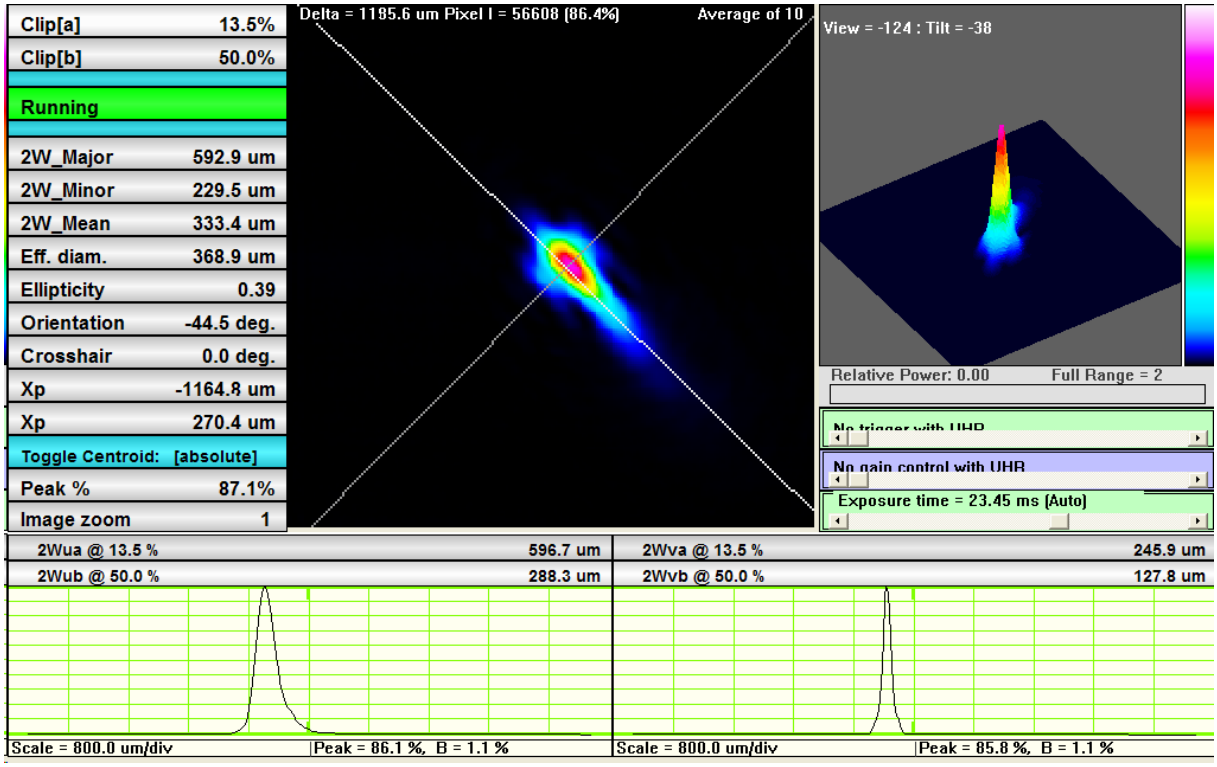

Figure 5.2 Beam profile with ellipticity 0.39

Figures 5.1 and 5.2. The beam geometry directly influences the removal process, as in some areas more energy is delivered and when overlapping of the craters is achieved it directly affects the material removal process.

1.1.1 Machine accuracy

Being part of a complex system the accuracy of the components is always going to be affected by the overall accuracy of the machine tool. The design of the machine, stages with their characteristics, temperature and humidity are very important factors that affect the stability of the system and can influence to a large extent the outcome of a removal process.

In order to minimise the influence of these factors a number of measures could be put in place:

- Air conditioning (temperature and humidity) of the room and internal enclosure
- Anti vibration base
- Granite or polymer concrete bases to absorb vibrations
- Active control for the position

1.2 Experiments

A series of experiments was carried out to investigate the influence of the process parameters over material removal. Laser pulse duration and power (average and peak) were investigated focusing on repeatability , accuracy and quality achieved during the removal of the material.

1.2.1 Overall accuracy

In order to investigate the accuracy of the laser milling process an experiment was conducted based on a real component. The geometry of the ceramic component, which has overall dimensions of 6mm x 2.9mm x 1.18mm, is shown in Figure 5.3. The properties of the material used, alumina 23, are listed in Table 5.1.

Note that both sides of the part have cavities, as well as a hole and a slot, which means that repositioning of the workpiece is necessary during manufacture. Because the laser spot diameter is very small (approximately 45μm), a very high set-up accuracy is required and repositioning is not desirable.

The wavelength of the Nd:YAG laser in the milling system used in this study was 1064 nm . Figure 5.4 gives approximate values of the light absorption of several materials in the 200nm to 1200nm spectrum. For alumina, the absorption at 1064 nm is about 10%, which is not favourable (too low) for laser machining. For this reason, a preliminary machinability test was conducted which showed that it is possible to machine alumina 23 with the milling system adopted.

The main requirements to be observed when selecting values for the process parameters were:

- a stable process

Stability in the process is required as material is removed in a layer by layer fashion. If the process is not stable it would lead to changes in the actual removal depth and subsequently at some point the interaction between the laser beam and the material would occur outside of the focal point of the beam. This would lead to a dramatic change in the removal mechanism and ultimately would result in no material being removed at all.

- the specified dimensional accuracy.

Specified by the contractor accuracy was ISO IT14

- an acceptable surface finish

When processing ceramic components with lasers a common problem is heat affected areas, where significant amounts of energy are being transferred into the bulk of the material, causing material properties to change. Usually a change in colour is an indicator that such events are occurring at an undesirable scale.

- reasonable cycle times

The material removal process should be a cost effective process completed within a reasonable time rather than just targeting ultimate quality. Utilizing a very small spot the material removal rate could reach impractical processing times.

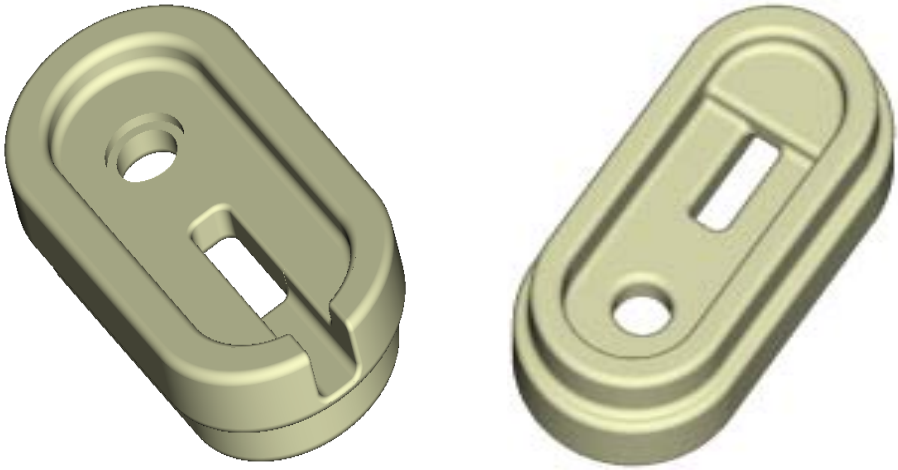

Bottom view Top view

Figure 5.3 Ceramic component.

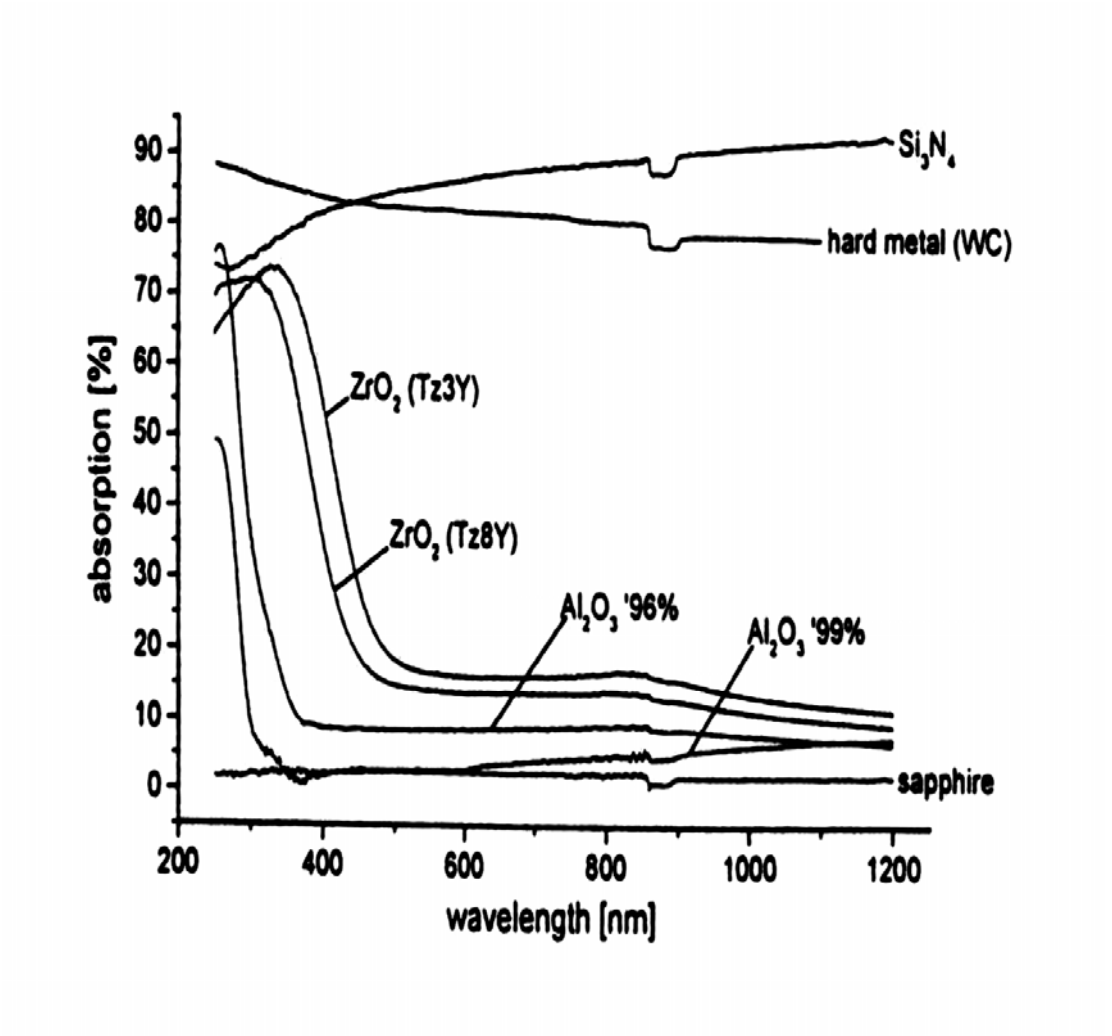

Figure 5.4 Light absorption for various materials (Hellrung et al, 1999)

Table 5.1 Material properties of alumina 23.

Material DIN VDE 0335/IEC 672	**Units**	
Principal constituent		99.7% Al_2O_3
Apparent density	g/cm^3	3.7-3.95
Main grain size	μm	10
Open porosity	%	0
Compressive strength	N/mm^2	3500
Bending strength	N/mm^2	300
Modulus of elasticity	GPa	380
Melting point/Maximum working temperature	° C	2030/1950
Specific heat	J/kg K	900
Thermal conductivity at 100 °C/1000 °C	W/m K	30/5
Emissivity at 1000 °C	%	21
Specific electrical resistance at: 20 °C/500 °C/1000 °C/1500 °C	Ohm. cm	$10^{14}/10^{12}/10^{7}/10^{4}$

1.2.1.1 Process set-up

Several single-factor experiments were carried out to determine the influence of the process parameters on the process output. Although they do not provide a complete picture of the different phenomena involved, because interactions between the factors are not considered, they do give an idea of the influence of the process parameters on a particular target process output, facilitating process tuning and reducing the amount of trial and error involved in process adjustment.

Figures 5.5 – 5.8 present the results obtained. It can be inferred that the most influential process parameter with respect to the layer thickness and the removal rate is the current in the lamp used to generate the laser beam (Figure 5.5). This is because the lamp current directly influences the energy of the laser pulses and the pulse peak power. This was the reason for using the lamp current as an approximate process tuning parameter.

The effect of pulse duration (Figure 5.6) is also linked to the pulse peak power. It was noticed that for longer pulses (τ_L >4μs) with lower peak powers the surface finish was poor and there was also a change in the surface colour. The latter might indicate that the chemical structure has been altered. In addition, for pulses longer than 4μs, the process was not stable resulting in a wide variation in layer thickness. The process window with regard to pulse duration was found to be in the range 2-4 μs. In general, shorter pulses are preferred for the machining of ceramics, because they give higher pulse peak powers, when the other parameters are fixed.

Pulse frequency (Figure 5.7) has two main influences on the laser milling results: (i) it directly controls the degree of overlapping of the craters produced by the laser pulses; and (ii) in machining ceramic materials, lower pulse frequencies are more efficient, because the pulse energy required for material removal is higher than that for other materials.

The scanning speed (Figure 5.8) also influences the overlap between craters, the lower the speed, the greater the overlap. When the overlap increases, the depth per layer also increases, because more material is subject to multipulse radiation.

From the single-factor experiments, it can be concluded that in order to achieve a stable process for machining alumina 23 ceramics, the following should be adopted:

- small pulse duration for higher pulse peak power
- low pulse frequency for sufficient pulse energy
- low scanning speed for better surface finish.(generally the lower the scanning speed – the better the surface finish, but at some point the opposite effect can be observed - increasing the roughness, while decreasing the scanning speed)

It should be stated that pre-machining (one or a few layers machined) is required to assure uniform absorption and process stability. Due to the preparation of the substrate (cutting, grinding) the first few layers would exhibit different absorption rates to the bulk of the material and if the process parameters are set, based on the laser-material interaction of these

first few layers, it would lead to a significant changes in stability and removal rate as the removal process progresses.

1.2.1.2 Results and discussion

A batch of 24 components was manufactured. The key dimensions of the components were measured. The results are given in Table 5.2. The dimensions in the slice plane XY are divided into two groups - internal and external. For the internal dimensions, hatching was performed from the inner side of the contour containing the corresponding dimension, while for the external dimensions hatching was from the outer side. For dimensions in the Z direction, this factor was not important as the manufacturing process is performed in a layer by layer fashion.

As shown in Figure 5.9 it was observed that for most internal dimensions, negative deviations from the nominal value were obtained, indicating that the actual dimensions were smaller than the nominal.

For external dimensions, the situation was the opposite and the actual dimensions were larger than the nominal. This could be explained by the fact that the effective laser spot diameter was smaller than the value employed in generating the laser path. This confirms that, as indicated above, a very important factor for an accurate removal process is the actual spot diameter. There are many theoretical models created to analyze and estimate the actual spot diameter, but due to the material composition (typically a few materials constitute the substrate exhibiting various heat absorption and conduction) and variance in material composition, a difference between theoretical and actual spot could be observed. As good practise the actual spot should always be measured.

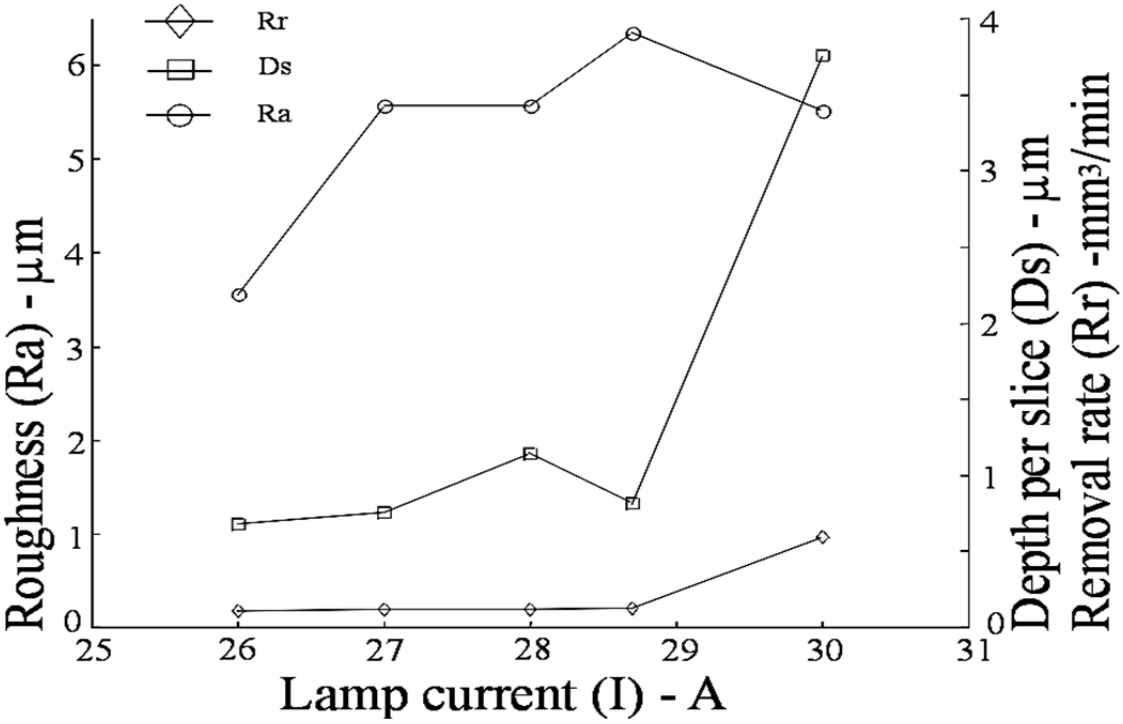

Figure 5.5 Influence of the process parameters on the process output – lamp current

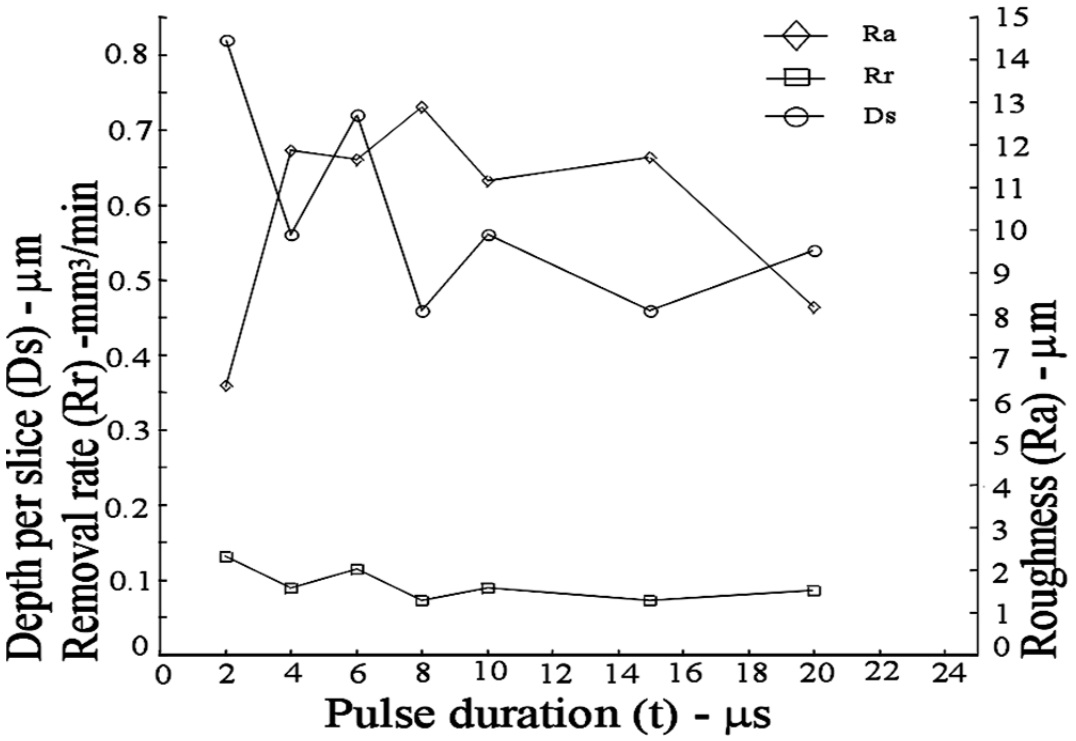

Figure 5.6 Influence of the process parameters on the process output – pulse duration

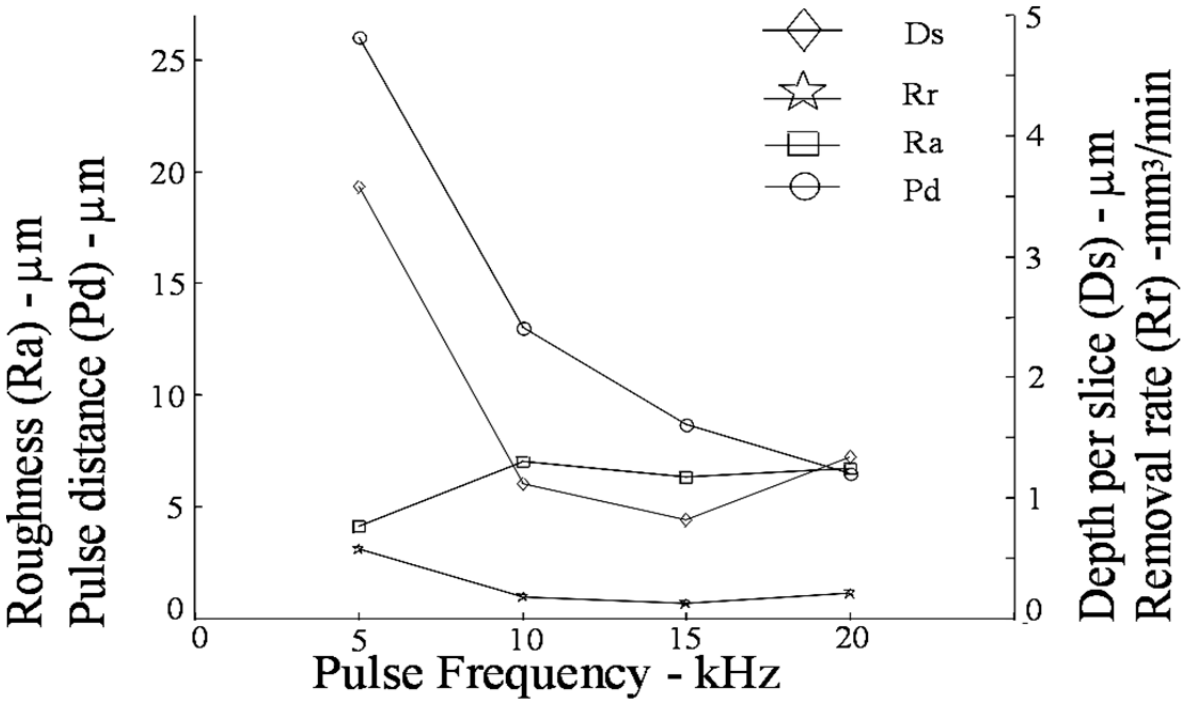

Figure 5.7 Influence of the process parameters on the process output – pulse frequency

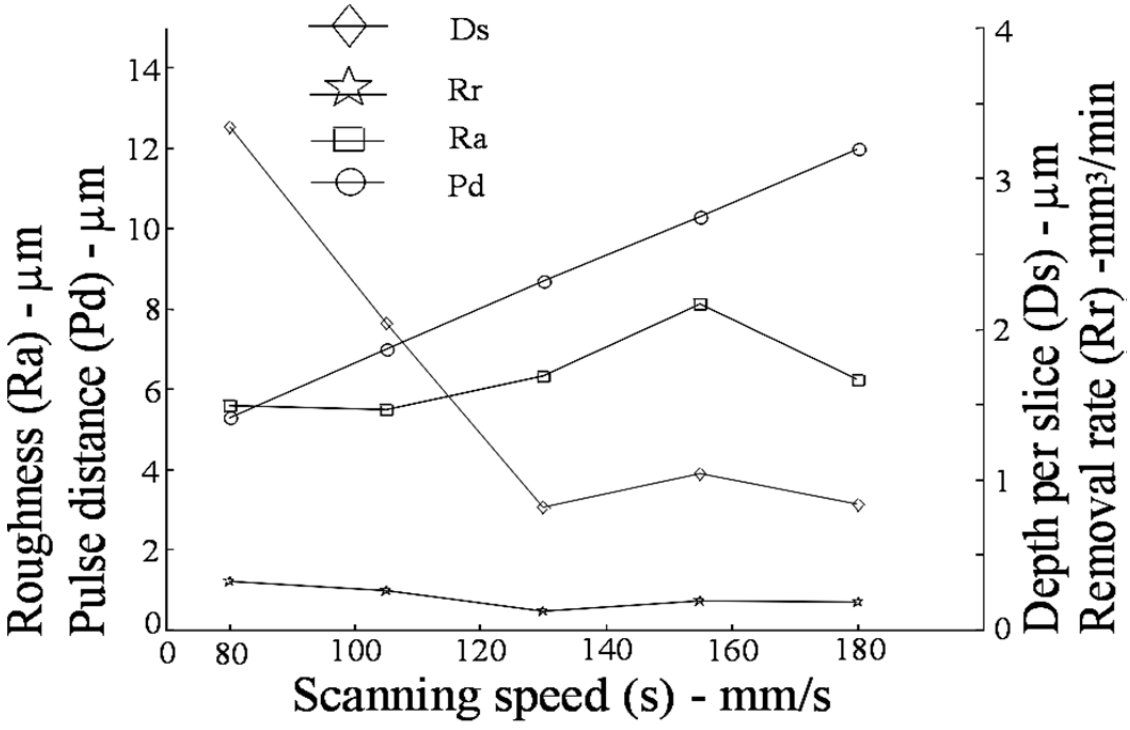

Figure 5.8 Influence of the process parameters on the process output – scanning speed

It was observed that, as the machined dimension increased, the absolute value of the deviation from the nominal also increased. This could be explained by the fact that both the diameter and the shape of the effective laser spot changes as the beam moves away from the optical axis of the system. A full analysis of the individual dimensions is included in the Appendix C.

However, the dimensional changes were not significant as shown by the measurements. In addition, the deviation from the nominal was also contributed to by losses of accuracy during the generation of the laser path as well as machine accuracy. Table 5.2 shows that most of the actual tolerances for the measured dimensions were between ISO Grade IT12 and IT14, which is within the prescribed tolerances for the component. For a small number of non-critical dimensions, the measured values were outside the specified limit, but this did not affect part functionality.

If compensation is applied to correct for the actual laser spot, it is exppected that the overall accuracy will be dramatically improved. This will shift the results closer to the nominal without changing the deviations and distributions. From the experiment it can be concluded that the effective crater diameter is a very important factor when it comes to overall accuracy of the process. In this case all other parameters were kept the same - laser power, repetition rate, pulse duration, scanning speed.

Repeatability of the process is good, although the processed material is one of the hardest to process with this type of laser - absorption around 10% and grain sizes 1-2 micrometers.

Nom	1	2	3	4	5	6	7	8	9	10	11	12	13	14	15	16	17	18	19	20	21	22	23	24	Dir
135	1339	1374	1372	1371	142	1381	136	1373	1326	1364	137	1359	1382	1375	138	1379	1413	1351	1399	145	1352	1392	1415	1398	X
3.75	3.653	3.697	3.69	3.714	3.814	3.695	3.7	3.727	3.687	3.702	3.68	3.711	3.725	3.714	3.761	3.731	3.734	3.689	3.725	3.764	3.689	3.717	3.694	3.691	X
4.75	4.717	4.678	4.673	4.666	4.724	4.671	4.694	4.682	4.689	4.677	4.664	4.676	4.68	4.701	4.703	4.667	4.679	4.69	4.679	4.674	4.687	4.692	4.683	4.676	X
5	4.899	4.823	4.863	4.835	4.844	4.841	4.866	4.843	4.874	4.858	4.83	4.822	4.844	4.844	4.846	4.843	4.838	4.847	4.831	4.856	4.857	4.86	4.853	4.881	X
6	6.088	6.03	6.062	6.022	6.033	6.05	6.058	6.015	6.087	6.035	6.026	6.025	5.98	6.017	6.045	6.034	6.02	6.052	6.043	6.011	6.04	6.055	6.039	6.016	X
0.5	0.456	0.452	0.465	0.47	0.458	0.456	0.452	0.472	0.392	0.48	0.476	0.46	0.481	0.468	0.481	0.481	0.478	0.446	0.464	0.486	0.468	0.47	0.47	0.47	Y
0.5	0.476	0.475	0.471	0.472	0.457	0.459	0.461	0.471	0.395	0.474	0.474	0.47	0.481	0.477	0.476	0.485	0.484	0.448	0.473	0.485	0.462	0.467	0.473	0.467	Y
17	1561	1528	1565	1554	1631	1563	1573	1557	1577	1554	1563	1552	1557	1552	1549	1542	1542	1567	1572	1536	1542	1551	1574	1568	Y
2.5	2.54	2.439	2.606	2.574	2.585	2.577	2.558	2.545	2.549	2.505	2.441	2.449	2.528	2.507	2.546	2.585	2.588	2.537	2.581	2.584	2.523	2.518	2.529	2.517	Y
2.9	2.989	2.969	2.962	2.974	2.98	2.997	2.996	2.979	3.03	2.927	2.978	2.994	2.913	2.925	2.957	2.97	2.979	2.993	2.996	2.97	2.968	2.982	2.985	2.937	Y
0.25	0.25	0.25	0.23	0.23	0.21	0.24	0.2	0.2	0.21	0.25	0.22	0.24	0.23	0.25	0.25	0.21	0.19	0.24	0.22	0.24	0.26	0.25	0.23	0.22	Z
0.3	0.29	0.29	0.3	0.28	0.26	0.3	0.29	0.3	0.2	0.29	0.3	0.3	0.3	0.29	0.29	0.28	0.28	0.27	0.3	0.28	0.28	0.27	0.28	0.28	Z
0.52	0.44	0.49	0.5	0.52	0.51	0.47	0.51	0.5	0.5	0.53	0.5	0.5	0.51	0.52	0.52	0.5	0.48	0.52	0.52	0.52	0.51	0.51	0.5	0.51	Z
1.18	1.19	1.17	1.15	1.18	1.17	1.18	1.18	1.18	1.16	1.19	1.18	1.19	1.17	1.18	1.19	1.17	1.15	1.21	1.17	1.15	1.21	1.21	1.16	1.17	Z

Table 5.2 24 Parts measured (mm)

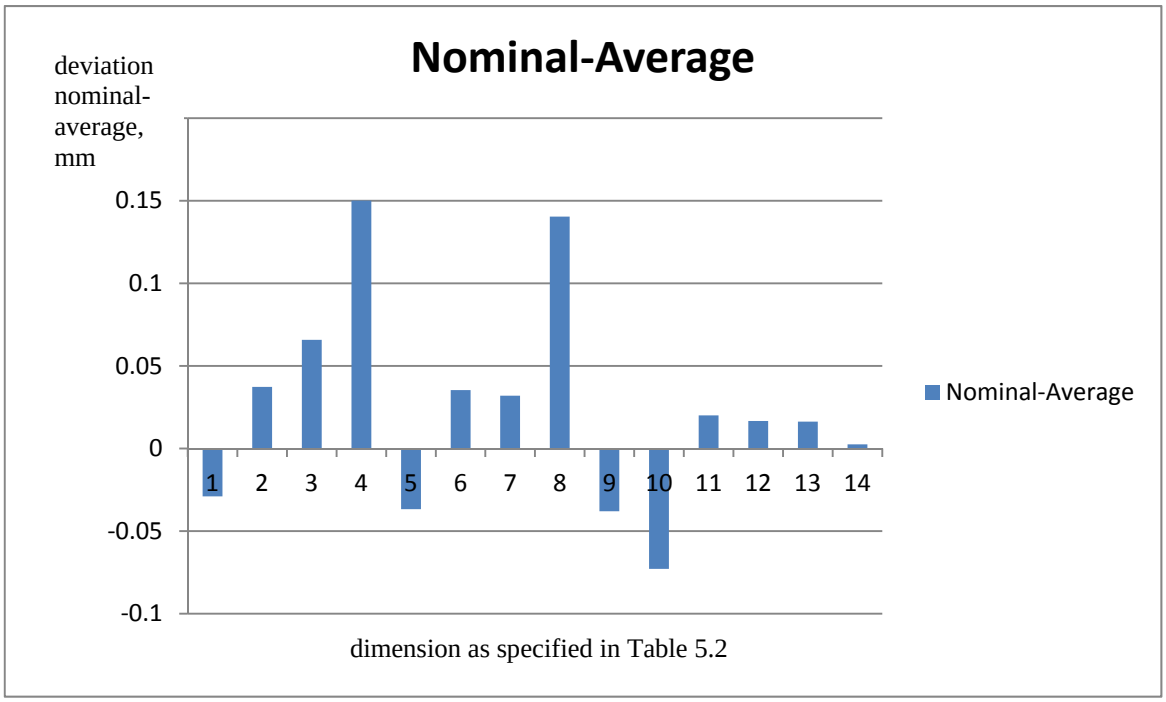

Figure 5.9 Nominal -average chart

1.2.2 Pulse duration and power influence

A series of experiments was conducted in order to estimate the effect that wavelength, pulse duration and power output has on the quality of the holes drilled in green ceramic tapes.

There are a few methods for hole drilling with lasers as described below in Figure 5.10. In this case trepanning was utilized but realized by galvo scanner.

In order to capture maximum data for this experiment a new MOPA based fiber laser was utilized. This laser allows 25 different waveforms to be created as shown in Figure 5.11 and in Figure 5.12. The laser is designed in such a fashion that not only pulse duration can be changed, from around 9 nanoseconds up to 200 nanoseconds, but also the pulse shape.

Most lasers have Gaussian distribution, where this laser has a variety of pulse shapes as described in Figures 5.11 and 5.12. This offers a unique possibility to study different mechanisms of material removal as a result of changing the shape of the pulse. In some cases it changes the absorption coefficient of the material and only triggers ablation at peak power, then gently carrying it through the pulse until the pulse is completed.

1.2.2.1 Process set-up

In order to investigate the influence of the pulse duration and the shape of the pulse the following experiment has been conducted:

Employing the SPI 20WSM Fiber laser in three different wave modes (different pulse lengths and shapes of the pulse as shown in the figures 5.11 and 5.12) and utilizing a galvo scanner a series of holes have been drilled in green ceramic tape at different power levels.

For each setting 20 holes were drilled, data captured and analyzed further.

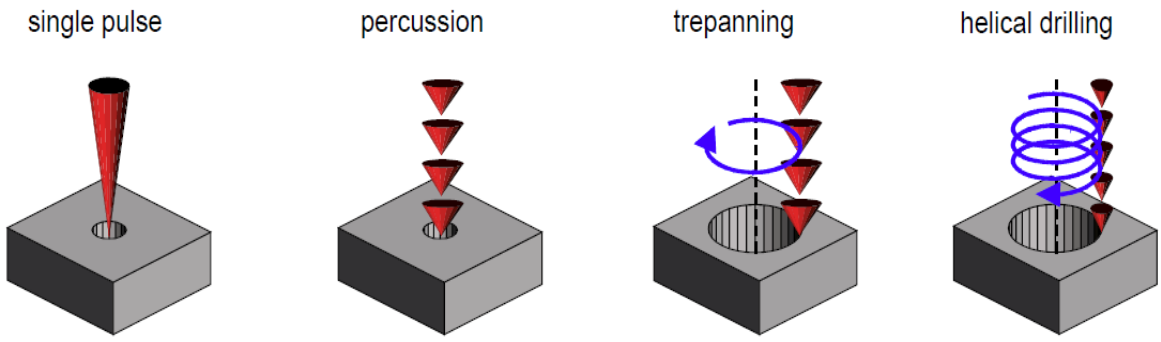

Figure 5.10 Methods for laser holes drilling (Dausinger et al, 2004)

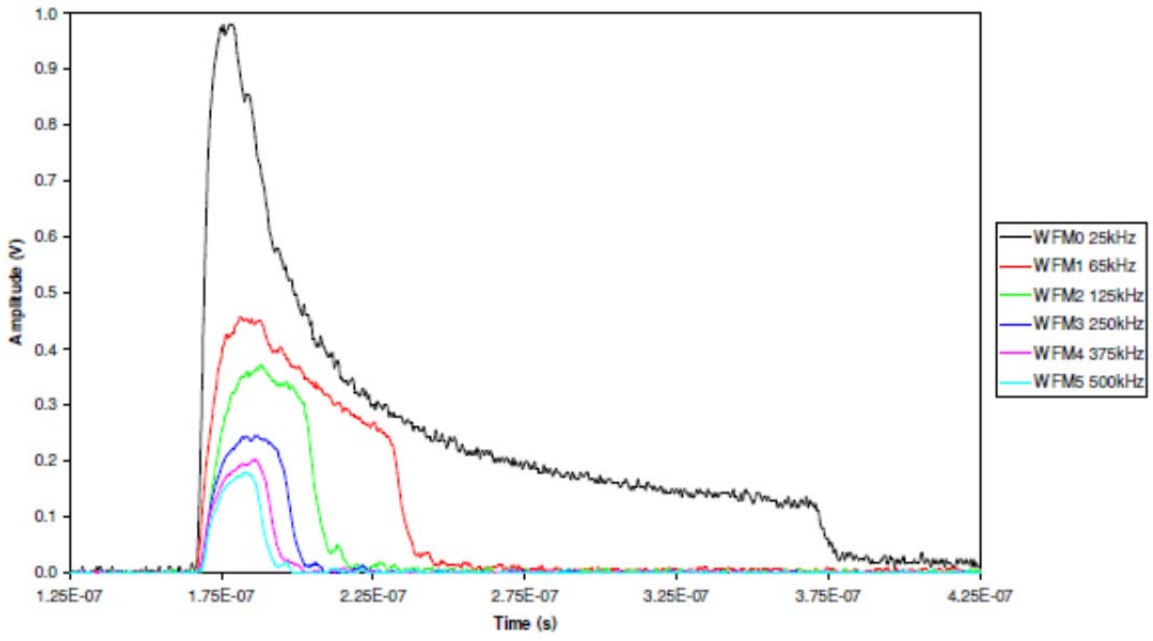

Figure 5.11 Example pulse shapes for waveform for 0-5 at PRF0

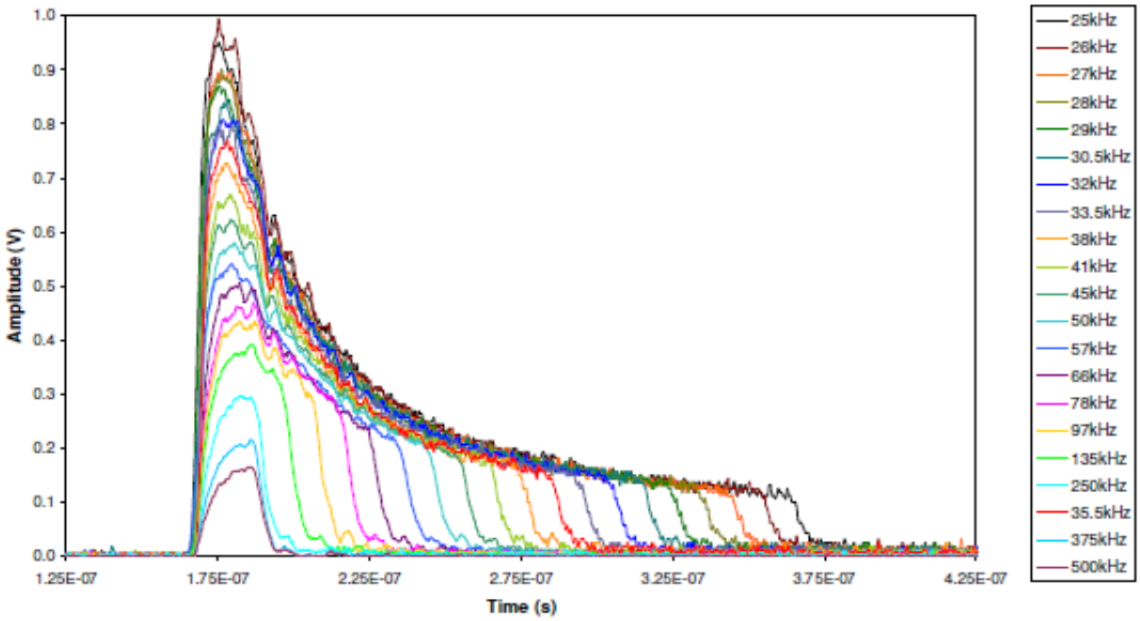

Figure 5.12 Example pulse shapes for waveform for 11-29 at PRF0

The system employed changes power as a percentage of the maximum available power. In order to convert this into real power, measurements were taken of the real power delivered by the laser system. Results are shown in Figure 5.13.

For the experiment 3 distinctive regimes were selected (details in Figure 5.14). The first regime (Figure 5.14- set1) utilizes the longest pulse the system can deliver (200 nanoseconds). Set 3 utilizes the shortest pulse duration available for this system (9 nanoseconds) and Set 2 is in the mid-range with a pulse duration of 90 nanoseconds.

The idea was to charter the response of the material to these three different pulse durations in terms of surface quality, hole radius and repeatability.

1.2.2.1 Results and discussion

Utilizing very long pulses did not work very well. As can be clearly seen in Figure 5.15 there are huge burns and shape deformations caused by the excess of energy supplied to the substrate. Such irregular shapes and burns makes this set inapplicable. Crystallization was observed around the edges of the processed area due to the excessive heat transfer into the bulk of the material, that triggered phase changes in the material which is an undesirable effect.

Clearly in this case the ablation threshold of the material has been exceeded by an intolerable margin.

When energy is not enough to trigger ablation - only heating of the material is observed.

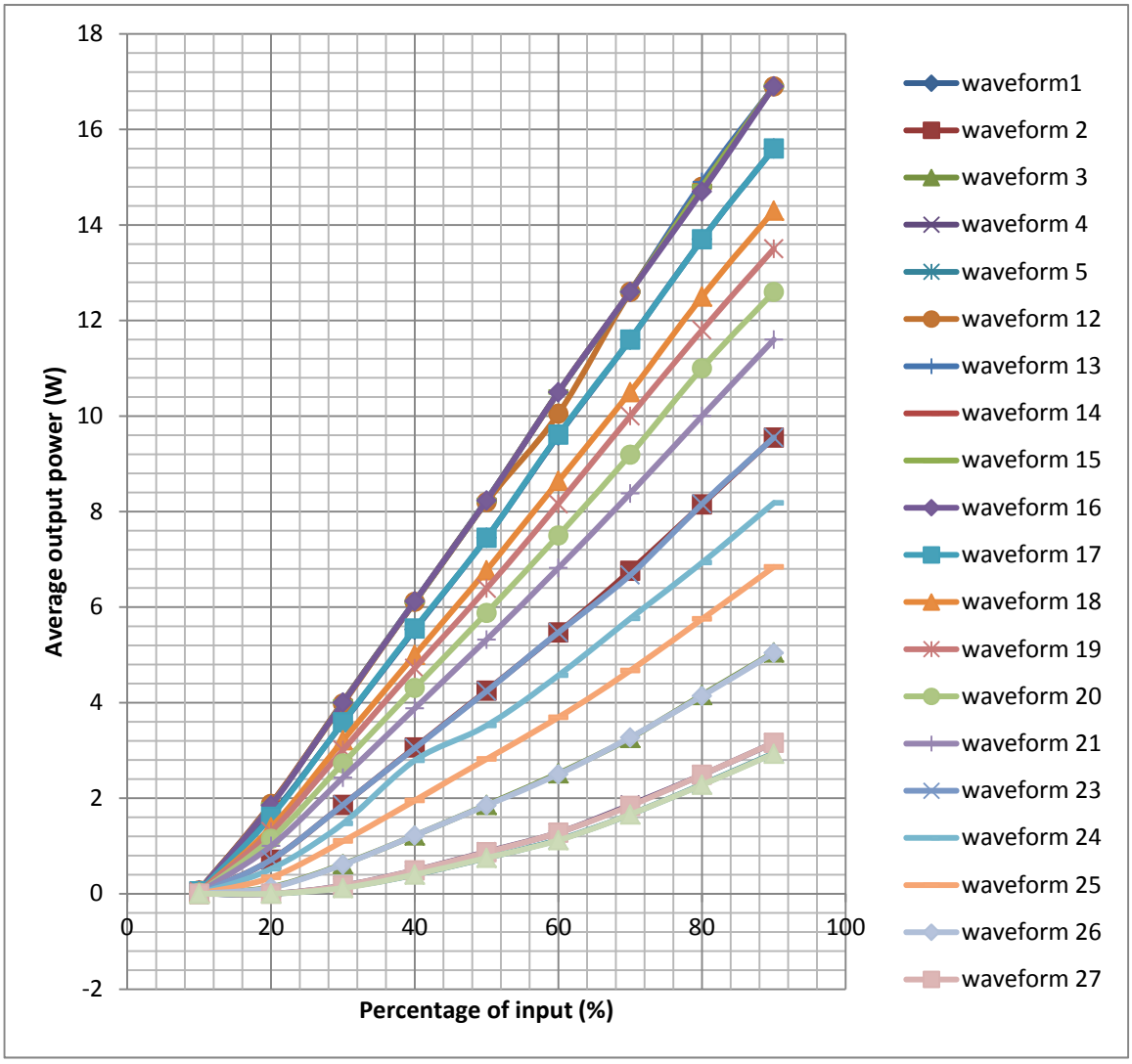

Figure 5.13 Actual average laser power

Number	Pulse Duration, ns	Frequency, kHz	Pulse energy(max), mJ	
1	200	25	0.8	Set1
2	90	45	0.44	Set2
3	9	500	0.04	Set3

Figure 5.14 Processing regimes

Exceeding the threshold levels allows the ablation process to start and this is the area where the best results are usually achieved. In this case we are way above the ablation threshold, where the energy supplied to the substrate exceeds the threshold and energy supplied is transferred to the bulk of the material as heat. As a result the heat affected zone is much bigger and more evident.

In some cases long pulse duration might be beneficial - for example for welding or rough material removal where quality is not an issue and the target is speed of processing, but in this case this was not a desired effect. From all power levels only one set was measured (Figure 5.16 and Figure 5.17) for estimating the effect of the pulse energy over the resulting diameter rather than analysis of the results for this pulse duration.

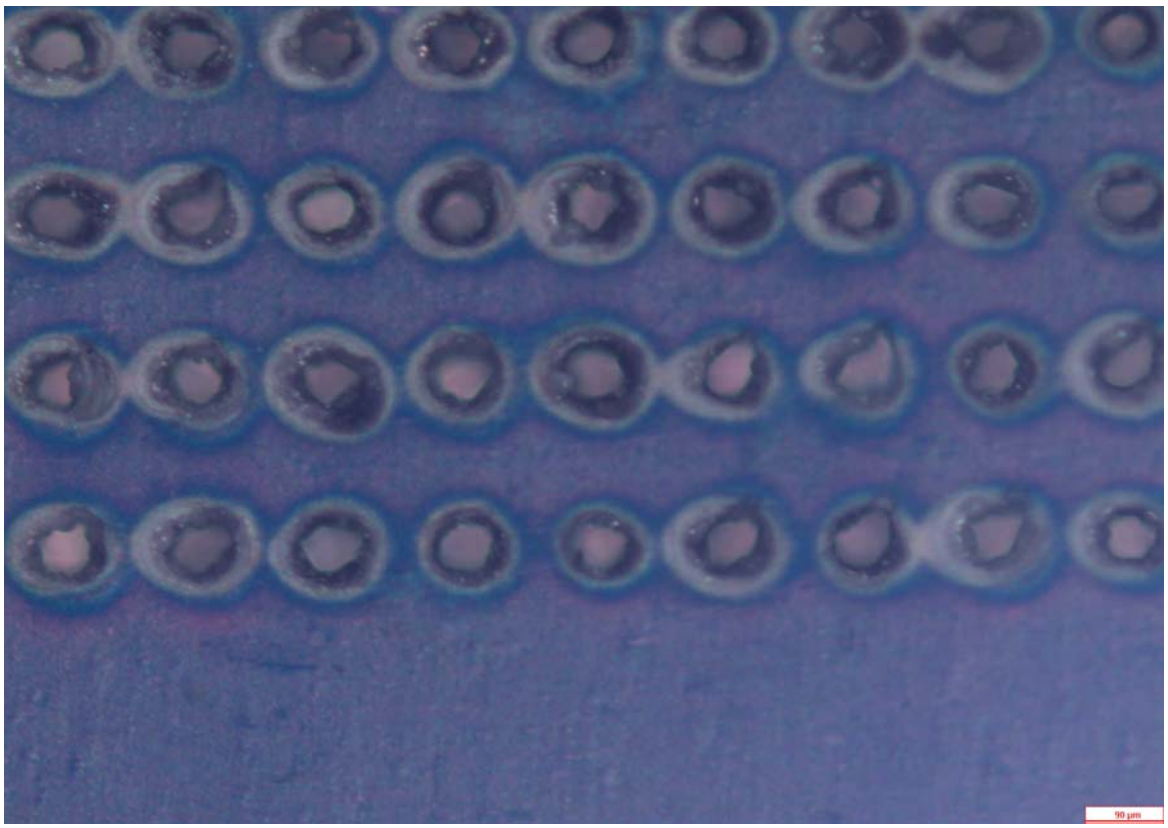

Figure 5.15 Set1 - Holes array

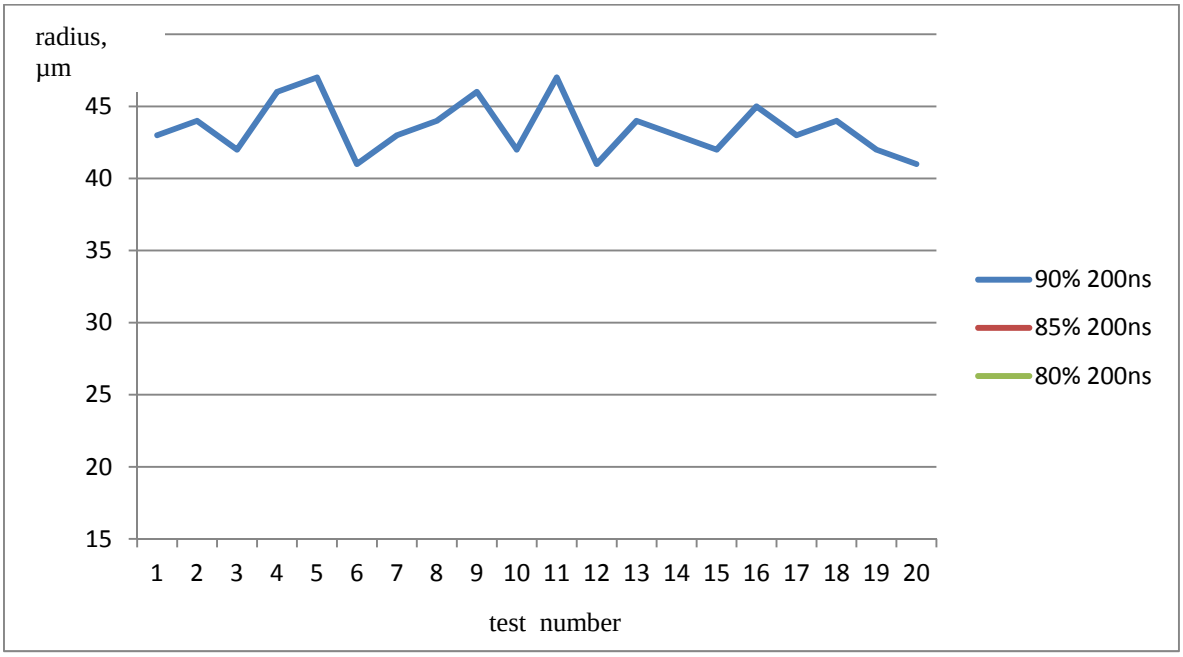

Figure 5.16 Set1 Actual dimensions (radius in µm)

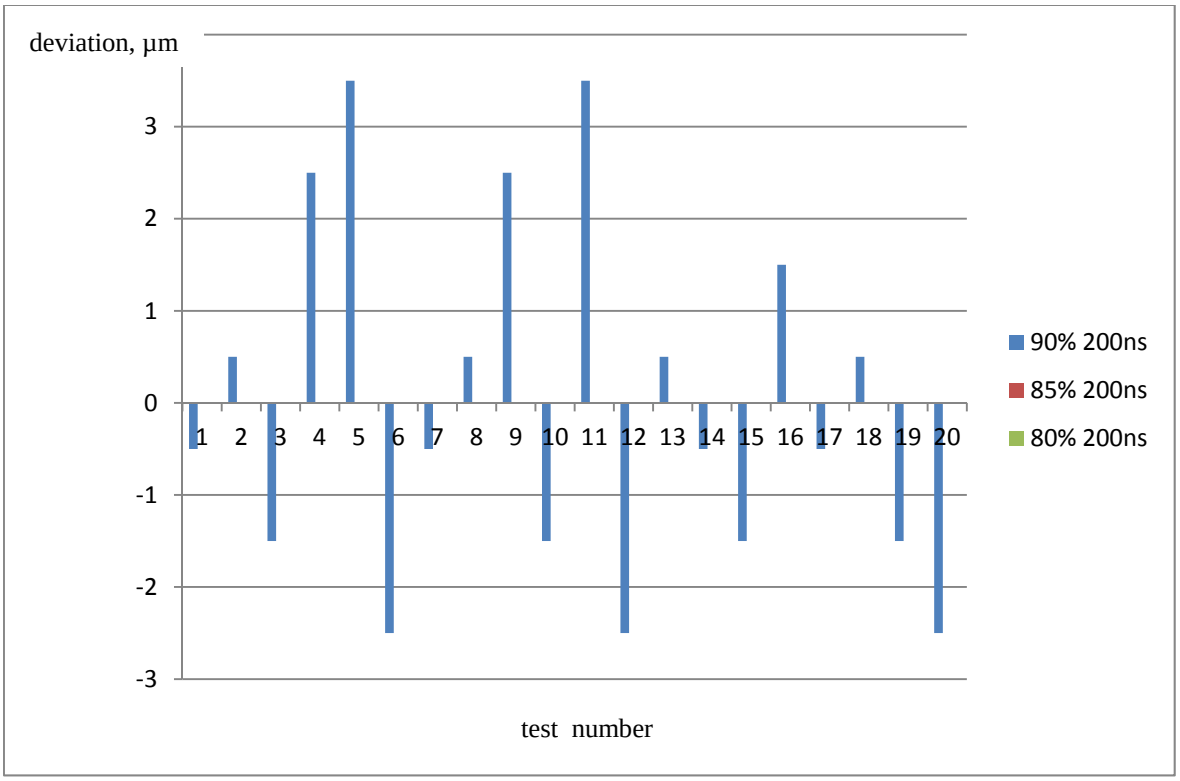

Figure 5.17 Set1 Deviations from mean radius (µm)

Set 2 of 90 ns pulse duration delivered results in the full range of power setting - from 90% P_{max} to 40% P_{max}(Figure 5.18). As can be seen in the Figure 5.19 from 90% P_{max} to 65% P_{max} there was really no change in the effective radius of the holes. After that level the radius starts to fall as expected. Above the threshold it seems applying more power did not change the effective radius of the hole. It only created more debris and heat affected zone, as the resulting heat dissipates into the substrate. Near the threshold of the material even small changes in laser power leads to a significant change in the effective crater and as the process removes material by simply overlapping the resulting craters it directly influences the effective radius of the hole. This configuration of the pulse - duration and energy distribution seems to suit much better this particular material. The laser-material coupling is the most important criteria for successful ablation. A variety of laser sources exist at present offering a huge range of wavelengths, pulse durations and beam qualities. Material ranges are also important as internal structure has a major impact on the material response.

As can be seen in Figure 5.20 process repeatability is very good in this process window - effective radius varies only a few micrometers. Considering the structure of the material - alumina particles in the range of 300nm, bonded by Recitel and not very short pulse duration of 90 nanoseconds of the laser source, these results can be considered rather good for this laser material coupling.

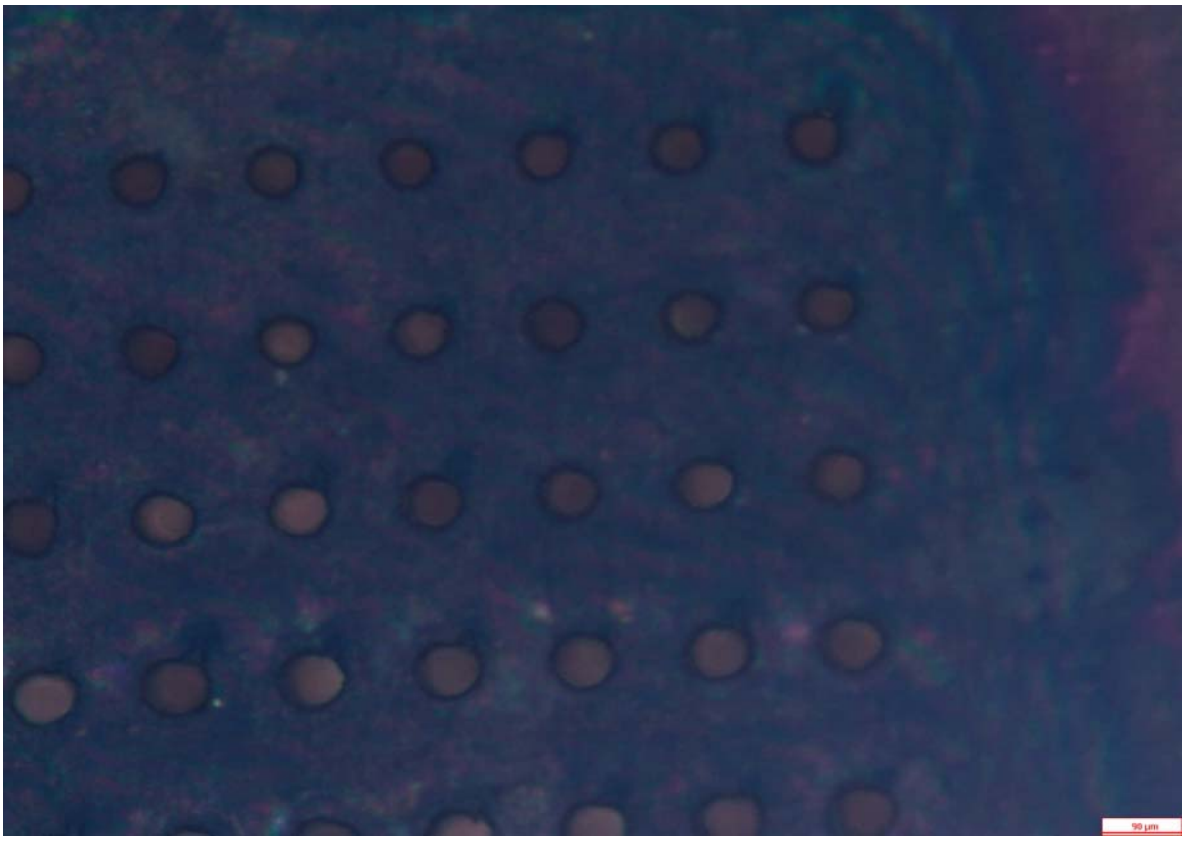

Figure 5.18 Set 2 - Holes array

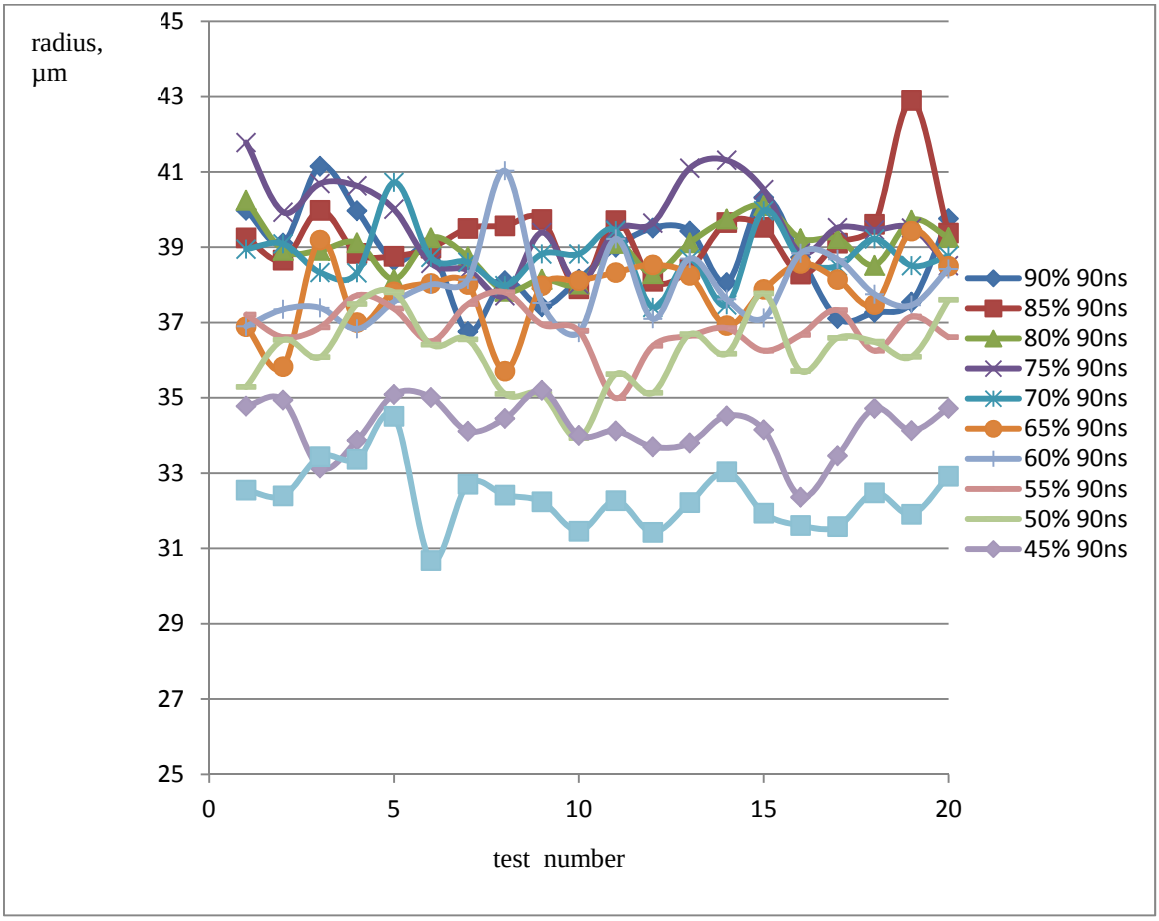

Figure 5.19 Set 2 Actual dimensions (radius in µm)

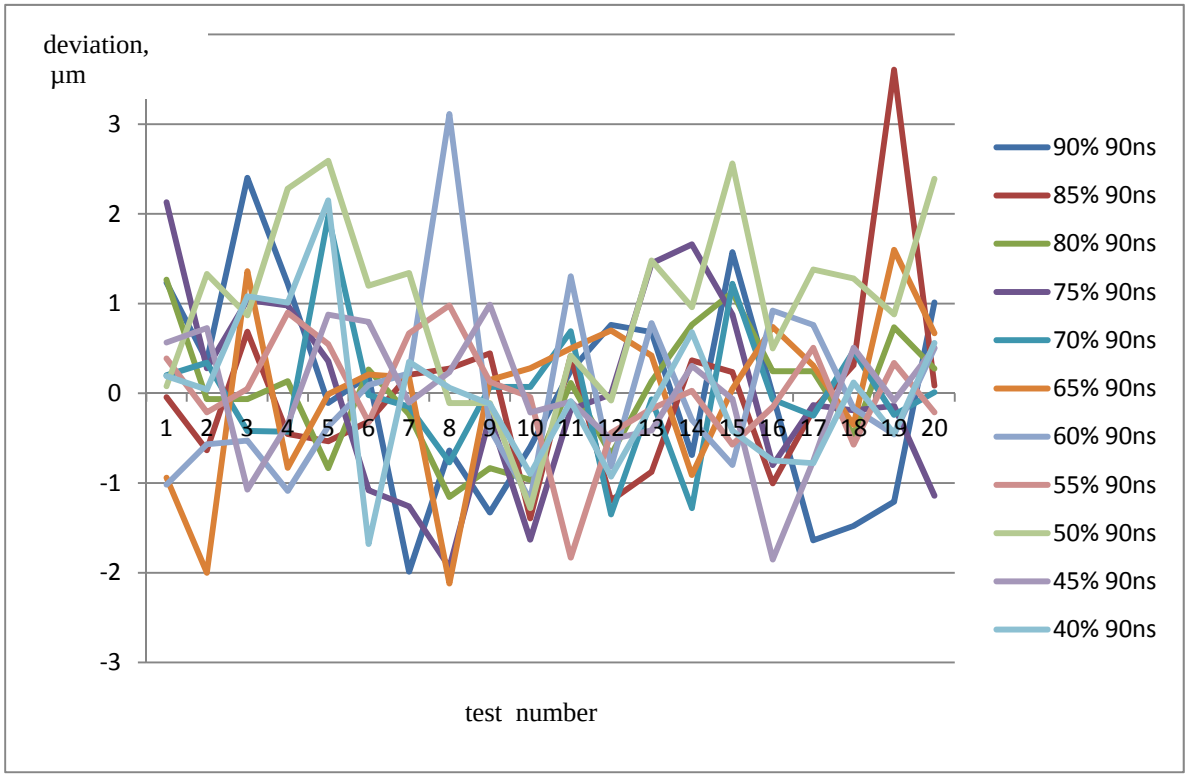

Figure 5.20 Set 2 Deviations from mean radius (µm)

Set 3 or 9 ns pulse duration - in this case the pulse utilised is the shortest and with an almost Gaussian distribution (Figure 5.11 - wave front 5). Power levels were very important as can be seen in Figure 5.22 – a small drop in the laser power delivered resulted in big changes in the effective hole radius. Furthermore, at 75% P_{max} there was no ablation at all as well as for settings lower than that. The repeatability of the process remains good as can be seen in Figure 5.23.

One pulse in this regime delivers only 0.04mJ energy, whereas with the 200ns long pulses the energy delivered per pulse is 0.8mJ. Such a difference is very influential especially with materials with low absorption coefficients, as most of the energy delivered is reflected or transmitted away. In this case the shape of the pulse is also quite different compared to the previous two cases. The near Gaussian distribution of this waveform brings this regime closer to the 'standard' pulses, rather than having a very powerful peak followed by a plateau and gradually lowering power to zero.

The main advantage of this waveform is the clean cut produced as the pulse duration is very short and there is no time for the heat to propagate into the bulk of material. Ablation threshold is achieved in a very narrow part of the pulse hence the effective spot is very small. On the negative side - process productivity or material removal rate is lower by a magnitude of 10 compared to previous regimes and so the time required to produce features/components might become impractical.

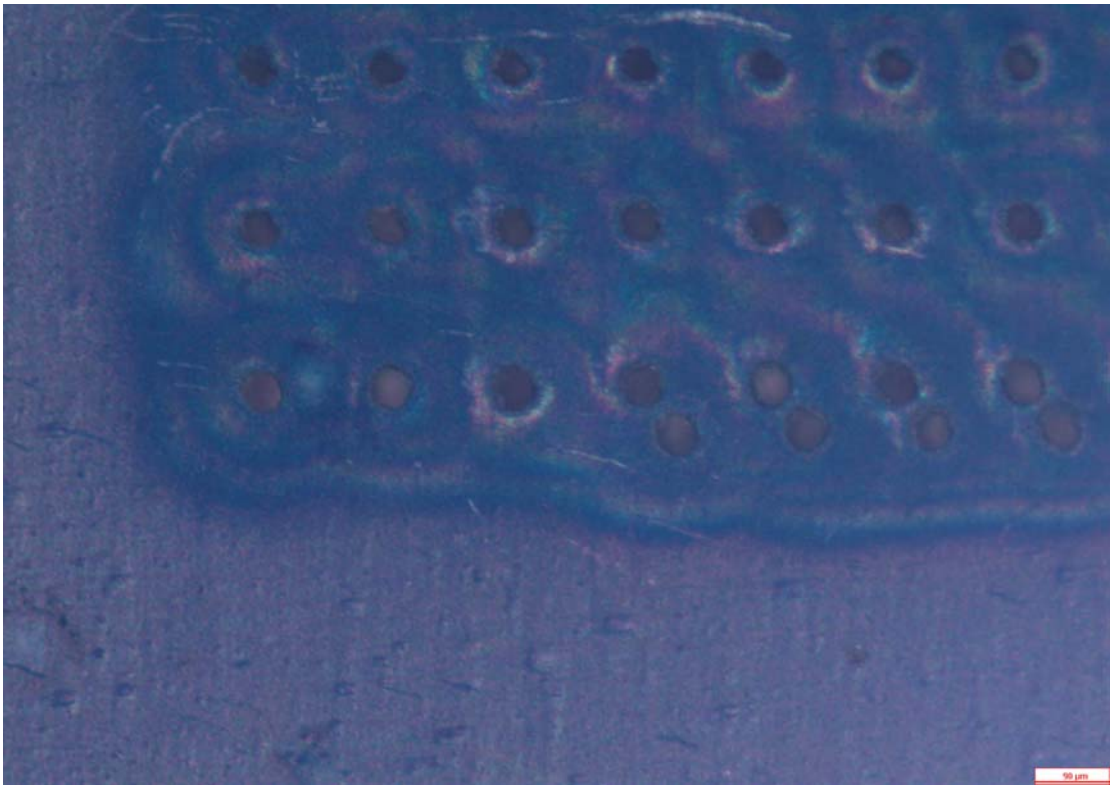

Figure 5.21 Set 3 - Holes array

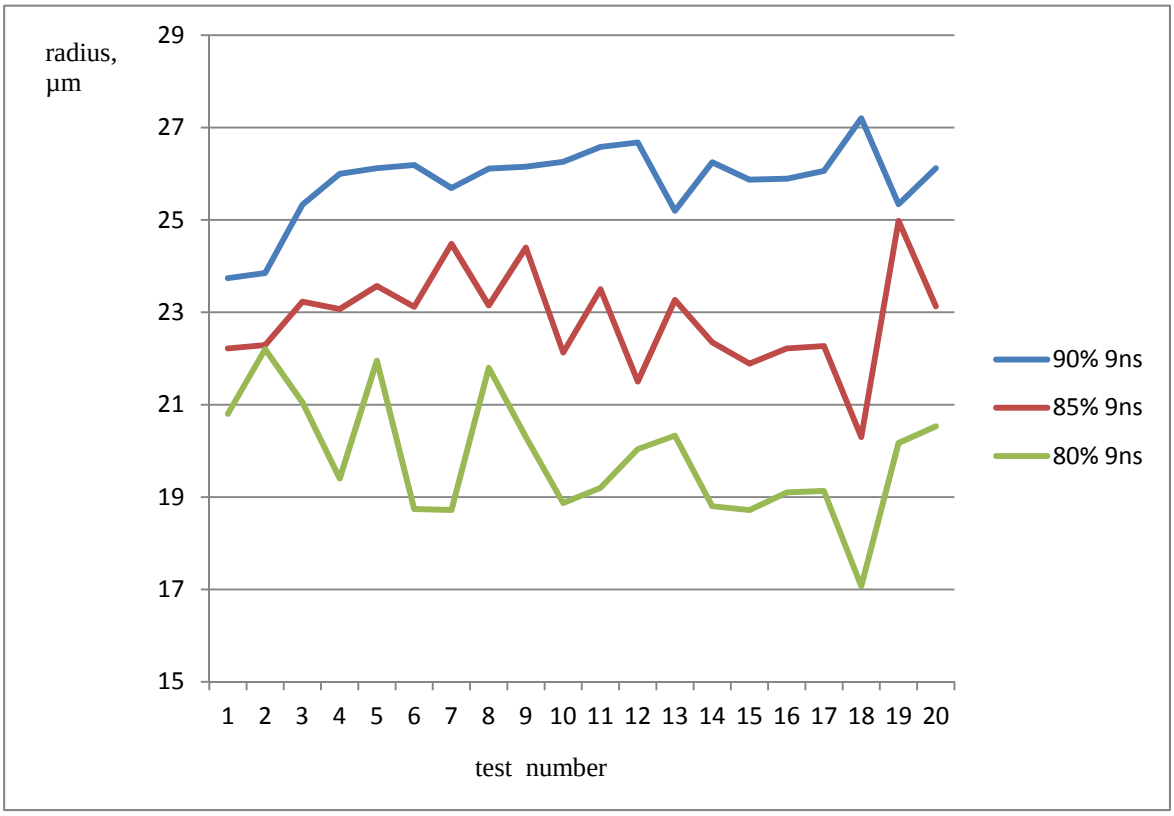

Figure 5.22 Set 3 Actual dimensions (radius in µm)

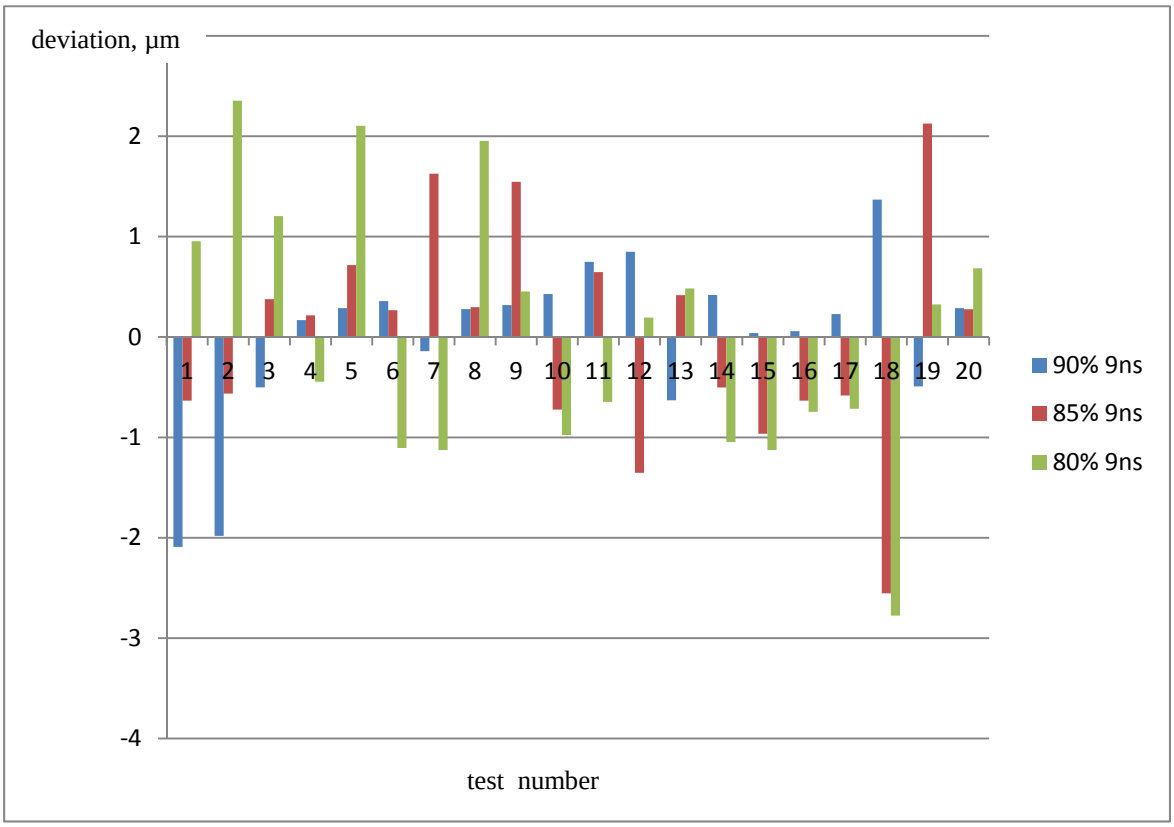

Figure 5.23 Set 3 Deviations from mean radius (µm)

1.3 Summary

Laser milling is a cost-effective process for manufacturing small batches of ceramic parts. It allows parts with complex shapes to be produced without the need for expensive tooling.

Laser milling is most suitable for machining parts with one-sided geometry or for partial machining of components from one side only. Complete laser milling of parts is also possible but difficulties in accurate re-positioning for additional set-ups would have to be addressed. The setting-up of the workpiece is most critical when small parts are to be manufactured. In cases where a through feature has to be machined, it is recommended that the support be made from a material that cannot be laser milled as vapour generated from the support may damage the part or influence its quality. It is therefore suggested that, for a machine employing a laser with a wavelength λ=1064 nm, a glass support plate be used to hold the workpiece.

The influence of the process parameters on laser milling is complex and must be optimised to obtain the highest part quality. Approximate tuning of the process for machining of alumina can be achieved by controlling the power and fine adjustments made by manipulating the scanning speed and/or pulse frequency. In addition, if available, different shaped pulses should be utilized as changes in the pulse duration and shape offer great flexibility of regimes. The accuracy of the process should be considered for each regime separately - as already demonstrated for each regime the effective spot size changes and this in turn triggers changes in the overall accuracy of the process. Preliminary tests should be completed considering all aspects that might change the accuracy of the process.

Process optimization is a tedious and lengthy process. However, given the fact that it needs to be done only once for a particular material - one can benefit from good results achieved each time that material is utilized again. Furthermore, as there are multiple solutions of the optimisation criteria, a full map of the material-laser interaction is recommended as different regimes could deliver similar results in terms of surface roughness, accuracy and heat affected zone, but achieved for significantly different periods of time.

As demonstrated in the experiments reported here, there are many factors that influence the overall accuracy of the process, but the ones related to the machine are usually fixed where much development can be done on the actual removal process in terms of accuracy.

It is strongly recommended that closed-loop control of the depth be used whenever possible in order to avoid instability in the layer thickness and associated accumulated errors.

Chapter 6 Contributions, conclusions and further work

6.1 Contributions

The effects of laser milling on the surface of the machined component have been investigated. An in depth analysis was carried out of the roughness achieved, heat penetration, hardness change as well as material grain refinement.

The laser parameters analyzed in this study were:

- Laser pulse duration
- Laser pulse shape
- Laser wavelength
- Overlapping of craters
- Laser type

Substrate-related parameters investigated were:

- Grain refinement
- Phase change
- Hardness change
- Roughness

The way the laser beam interacts with the substrate was also under investigation in terms of:

- Removal strategy
- Machine control program
- Accuracy

In this research, the effects of pulse duration, wavelength, pulse shape and overlapping of the pulses of four different laser sources on surface integrity were investigated. In particular, an attempt was made to assess the impact of four distinctly different laser regimes on surface quality and material microstructure.

In order to assess the thermal impact on the substrate caused by the laser milling process, a novel methodology was created for analysis, based on the grain refinement in the bulk of the material. Additional information was obtained by investigating hardness changes near the processed area.

Surface roughness is a critical factor for many applications and a thorough analysis of the resulting topography was concluded that, for each material, the best laser – material coupling has to be found. Laser milling is a material dependent process and the thermal and optical properties of the material have a strong impact on the removal process.

The characteristics of the laser source are as important as the material that undergoes ablation. The relation between the pulse duration, pulse shape and accuracy of the process was demonstrated through a series of experiments designed to expose the correlation between these parameters and to assess their impact.

An often omitted aspect of the laser material interaction was studied, the material removal strategies and their impact on surface quality, removal rate and feature definition.
Through a carefully selected test structure all strategy related aspects of the removal process were investigated. The results obtained clearly confirm the importance of the selected

strategy and, as a consequence, guidance is created based on feature topography and application.

1.1 Conclusions

Laser milling is capable of processing a large range of materials which are not machinable with conventional manufacturing processes. It was demonstrated here that engineering ceramics can be machined without requiring expensive special tools and without any limitations on the 3D complexity of the component.

Nevertheless, laser milling is still in its infancy. Laser-material interactions are not yet fully understood. Much effort in the research and development of the available laser sources is still required. Ultrafast lasers are beginning to be applied. They can offer more precise machining without the thermal damage that accompanies long-pulse laser manufacturing.

The aim of this work was to investigate the effects on the substrate caused by laser ablation when utilized in ‘milling’ fashion and especially the heat affected zones created. Then, through a material removal strategy and accuracy estimation, to apply optimization for micro structuring applications.

In this research, the effects of pulse duration of four different laser sources on surface integrity were investigated. In particular, an attempt was made to assess the impact of four different laser regimes on surface quality and material microstructure. These are the issues that have to be taken into account when considering the tradeoffs between high removal rates

and the resulting surface integrity. This is a particular dilemma when selecting the most appropriate ablation regime for performing micro structuring.

During laser milling applying different ablation mechanisms, the material goes through several phase transitions that have a direct impact on surface integrity of the processed area. Thus, the relevant material characteristics are transition energies, such as evaporation energy and melting energy. In addition, thermal conductivity is a key material factor affecting the resulting surface integrity. In particular, this affects the dissipation of the absorbed energy into the bulk of the material and the energy losses, and hence determines the size of the HAZ.

The following generic conclusions can be drawn from this study:

For both ms and ns laser milling, the HAZ on the ablated surface was estimated to be within 50µm. However, there were some differences in grain size refinements when comparing the resulting microstructures. The melt phase during µs laser processing was larger, and more heat was transferred into the substrate, leading to the formation of a finer grain structure.

When performing ultra short pulsed laser ablation, the effects of heat transfer are not evident as was the case with longer laser pulse durations. Although some heat is transferred into the bulk, it is not sufficient to trigger significant structural changes. Heat penetration is much smaller and grain refinement is minimal. The effects of pulse duration on the resulting material microstructure are more evident in the micrograph of the field exposed to ps laser ablation than that of the area which underwent processing with fs laser pulses.

Due to the ablation mechanism that is in place when applying ultra-short pulses, significant improvements of surface roughness can be achieved by applying ps and fs pulse lasers. In this research, a marginally better surface quality was achieved when performing laser milling with a ps laser source. This could be explained with nonlinear effects that are typical for processing materials at fs regimes, and also with the specific machining response of the tooling steel to the selected processing parameters, especially the lasers' wavelength.

These generic conclusions again underline the tradeoffs that exist between the resulting surface integrity and removal rates. Therefore, it is necessary to look for the best compromise when selecting the optimum laser source for each specific application. Taking into account the specific requirements of micro tooling applications, in particular as high as possible surface quality, and the relatively small volumes of material that have to be removed, ultra-short pulsed laser ablation regimes present a viable solution. Furthermore, this research suggests that ps pulse lasers offer some advantages over fs laser sources when they are utilised for machining micro cavities in tooling steel. Taking into account that the fluence of the ps laser source is four times higher than that of the fs laser, it can be expected that through further process optimisation an even better surface quality could be achieved. This answers the first research question.

A very important, but commonly ignored aspect of laser material removal is the effect of tool path optimisation and material removal strategies on the resultant surface quality and edge definition. The conducted experimental study shows clearly that the applied milling strategies have a significant effect on the resulting surface topography and the edge definition. This answers the second research question.

Also, the research has demonstrated that by optimising the laser path and material removal strategies it is possible to reduce significantly the thermal load when milling micro features, and thus to minimise the HAZ and other secondary effects. This addresses the third research question.

1.2 Further work

A significant improvement on all aspects of the laser milling process is expected from the development of new laser sources. Utilizing lower wavelengths and shorter pulses will help to achieve lower surface roughness and smaller heat affected zones. Furthermore optimization of the material removal strategies will be developed and hence improvement is expected in the surface quality and processing time. A new generation of fiber lasers is emerging, allowing different pulse shapes to be utilized for processing materials at unfavourable wavelengths and pulse durations.

Appendixes

APPENDIX A

MACRO PROGRAM

Appendixes

```
DELETE ALL

YES

RESET ALL

DIALOGS MESSAGE OFF

IMPORT MODEL FILEOPEN "D:\PROJECTS\ARees insert\realsession\realposition.dgk"

DELETE SCALE VIEWMILL RESIZEVIEW

VIEW MODEL ; SHADE NORMAL

FORM BLOCK

EDIT BLOCK RESET

BLOCK ACCEPT

CREATE TOOL ; TAPERSPHERICAL  FORM TOOL

RENAME TOOL "1" 'laser_pen'

EDIT TOOL 'laser_pen' TAPERANGLE "15"

EDIT TOOL 'laser_pen' LENGTH "0.1"

EDIT TOOL 'laser_pen' TIPRADIUS 0.00433

EDIT TOOL 'laser_pen' DIAMETER 0.013

EDIT TOOL 'laser_pen' NUMBER COMMANDFROMUI 1

EDIT PREFERENCE CUTTINGDATATDU NO

EDIT TOOL 'laser_pen' AXIAL_DOC_REC 0.002

EDIT TOOL 'laser_pen' RADIAL_DOC_REC 0.004

EDIT TOOL 'laser_pen' FEED_PER_TOOTH_REC "0.001"

EDIT TOOL 'laser_pen' CUTTING_SPEED_REC 5000
```

EDIT TOOL 'laser_pen' SPINDLE_SPEED_REC 0.001

EDIT TOOL 'laser_pen' FEED_RATE_REC 2700

TOOL ACCEPT

FORM FEEDRATE

EDIT RPM 0.001

EDIT FRATE 2700

EDIT PRATE "7"

EDIT RSPEED 5000

FEEDRATE ACCEPT

FORM TOOLZHEIGHTS

EDIT TOOLPATH SAFEAREA DIRECTION I "0"

EDIT TOOLPATH SAFEAREA DIRECTION J "0"

EDIT TOOLPATH SAFEAREA DIRECTION K "1"

EDIT TOOLPATH SAFEAREA SIZE 0

EDIT TOOLPATH SAFEAREA PLUNGE_SIZE "0"

EDIT RMOVES ABSOLUTE

TOOLZHEIGHTS ACCEPT

FORM TOOLZHEIGHTS

EDIT TOOLPATH SAFEAREA DIRECTION I "0"

EDIT TOOLPATH SAFEAREA DIRECTION J "0"

EDIT TOOLPATH SAFEAREA DIRECTION K "1"

EDIT TOOLPATH SAFEAREA SIZE 0

EDIT TOOLPATH SAFEAREA PLUNGE_SIZE "0"

EDIT RMOVES ABSOLUTE

TOOLZHEIGHTS ACCEPT

IMPORT TEMPLATE ENTITY TOOLPATH TMPLTSELECTORGUI

"3D-Area-Clearance\Raster-AreaClear-Model.ptf"

SET AREACLEAREXPERT

ACTIVATE TOOL "laser_pen"

EDIT RTOLERANCE 0.001

EDIT RTHICKNESS 0.002

EDIT OVER 0.004

EDIT ZHEIGHTS AUTOMATIC OFF

FORM ZHEIGHTS

EDIT ZHEIGHTS MODE VALUE

EDIT ZHEIGHTS MODEVALUE 0

EDIT ZHEIGHTS REFERENCE TYPE TOOLPATH

EDIT ZHEIGHTS REFERENCE ACTION APPENDALL

PROCESS ZHEIGHTS

ZHEIGHTS ACCEPT

EDIT ACUTDIR CONVENTIONAL

EDIT PMOVES AFTER

FORM TOOLAXIS

EDIT TOOLAXIS TYPE VERTICAL

TOOLAXIS ACCEPT

EDIT LMOVES PLUNGE

SET POCKET

EDIT AUTOANGLEMODE MANUAL

```
EDIT RANGLE

EDIT AREACLEAR TYPE MODEL

EDIT CUTTERCOMP TYPE AUTOMATIC

EDIT FLAT_TOLERANCE 0.001

EDIT TOOLPATH "1" CALCULATE

EDIT TOOLPATH "1" RECYCLE

EDIT TOOLPATH "1" REAPPLYFROMGUI

VIEW MODEL ; SHADE OFF

VIEW MODEL ; WIREFRAME OFF

EXPLORER SELECT Toolpath "Toolpath\1" NEW

FORM TOOLPATH

ACTIVATE TOOLPATH "1"

EDIT TOOLPATH "1" CLONE

SET AREACLEAREXPERT

ACTIVATE TOOL "laser_pen"

FORM TOOLZHEIGHTS

EDIT TOOLPATH SAFEAREA DIRECTION I "0"

EDIT TOOLPATH SAFEAREA DIRECTION J "0"

EDIT TOOLPATH SAFEAREA DIRECTION K "1"

EDIT TOOLPATH SAFEAREA SIZE  -0.002

EDIT TOOLPATH SAFEAREA PLUNGE_SIZE  "0"

EDIT RMOVES ABSOLUTE

TOOLZHEIGHTS ACCEPT

EDIT RTOLERANCE 0.001
```

EDIT RTHICKNESS 0.002

EDIT OVER 0.004

EDIT LMOVES PLUNGE

DRAW SLICES

EDIT ZHEIGHTS AUTOMATIC OFF

FORM ZHEIGHTS

DELETE ZHEIGHTS ALL

EDIT ZHEIGHTS MODE VALUE

EDIT ZHEIGHTS MODEVALUE -0.002

PROCESS ZHEIGHTS

EDIT ZHEIGHTS REFERENCE TYPE TOOLPATH

EDIT ZHEIGHTS REFERENCE ACTION APPENDTOP

EDIT ZHEIGHTS REFERENCE select "2"

EDIT PCUTDIR CLIMB

ZHEIGHTS ACCEPT

EDIT ACUTDIR CONVENTIONAL

EDIT PMOVES AFTER

FORM TOOLAXIS

EDIT TOOLAXIS TYPE VERTICAL

TOOLAXIS ACCEPT

EDIT LMOVES PLUNGE

SET POCKET

EDIT AUTOANGLEMODE MANUAL

EDIT RANGLE 126

```
EDIT AREACLEAR TYPE MODEL

EDIT CUTTERCOMP TYPE AUTOMATIC

EDIT FLAT_TOLERANCE 0.001

PROCESS ZHEIGHTS

ZHEIGHTS ACCEPT

EDIT PMOVES AFTER

BATCH TOOLPATH "1_1" OFF

EDIT TOOLPATH "1_1" CALCULATE

EDIT TOOLPATH "1_1" RECYCLE

EDIT TOOLPATH "1_1" REAPPLYFROMGUI

EXPLORER SELECT Toolpath "Toolpath\1_1" NEW

RENAME Toolpath "1_1" "2"

EXPLORER SELECT Toolpath "Toolpath\1" NEW

FORM TOOLPATH

ACTIVATE TOOLPATH "1"

EDIT TOOLPATH "1" CLONE

SET AREACLEAREXPERT

ACTIVATE TOOL "laser_pen"

FORM TOOLZHEIGHTS

EDIT TOOLPATH SAFEAREA DIRECTION I "0"

EDIT TOOLPATH SAFEAREA DIRECTION J "0"

EDIT TOOLPATH SAFEAREA DIRECTION K "1"

EDIT TOOLPATH SAFEAREA SIZE  -0.004

EDIT TOOLPATH SAFEAREA PLUNGE_SIZE  "0"
```

EDIT RMOVES ABSOLUTE

TOOLZHEIGHTS ACCEPT

EDIT RTOLERANCE 0.001

EDIT RTHICKNESS 0.002

EDIT OVER 0.004

EDIT LMOVES PLUNGE

DRAW SLICES

EDIT ZHEIGHTS AUTOMATIC OFF

FORM ZHEIGHTS

DELETE ZHEIGHTS ALL

EDIT ZHEIGHTS MODE VALUE

EDIT ZHEIGHTS MODEVALUE -0.004

PROCESS ZHEIGHTS

EDIT ZHEIGHTS REFERENCE TYPE TOOLPATH

EDIT ZHEIGHTS REFERENCE ACTION APPENDTOP

EDIT ZHEIGHTS REFERENCE select "3"

EDIT PCUTDIR CLIMB

ZHEIGHTS ACCEPT

EDIT ACUTDIR CONVENTIONAL

EDIT PMOVES AFTER

FORM TOOLAXIS

EDIT TOOLAXIS TYPE VERTICAL

TOOLAXIS ACCEPT

EDIT LMOVES PLUNGE

SET POCKET

EDIT AUTOANGLEMODE MANUAL

EDIT RANGLE 19

EDIT AREACLEAR TYPE MODEL

EDIT CUTTERCOMP TYPE AUTOMATIC

EDIT FLAT_TOLERANCE 0.001

PROCESS ZHEIGHTS

ZHEIGHTS ACCEPT

EDIT PMOVES AFTER

BATCH TOOLPATH "1_1" OFF

EDIT TOOLPATH "1_1" CALCULATE

EDIT TOOLPATH "1_1" RECYCLE

EDIT TOOLPATH "1_1" REAPPLYFROMGUI

EXPLORER SELECT Toolpath "Toolpath\1_1" NEW

RENAME Toolpath "1_1" "3"

…

…

NCTOOLPATH APPLY

NCTOOLPATH ACCEPT

EDIT TOOLPATH "124" REAPPLYFROMGUI

EXPLORER SELECT Toolpath "Toolpath\125" NEW

ACTIVATE TOOLPATH "125"

CREATE NCPROGRAM "125" EDIT NCPROGRAM "125" APPEND TOOLPATH "125"

DEACTIVATE NCPROGRAM

```
EXPLORER SELECT NCProgram "NCProgram\125" NEW
 EDIT NCPROGRAM "125" LOADTOOL AUTOMATIC
 EDIT NCPROGRAM "125" ITEM 0 COMPONENT 4 TOOLNUMBER "1"
 EDIT NCPROGRAM "125" ITEM 0 COMPONENT 4 COOLANT NONE
 EDIT NCPROGRAM "125" ITEM 0 COMPONENT 4 CYCLES OFF
 EDIT NCPROGRAM "125" ITEM 0 COMPONENT 4 LENGTHCOMP OFF
 EDIT NCPROGRAM "125" ITEM 0 COMPONENT 4 COMP_CODE NONE
 ACTIVATE NCPROGRAM "125" KEEP NCPROGRAM ;
YES
NCTOOLPATH APPLY
NCTOOLPATH ACCEPT
 EDIT TOOLPATH "125" REAPPLYFROMGUI
```

APPENDIX B

POST PROCESSOR

```
machine fanuc15m

#################################################
# Company   - Cardiff MEC                       #
# Machine   - Oxford Laser                              #
# Control           - Aerotech                                  #
#                                                               #
# Axis Configuration Code : 5220                #
#               ---------------                 #
#                               | HEAD  | TABLE |               #
#  ---------------|-------|-------|              #
# |    A axis         |   -         |   Y   |                  #
# |---------------|-------|-------|              #
# |    B axis         |   -   |   Z   |          #
# |---------------|-------|-------|              #
# |    C axis         |   -         |   -   |  #
#  ------------------------------               #
#                                                               #
# Metric output                         |  1  |         #
# Absolute output                       |  1  |         #
# Cutter Compensation                   |  1  |         #
# Drilling cycles               |  0  |           #
# Drilling cycles 200 series            |  0  |         #
# Parameterised feedrates   |  0  |           #
# Inverse time feedrates    |  0  |           #
# RTCP                                  |  0  |         #
# Active Working Plane                  |  0  |         #
# Connection moves enabled              |  1  |         #
# Spline machining                      |  0  |         #
#                                                               #
#################################################
#
#
# # Modified by PVP - 16.08.2008
# Modified by PVP - 17.01.2009 - without pso output
# Modified by PVP - 13.02.2009 - = removed for skim rate
# pvp - G108 and G301 added
# PVP - G108 and G301 Blanked    17-04-09
#50
  define word %D
    address letter  = " "
    address width   = 1
    field width     = 2
    decimal places  = 0
    decimal point   = false
    leading zeros   = true
    trailing zeros  = true
    imperial formats = metric formats
  end define
#61
  define word %M
    address letter  = "."
    address width   = 1
    field width     = 2
    decimal places  = 0
    decimal point   = false
```

```
    leading zeros   = true
    trailing zeros  = true
    imperial formats = metric formats
  end define
#72
  define word %Y
    address letter  = "."
    address width   = 1
    field width     = 2
    decimal places  = 0
    decimal point   = false
    leading zeros   = true
    trailing zeros  = true
    imperial formats = metric formats
  end define
#83
  define word %h
    address letter  = " - "
    address width   = 3
    field width     = 2
    decimal places  = 0
    decimal point   = false
    leading zeros   = true
    trailing zeros  = true
    imperial formats = metric formats
  end define
#94
  define word %m
    address letter  = ":"
    address width   = 1
    field width     = 2
    decimal places  = 0
    decimal point   = false
    leading zeros   = true
    trailing zeros  = true
    imperial formats = metric formats
  end define
#105
  define word %s
    address letter  = ":"
    address width   = 1
    field width     = 2
    decimal places  = 0
    decimal point   = false
    leading zeros   = true
    trailing zeros  = true
    imperial formats = metric formats
  end define
#116
  define word TOL
    address letter = " "
    address width  = 1
    field width    = 5
    metric formats
    decimal places = 3
    decimal point  = true
    leading zeros  = false
    trailing zeros = false
```

```
    imperial formats
    decimal places = 4
    decimal point  = true
    leading zeros  = false
    trailing zeros = false
  end define
#132
   define word PMCB
    address letter = ""
    address width  = 0
    field width    = 5
    tape position  = 1
    upper case
    imperial formats = metric formats
  end define
#141
  define word PMCBR
    address letter = ""
    address width  = 0
    field width    = 2
    tape position  = 0
    upper case
    imperial formats = metric formats
  end define
#150
 define word TXT
    address letter = " "
    address width  = 1
    field width    = 32
    tape position  = 0
    upper case
    imperial formats = metric formats
  end define
#159
#  ======== Toolpath time Words ========
#
   define word STORE
    address width  = 1
    field width    = 30
    leading zeros  = false
    trailing zeros = true
    decimal point  = false
    decimal places = 0
    sign           = none
    tape position  = 1
    permanent
    modal
    imperial formats = metric formats
  end define
#175
  define word tpt
    address letter = ""
    address width  = 0
    field width    = 0
    decimal places = 3
    scale factor   = 1
    decimal point  = true
    leading zeros  = true
```

```
    trailing zeros = true
    permanent
    imperial formats = metric formats
  end define
#188
  define word secs
    address letter = ""
    address width  = 0
    field width    = 0
    decimal places = 0
    decimal point  = false
    leading zeros  = true
    trailing zeros = true
    imperial formats = metric formats
  end define
#199
  define word mins
    address letter = ""
    address width  = 0
    field width    = 0
    decimal places = 0
    decimal point  = false
    leading zeros  = true
    trailing zeros = true
    imperial formats = metric formats
  end define
#210
  define word hrs
    address letter = ""
    address width  = 0
    field width    = 0
    decimal places = 0
    decimal point  = false
    leading zeros  = true
    trailing zeros = true
    imperial formats = metric formats
  end define
#221
  define word act
    address letter = ""
    address width  = 0
    field width    = 0
    decimal places = 3
    scale factor   = 1
    decimal point  = true
    leading zeros  = true
    trailing zeros = true
    permanent
    imperial formats = metric formats
  end define
#234
  define word %th
    address letter = " "
    address width  = 1
    field width    = 2
    decimal point  = false
    leading zeros  = true
    trailing zeros = true
```

```
    imperial formats = metric formats
  end define
#244
#  ===================================
#246
  define word M3
    address letter = "M"
    address width  = 1
    field width    = 3
    tape position  = 1
    imperial formats = metric formats
  end define
#254
  define word M4
    address letter = "M"
    imperial formats = metric formats
  end define
#259
  define word M5
    address letter = "M"
    imperial formats = metric formats
  end define
#264
  define word DW
    address letter = "P"
    address width  = 1
    metric formats
    scale factor   = 100
    decimal places = 0
    decimal point  = false
    trailing zeros = true
    tape position  = 1
    imperial formats = metric formats
  end define
#276
  define word G8
    address letter = "G"
    address width  = 1
    field width    = 2
    metric formats
    decimal places = 0
    decimal point  = false
    leading zeros  = true
    trailing zeros = true
    tape position  = 1
    imperial formats = metric formats
  end define
#289
  define word DTM
    address letter  = ""
    address width   = 0
    field width     = 2
    tape position   = 1
    permanent
    imperial formats = metric formats
  end define
#298
  define format ( ID )
```

```
    address letter = "O"
    address width  = 1
    field width    = 4
    upper case
    imperial formats = metric formats
  end define
#306
  define format ( N )
    not permanent
  end define
#310
  define format ( G4 H )
    leading zeros  = true
  end define
#314
  define format ( G7 )
    address width  = 1
    field width    = 3
    leading zeros  = true
    trailing zeros = true
    imperial formats = metric formats
  end define
#
define format ( X )
    address letter = "GX"
    address width  = 2
    scale factor = -1
  end define
#335
  define format ( Y )
    address letter = "GY"
    address width  = 2
    scale factor = -1
  end define
#322
  define format ( X Y Z I J K R )
    metric formats
    decimal places = 3
    decimal point  = true
    leading zeros  = false
    trailing zeros = false
    imperial formats
    decimal places = 6
    decimal point  = true
    leading zeros  = false
    trailing zeros = false
  end define
#335
  define format ( A B C )
    field width    = 8
    metric formats
    decimal place  = 3
    decimal point  = true
    leading zeros  = false
    trailing zeros = false
    sign           = if negative
    tape position  = 1
    modal
```

```
    imperial formats = metric formats
  end define
#348
  define format ( Z )
    scale factor  = -1
  end define
#335
  define format ( K )
    scale factor = -1
  end define
#352
  define format ( P )
    field width   = 4
    leading zeros = true
    imperial formats = metric formats
  end define
#358
  define word E
    field width     = 5
    tape position   = 1
    modal
    imperial formats = metric formats
  end define
#360
  define format ( S )
    address letter = "FireDistance = "
    address width  = 15
    field width    = 8
    metric formats
    leading zeros  = true
    trailing zeros = true
    decimal places = 5
    decimal point  = true
    imperial formats = metric formats
  end define
#362
  define format ( E F )
    scale divisor  = 60
    imperial formats = metric formats
  end define
#365
  define format ( H M1 M2 S )
    modal
  end define
#369
  define format ( tpt )
    tape position  = -25
  end define
#373
  word order = ( N MS msg EM )
#375
  define keys
    azimuth axis     = A
    elevation axis   = B
    radius           = R
  end define
#381
  define codes
```

```
    imperial data    = G4 70
    metric data      = G4 71
    cycle retract    not used
    drill            not used
    break chip       not used
    deep drill       not used
    tap              not used
    bore 1           not used
    bore 2           not used
    coolant on mist  not used
    coolant on       not used
    coolant on flood not used
    coolant off      not used
  end define
#397
  units                = input
  option file units      = metric
  message output         = false
  block order            = true
  block start            = 10
  block increment        = 1
  tool reset coordinates = 1
  integer 6              = 0
  integer 26             = 1
  integer 51             = 4
  integer 69             = 2
  full circle            = false
  incremental centre     = true
  suppress xz arc        = false
  suppress yz arc        = false
  arc radius limit       = 10000.0
  arc minimum radius     = 0.2
  maximum feedrate       = 20000.0
  rapid feedrate         = 20000.0
  zero                   = "0.0"
  segment type           = 2
  maximum tape blocks    = 100
  tape split retract distance = 0
#418
  spindle azimuth rotation   = false
  azimuth axis units         = degrees
  azimuth axis direction     = positive
  azimuth centre             = ( 0.0 0.0 0.0 )
  azimuth axis param         = ( 431.388 165.643 -30.66  -1.0 0.0 0.0 )
#424
  spindle elevation rotation = false
  elevation axis units       = degrees
  elevation axis direction   = positive
  elevation centre           = ( 0.0 0.0 0.0 )
  elevation axis param       = ( 431.388 165.643 -30.66  0.0 -1.0 0.0 )
#430
  pcs origin                 = ( 0.0 0.0 0.0  0.0 0.0 0.0 )
  linear axis limits         = ( -3000.0 3000.0 -2000.0 2000.0 -1000.0 1000.0 )
  rotary axis limits         = ( -10.0  10.0 -10.0 10.0 0.05 1 )
#434
  initial tool vector        = ( 0 0 1 )
  workplane angles             = none
  retract at angular limit     = true
```

```
  retract and reconfigure style  = linearise
  unwind at tool change          = false
  multiaxis coordinate transform = true
  linearise multiaxis moves      = true
  linearise first move           = false
  use fiveaxis always            = true
  multiaxis toollength used      = true
  withdrawal amount              = 100.0
  integer 3                      = 1
#447
  define block tape start
    if ( DPversion < 1470 )
      error " MINIMUM DUCTPOST VERSION REQUIRED = 1470"
    end if
    "%"
  end define
#455
  define block tool change first
    ID SpecialRecord[45]
    N ; "; PROGRAM NAME  : " ; TXT JobName
    N ; "; PART NAME     : " ; TXT PartID
    N ; "; PROGRAM DATE  : " ; %D Day  ; %M Month   ; %Y Year ;
                               %h Hour ; %m Minutes ; %s Seconds
    N ; "; PROGRAMMED BY : " ; TXT Programmer
    N ; "; POWERMILL CB  : " ; PMCB  PMCodeBase ; PMCBR PMCodeBaseRevision
    N ; "; DP VERSION    : " ; TXT DPversion
    N ; "; OPTION FILE   : " ; TXT OptionFileName
    N ; "; OUTPUT WORKPLANE :" ; TXT OutputWorkPlaneName
    N ; ";   "
    repeat ( NumberToolPaths )
      tpt ToolPathTime[LoopCounter] ; act ( Word{act} + Word{tpt} )
    end repeat
    N ; "; ESTIMATED CUTTING TIME :" ; STORE NumberToolPaths =C ; " TOOLPATHS = " ;
      secs ( Word{act} % 60 ) ;
      mins ( Word{act} - Word{secs} / 60 % 60 ) ;
      hrs  ( Word{act} / 60 - Word{mins} / 60 ) ;
      %th Word{hrs} ; %m Word{mins} ; %s Word{secs}
    N ; ";   "
    tpt 0
    act 0
    N ; "#define FireDistance $global1"
    N ; S ToolSpeed[ToolNum]
    N ; "MSGCLEAR -1"
    #N ; "ENABLE X Y Z A B GX GY"
    N ; "BEAMOFF"
    #N ; "HOME Z X Y GX GY A B"
    #N ; ":UseCurrentFireDistance"
    N ; "MSGDISPLAY 1, \""; TXT JobName ; ": Program Started\""
    N ; "MSGDISPLAY 1, \"{#F3 #F}\" \"Time is #TM\""
    # N ; "MSGDISPLAY 1, \"Using Without PSO \"
    N ; G4 TapeUnits
    N ; G6 76
    N ; absolute data =C
    N ; "DRIVECMD GX 67 3 1 0 0 0 0 0"
    N ; "DRIVECMD GY 67 3 1 0 0 0 0 0"
    N ; "A-0.1297 B-0.3"
    # N ; "G108"
    # N ; "G301"
```

```
    set swb
  end define
#485
  define block tool change
    N ; absolute data =C
    set swb
  end define
#490
  define block move from
  end define
#493
  # swa - controls output of toolpath and workplane names
  # swb - controls first move after tool change
  # swc - controls laser on
  # swd - controls laser off
  # swe - controls macro call to camera 1
  # swf - controls macro call to camera 2
  # swg - controls macro call to Laser power check
#499
  define block cldat 1094
    set swa
    set swc
  end define
#504
   define block ppfun camera1
     set swe
   end define
#508
   define block ppfun camera2
     set swf
   end define
#508
   define block ppfun pm532
     set swh
   end define
#508
 define block tape segment
   if ( swe )
     N ; "/CALL CAM1"
   end if
   if ( swf )
     N ; "/CALL CAM2"
   end if
   if ( swg )
     N ; "/CALL PM532"
   end if
 end define
#511
 define block move rapid
    if ( swa )
      N ; "; ========= "
      N ; "; TOOLPATH  : " ; TXT ToolPathName
      N ; "; ========= "
      unset swa
    end if
    if ( swb )
      N ; rapid ; absolute data ; x coord ; y coord
      N ; rapid ; z coord
```

```
    unset swb
   else
    N ; rapid ; absolute data ; x coord ; y coord ; z coord
   end if
  end define
#524
  define block move linear
   if ( swa )
    N ; "; ========= "
    N ; "; TOOLPATH  : " ; TXT ToolPathName
    N ; "; ========= "
    unset swa
   end if
   if ( swb )
    N ; linear ; G8 98 ; elevation axis ; azimuth axis ; E Srat ; feedrate Srat
    N ; linear ; x coord ; y coord
    N ; linear ; z coord
    unset swb
   else
    if ( feedrate == Frat and swc )
     N ; "BEAMON"
     N ; linear ; x coord ; y coord ; z coord ;
        elevation axis ; azimuth axis ; E feedrate ; feedrate
     unset swc
     set swd
    else if ( feedrate > Srat )
     if ( swd )
      N ; "BEAMOFF"
      unset swd
      set swc
     end if
     N ; linear ; x coord ; y coord ; z coord ;
        elevation axis ; azimuth axis ; E Srat ; feedrate Srat
     set swc
    else
     N ; linear ; G2 ; x coord ; y coord ; z coord ;
        elevation axis ; azimuth axis ; E feedrate ; feedrate
     set swd
    end if
   end if
  end define
#559
  define block move circle
   N ; G1 ; G3 ; x coord ; y coord ; z coord ;
            key i ; key j ; key k ; E feedrate ; feedrate
  end define
#563
  define block tape end
   N ; "BEAMOFF"
   N ; "MSGDISPLAY 1, \"{#F3 #F}\" \"Time is #TM\""
   N ; "MSGDISPLAY 1, \"Local Program Finished\""
   # N ; M1 2
  end define
#567
end
```

APPENDIX C

INDIVIDUAL STATISTICAL ANALYSIS

Appendixes

1.35		Average-cell
1.339	1.378958	0.039958
1.374	1.378958	0.004958
1.372	1.378958	0.006958
1.371	1.378958	0.007958
1.42	1.378958	-0.04104
1.381	1.378958	-0.00204
1.36	1.378958	0.018958
1.373	1.378958	0.005958
1.326	1.378958	0.052958
1.364	1.378958	0.014958
1.37	1.378958	0.008958
1.359	1.378958	0.019958
1.382	1.378958	-0.00304
1.375	1.378958	0.003958
1.38	1.378958	-0.00104
1.379	1.378958	-4.2E-05
1.413	1.378958	-0.03404
1.351	1.378958	0.027958
1.399	1.378958	-0.02004
1.45	1.378958	-0.07104
1.352	1.378958	0.026958
1.392	1.378958	-0.01304
1.415	1.378958	-0.03604
1.398	1.378958	-0.01904
1.378958	Aver	
1.35	Nom	
-0.02896		
0.027423	STDEV	

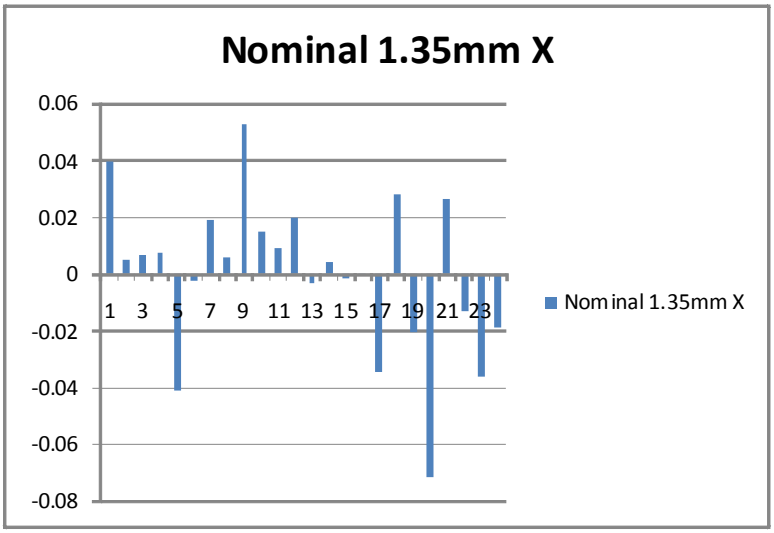

3.75	Average	Average-cell
3.653	3.712667	0.059667
3.697	3.712667	0.015667
3.69	3.712667	0.022667
3.714	3.712667	-0.00133
3.814	3.712667	-0.10133
3.695	3.712667	0.017667
3.7	3.712667	0.012667
3.727	3.712667	-0.01433
3.687	3.712667	0.025667
3.702	3.712667	0.010667
3.68	3.712667	0.032667
3.711	3.712667	0.001667
3.725	3.712667	-0.01233
3.714	3.712667	-0.00133
3.761	3.712667	-0.04833
3.731	3.712667	-0.01833
3.734	3.712667	-0.02133
3.689	3.712667	0.023667
3.725	3.712667	-0.01233
3.764	3.712667	-0.05133
3.689	3.712667	0.023667
3.717	3.712667	-0.00433
3.694	3.712667	0.018667
3.691	3.712667	0.021667
3.712667	Aver	
3.75	Nom	
0.037333	Nom-Aver	
0.033058	STDEV	

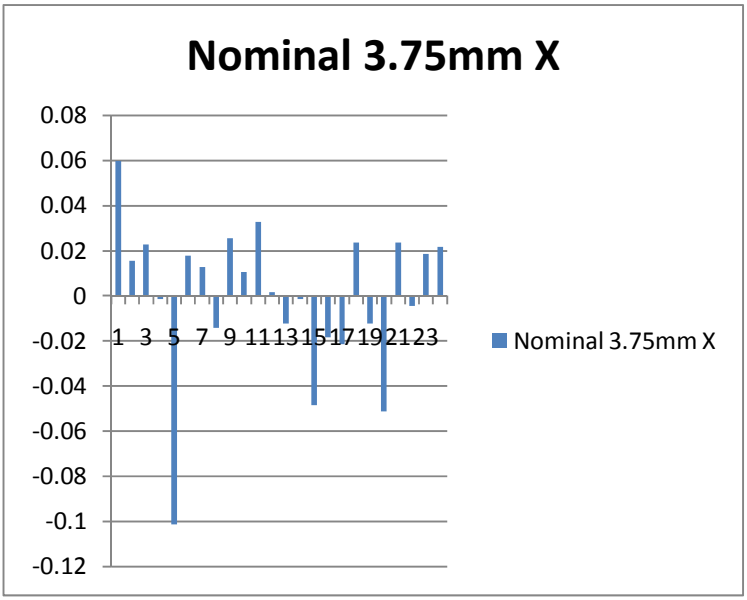

4.75	Average	Average-cell
4.717	4.68425	-0.03275
4.678	4.68425	0.00625
4.673	4.68425	0.01125
4.666	4.68425	0.01825
4.724	4.68425	-0.03975
4.671	4.68425	0.01325
4.694	4.68425	-0.00975
4.682	4.68425	0.00225
4.689	4.68425	-0.00475
4.677	4.68425	0.00725
4.664	4.68425	0.02025
4.676	4.68425	0.00825
4.68	4.68425	0.00425
4.701	4.68425	-0.01675
4.703	4.68425	-0.01875
4.667	4.68425	0.01725
4.679	4.68425	0.00525
4.69	4.68425	-0.00575
4.679	4.68425	0.00525
4.674	4.68425	0.01025
4.687	4.68425	-0.00275
4.692	4.68425	-0.00775
4.683	4.68425	0.00125
4.676	4.68425	0.00825
4.68425	Aver	
4.75	Nom	
0.06575	Nom-Aver	
0.015121	STDEV	

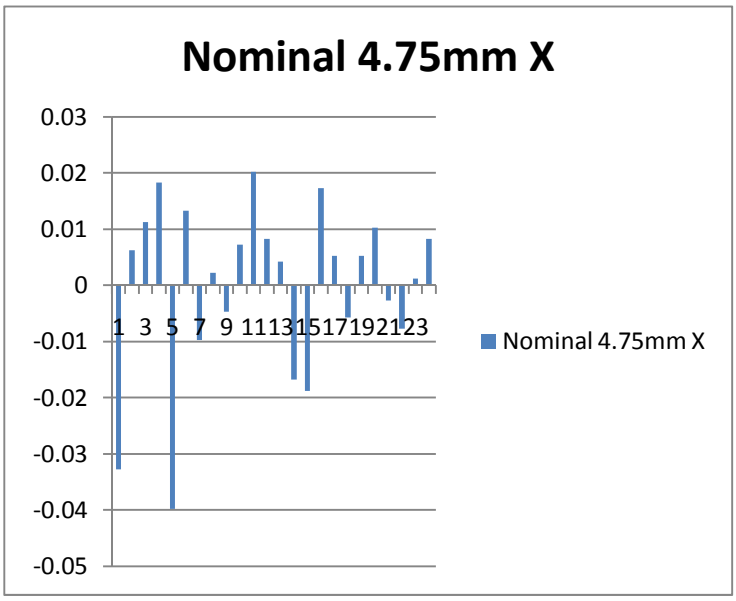

Appendixes

5	Average	Average-cell
4.899	4.849917	-0.04908
4.823	4.849917	0.026917
4.863	4.849917	-0.01308
4.835	4.849917	0.014917
4.844	4.849917	0.005917
4.841	4.849917	0.008917
4.866	4.849917	-0.01608
4.843	4.849917	0.006917
4.874	4.849917	-0.02408
4.858	4.849917	-0.00808
4.83	4.849917	0.019917
4.822	4.849917	0.027917
4.844	4.849917	0.005917
4.844	4.849917	0.005917
4.846	4.849917	0.003917
4.843	4.849917	0.006917
4.838	4.849917	0.011917
4.847	4.849917	0.002917
4.831	4.849917	0.018917
4.856	4.849917	-0.00608
4.857	4.849917	-0.00708
4.86	4.849917	-0.01008
4.853	4.849917	-0.00308
4.881	4.849917	-0.03108
4.849917	Aver	
5	Nom	
0.150083	Nom-Aver	
0.018149	STDEV	

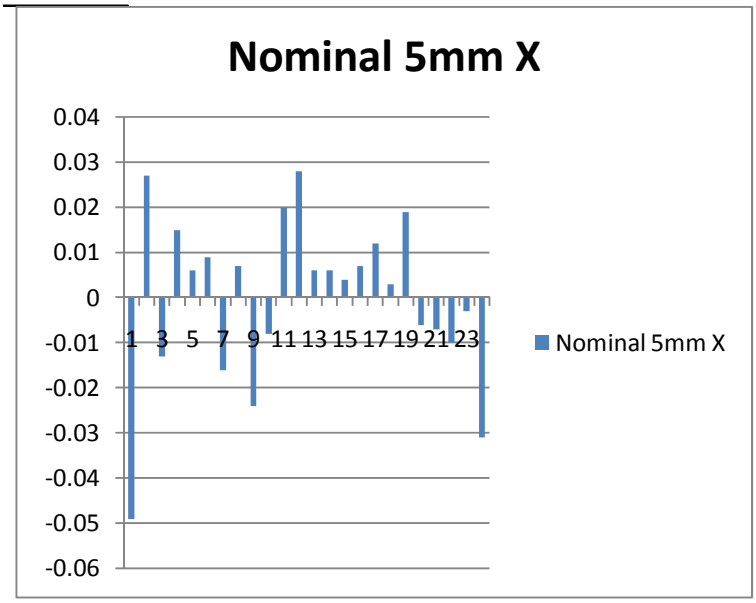

Appendixes

6	Average	Average-cell
6.088	6.036792	-0.05121
6.03	6.036792	0.006792
6.062	6.036792	-0.02521
6.022	6.036792	0.014792
6.033	6.036792	0.003792
6.05	6.036792	-0.01321
6.058	6.036792	-0.02121
6.015	6.036792	0.021792
6.087	6.036792	-0.05021
6.035	6.036792	0.001792
6.026	6.036792	0.010792
6.025	6.036792	0.011792
5.98	6.036792	0.056792
6.017	6.036792	0.019792
6.045	6.036792	-0.00821
6.034	6.036792	0.002792
6.02	6.036792	0.016792
6.052	6.036792	-0.01521
6.043	6.036792	-0.00621
6.011	6.036792	0.025792
6.04	6.036792	-0.00321
6.055	6.036792	-0.01821
6.039	6.036792	-0.00221
6.016	6.036792	0.020792
6.036792	Aver	
6	Nom	
-0.03679	Nom-Aver	
0.023869	STDEV	

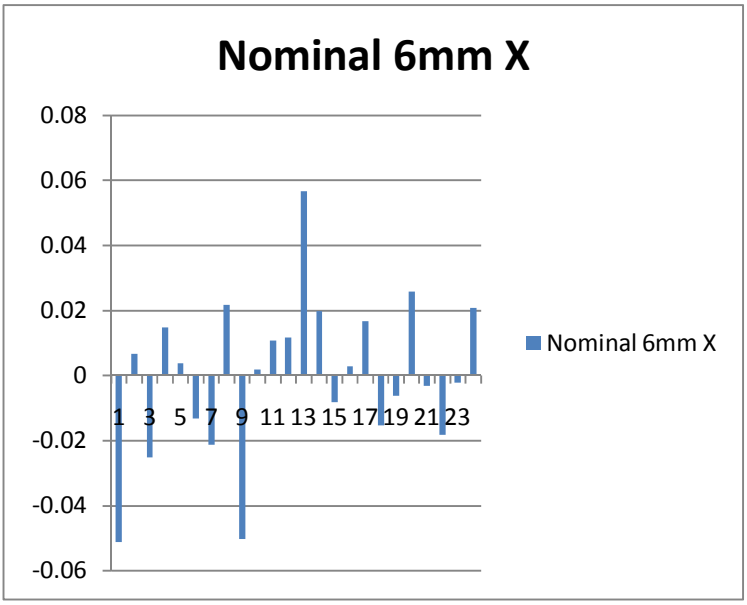

Appendixes

0.5	Average	Average-cell
0.456	0.464667	0.008667
0.452	0.464667	0.012667
0.465	0.464667	-0.00033
0.47	0.464667	-0.00533
0.458	0.464667	0.006667
0.456	0.464667	0.008667
0.452	0.464667	0.012667
0.472	0.464667	-0.00733
0.392	0.464667	0.072667
0.48	0.464667	-0.01533
0.476	0.464667	-0.01133
0.46	0.464667	0.004667
0.481	0.464667	-0.01633
0.468	0.464667	-0.00333
0.481	0.464667	-0.01633
0.481	0.464667	-0.01633
0.478	0.464667	-0.01333
0.446	0.464667	0.018667
0.464	0.464667	0.000667
0.486	0.464667	-0.02133
0.468	0.464667	-0.00333
0.47	0.464667	-0.00533
0.47	0.464667	-0.00533
0.47	0.464667	-0.00533
0.464667	Aver	
0.5	Nom	
0.035333	Nom-Aver	
0.018828	STDEV	

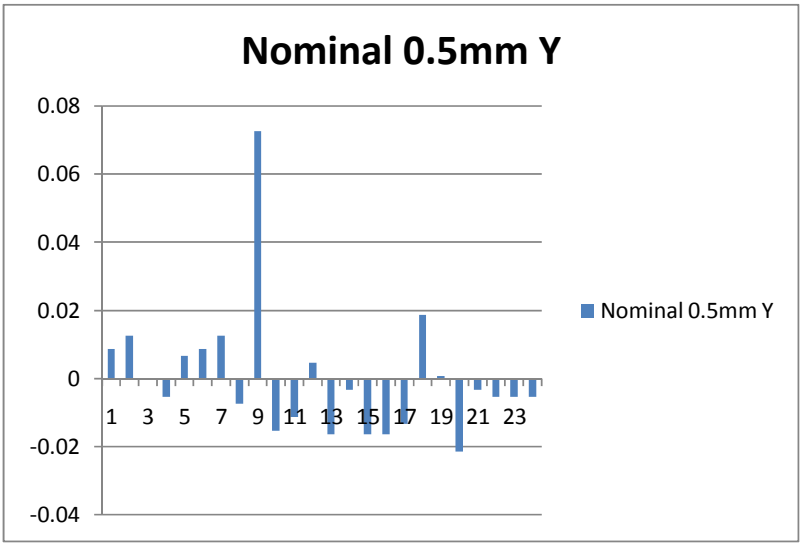

0.5	Average-cell	Average-cell
0.476	0.468042	-0.00796
0.475	0.468042	-0.00696
0.471	0.468042	-0.00296
0.472	0.468042	-0.00396
0.457	0.468042	0.011042
0.459	0.468042	0.009042
0.461	0.468042	0.007042
0.471	0.468042	-0.00296
0.395	0.468042	0.073042
0.474	0.468042	-0.00596
0.474	0.468042	-0.00596
0.47	0.468042	-0.00196
0.481	0.468042	-0.01296
0.477	0.468042	-0.00896
0.476	0.468042	-0.00796
0.485	0.468042	-0.01696
0.484	0.468042	-0.01596
0.448	0.468042	0.020042
0.473	0.468042	-0.00496
0.485	0.468042	-0.01696
0.462	0.468042	0.006042
0.467	0.468042	0.001042
0.473	0.468042	-0.00496
0.467	0.468042	0.001042
0.468042	Aver	
0.5	Nom	
0.031958	Nom-Aver	
0.017984	STDEV	

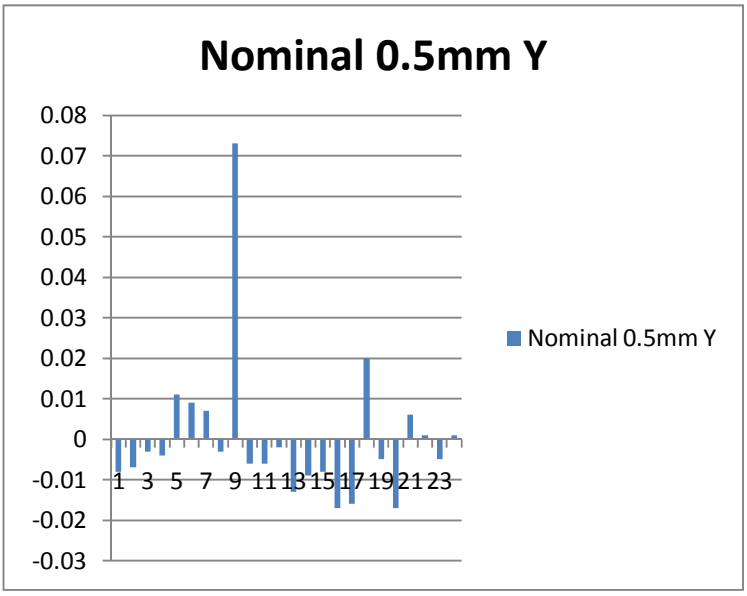

1.7	Average-cell	Average-cell
1.561	1.559583	-0.00142
1.528	1.559584	0.031584
1.565	1.559584	-0.00542
1.554	1.559584	0.005584
1.631	1.559585	-0.07142
1.563	1.559585	-0.00342
1.573	1.559585	-0.01341
1.557	1.559585	0.002585
1.577	1.559586	-0.01741
1.554	1.559586	0.005586
1.563	1.559586	-0.00341
1.552	1.559587	0.007587
1.557	1.559587	0.002587
1.552	1.559587	0.007587
1.549	1.559588	0.010588
1.542	1.559588	0.017588
1.542	1.559588	0.017588
1.567	1.559588	-0.00741
1.572	1.559589	-0.01241
1.536	1.559589	0.023589
1.542	1.559589	0.017589
1.551	1.55959	0.00859
1.574	1.55959	-0.01441
1.568	1.55959	-0.00841
1.559583	Aver	
1.7	Nom	
0.140417	Nom-Aver	
0.019764	STDEV	

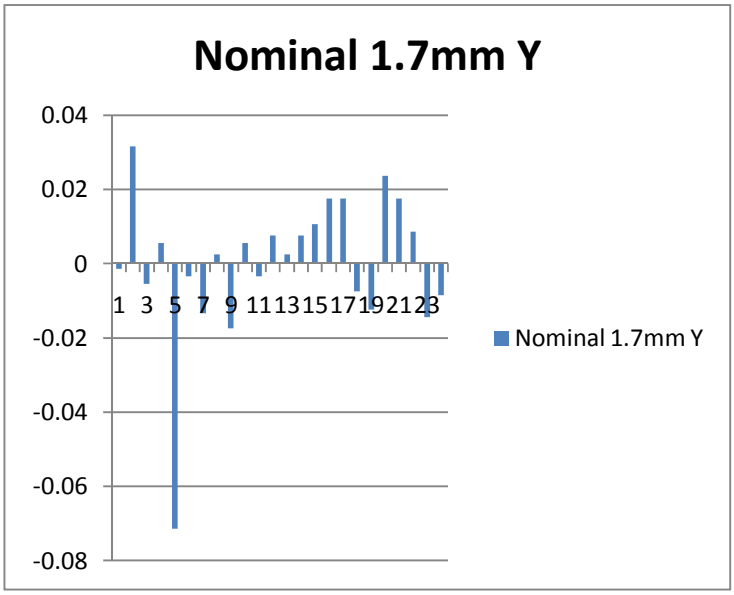

2.5	Average-cell	Average-cell
2.54	2.537958	-0.00204
2.439	2.537958	0.098958
2.606	2.537958	-0.06804
2.574	2.537958	-0.03604
2.585	2.537958	-0.04704
2.577	2.537958	-0.03904
2.558	2.537958	-0.02004
2.545	2.537958	-0.00704
2.549	2.537958	-0.01104
2.505	2.537958	0.032958
2.441	2.537958	0.096958
2.449	2.537958	0.088958
2.528	2.537958	0.009958
2.507	2.537958	0.030958
2.546	2.537958	-0.00804
2.585	2.537958	-0.04704
2.588	2.537958	-0.05004
2.537	2.537958	0.000958
2.581	2.537958	-0.04304
2.584	2.537958	-0.04604
2.523	2.537958	0.014958
2.518	2.537958	0.019958
2.529	2.537958	0.008958
2.517	2.537958	0.020958
2.537958	Aver	
2.5	Nom	
-0.03796	Nom-Aver	
0.04634	STDEV	

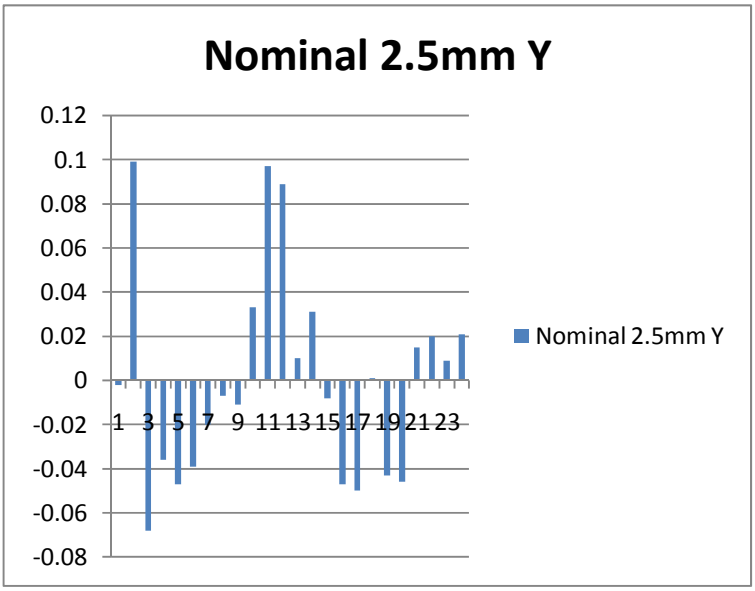

2.9	Average-cell	Average-cell
2.989	2.972917	-0.01608
2.969	2.972917	0.003917
2.962	2.972917	0.010917
2.974	2.972917	-0.00108
2.98	2.972917	-0.00708
2.997	2.972917	-0.02408
2.996	2.972917	-0.02308
2.979	2.972917	-0.00608
3.03	2.972917	-0.05708
2.927	2.972917	0.045917
2.978	2.972917	-0.00508
2.994	2.972917	-0.02108
2.913	2.972917	0.059917
2.925	2.972917	0.047917
2.957	2.972917	0.015917
2.97	2.972917	0.002917
2.979	2.972917	-0.00608
2.993	2.972917	-0.02008
2.996	2.972917	-0.02308
2.97	2.972917	0.002917
2.968	2.972917	0.004917
2.982	2.972917	-0.00908
2.985	2.972917	-0.01208
2.937	2.972917	0.035917
2.972917	Aver	
2.9	Nom	
-0.07292	Nom-Aver	
0.026461	STDEV	

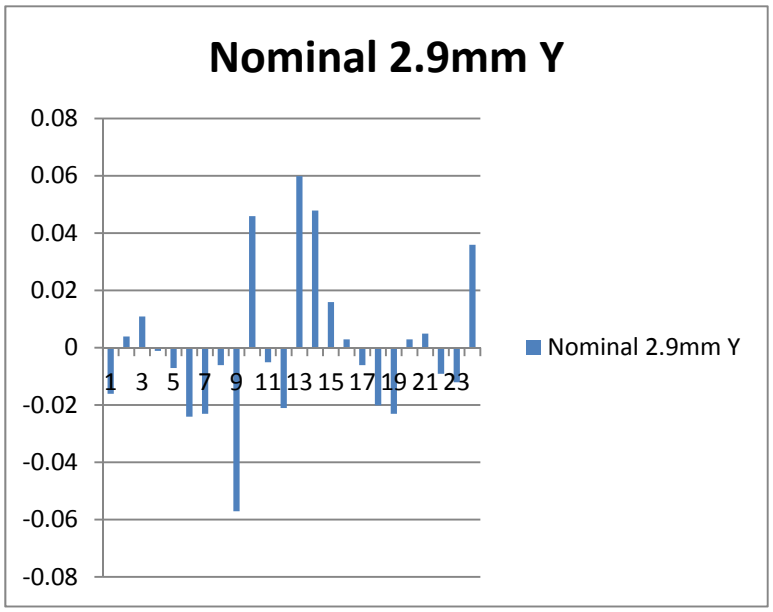

2.9	Average-cell	Average-cell
2.989	2.972917	-0.01608
2.969	2.972917	0.003917
2.962	2.972917	0.010917
2.974	2.972917	-0.00108
2.98	2.972917	-0.00708
2.997	2.972917	-0.02408
2.996	2.972917	-0.02308
2.979	2.972917	-0.00608
3.03	2.972917	-0.05708
2.927	2.972917	0.045917
2.978	2.972917	-0.00508
2.994	2.972917	-0.02108
2.913	2.972917	0.059917
2.925	2.972917	0.047917
2.957	2.972917	0.015917
2.97	2.972917	0.002917
2.979	2.972917	-0.00608
2.993	2.972917	-0.02008
2.996	2.972917	-0.02308
2.97	2.972917	0.002917
2.968	2.972917	0.004917
2.982	2.972917	-0.00908
2.985	2.972917	-0.01208
2.937	2.972917	0.035917
2.972917	Aver	
2.9	Nom	
-0.07292	Nom-Aver	
0.026461	STDEV	

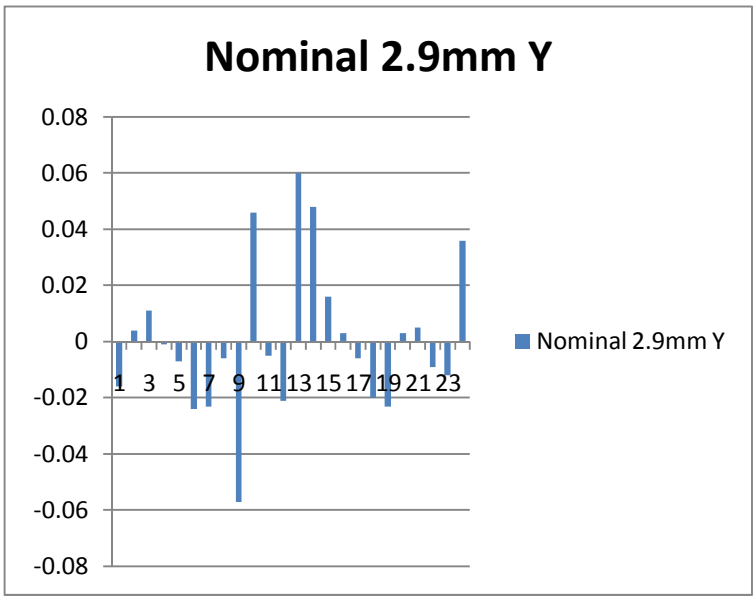

0.3	Average	Average-cell
0.29	0.283333	-0.00667
0.29	0.283333	-0.00667
0.3	0.283333	-0.01667
0.28	0.283333	0.003333
0.26	0.283333	0.023333
0.3	0.283333	-0.01667
0.29	0.283333	-0.00667
0.3	0.283333	-0.01667
0.2	0.283333	0.083333
0.29	0.283333	-0.00667
0.3	0.283333	-0.01667
0.3	0.283333	-0.01667
0.3	0.283333	-0.01667
0.29	0.283333	-0.00667
0.29	0.283333	-0.00667
0.28	0.283333	0.003333
0.28	0.283333	0.003333
0.27	0.283333	0.013333
0.3	0.283333	-0.01667
0.28	0.283333	0.003333
0.28	0.283333	0.003333
0.27	0.283333	0.013333
0.28	0.283333	0.003333
0.28	0.283333	0.003333
0.283333	Aver	
0.3	Nom	
0.016667	Nom-Aver	
0.02099	STDEV	

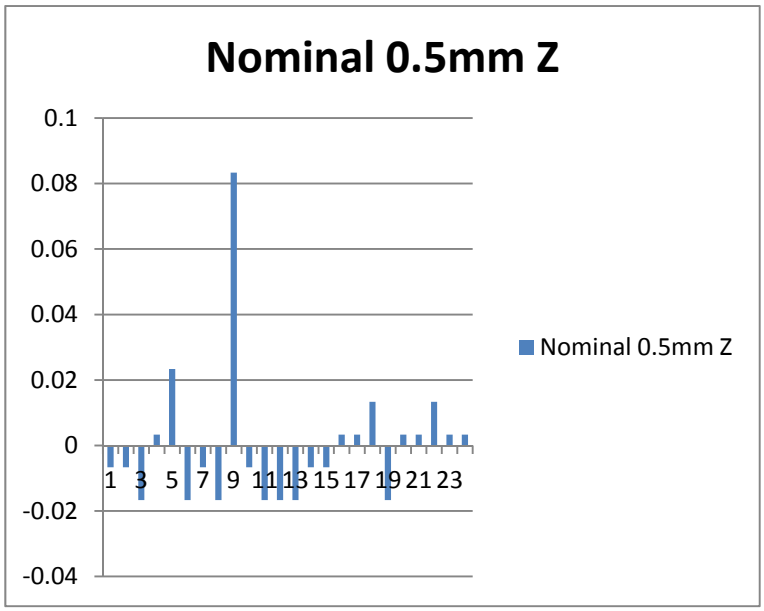

Appendixes

0.52	Average	Average-cell
0.44	0.50375	0.06375
0.49	0.50375	0.01375
0.5	0.50375	0.00375
0.52	0.50375	-0.01625
0.51	0.50375	-0.00625
0.47	0.50375	0.03375
0.51	0.50375	-0.00625
0.5	0.50375	0.00375
0.5	0.50375	0.00375
0.53	0.50375	-0.02625
0.5	0.50375	0.00375
0.5	0.50375	0.00375
0.51	0.50375	-0.00625
0.52	0.50375	-0.01625
0.52	0.50375	-0.01625
0.5	0.50375	0.00375
0.48	0.50375	0.02375
0.52	0.50375	-0.01625
0.52	0.50375	-0.01625
0.52	0.50375	-0.01625
0.51	0.50375	-0.00625
0.51	0.50375	-0.00625
0.5	0.50375	0.00375
0.51	0.50375	-0.00625
0.50375	Aver	
0.52	Nom	
0.01625	Nom-Aver	
0.019295	STDEV	

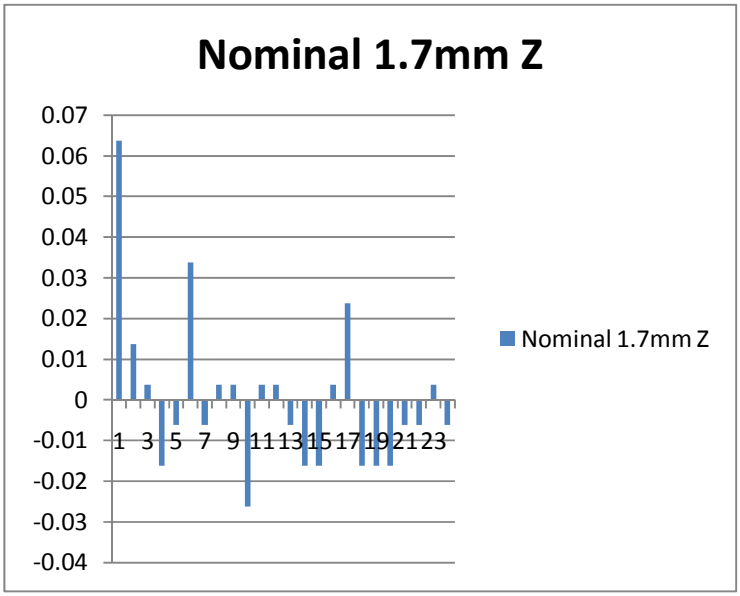

1.18	Average	Average-cell
1.19	1.1775	-0.0125
1.17	1.1775	0.0075
1.15	1.1775	0.0275
1.18	1.1775	-0.0025
1.17	1.1775	0.0075
1.18	1.1775	-0.0025
1.18	1.1775	-0.0025
1.18	1.1775	-0.0025
1.16	1.1775	0.0175
1.19	1.1775	-0.0125
1.18	1.1775	-0.0025
1.19	1.1775	-0.0125
1.17	1.1775	0.0075
1.18	1.1775	-0.0025
1.19	1.1775	-0.0125
1.17	1.1775	0.0075
1.15	1.1775	0.0275
1.21	1.1775	-0.0325
1.17	1.1775	0.0075
1.15	1.1775	0.0275
1.21	1.1775	-0.0325
1.21	1.1775	-0.0325
1.16	1.1775	0.0175
1.17	1.1775	0.0075
1.1775	Aver	
1.18	Nom	
0.0025	Nom-Aver	
0.017508	STDEV	

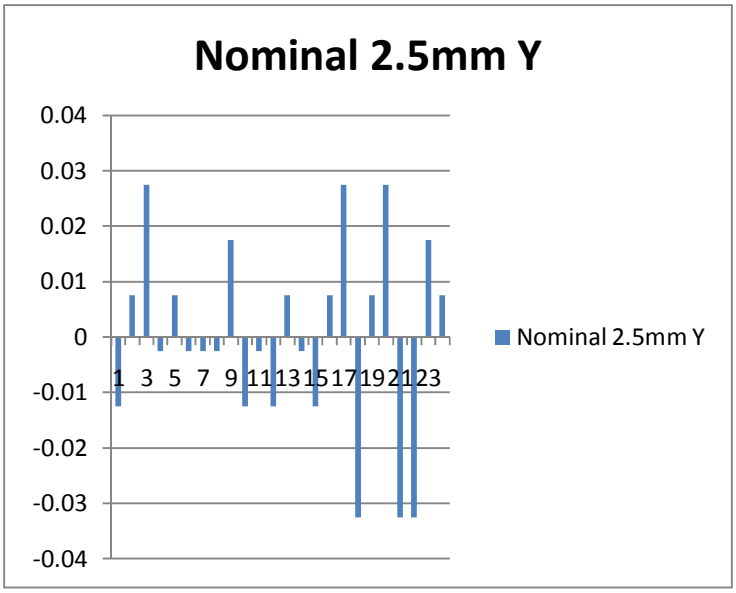

References

Aerotech 3200 **Instructions Manual**, 2005, Aerotech, USA

Beck W, 2000.**Recent advances in laser micro-machining**. Proceedings SPIE,2000, Vol. 4002, pp 2-15

Beyer E, Petring D, Zefferer H and Eberl G.,1994**. Laser caving: Rapid progress in an advanced technology**. Laser Assisted Net shape Engineering, Meisenbach Bamberg, Proceedings of the LANE'94, Vol. 1, pp 477-490

Breitlung D., Ruf A., Dausinger F.,2004. **Fundamental aspects in machining of metals with short and ultrashort laser pulses**.Proceedings of the SPIE, Volume 5339, pp. 49-63 (2004)

Buehler-Omnimet software manual, 2000. Buhler, USA

Burck P and Wiegel K, 1995. **Laser machining of Si3N4 ceramics**. Optical and Quantum Electronics, Vol. 27, pp 1349-1358

CarlZeiss SE/FIB, **Cross Beam®/FIB-SEM Instruction manual**, 2005,Zeiss, Germany

Chen K and Yao Y L, 2000. **Process optimisation in pulsed laser micromachining with applications in medical device manufacturing**. International Journal of Advanced Manufacturing Technology, Vol.16, pp 243-249

References

Chichkov B N, Momma C, Nolte S, von Alvensleben F and Tuennermann A, 1996. **Femtosecond, picosecond and nanosecond laser ablation of solids**. Applied Physics, A63, pp 109-115

Cline, H. E. And Anthony, T.R., 1977. **Heattreating and melting material with a scaning laser or electron beam**. Journal of Applied Physics, 1977, Vol. 48, pp.3895-3900

Costa A.P., Quintino L. And Greitmann M., 2003. **Laser beam welding hard metals to steel**. Journal of Materials Processing Technology, Volume 141, Issue2, 2003, pp.163-173

Dobrev T, S S Dimov, and A J Thomas.2008. **Laser milling: modelling crater and surface formation.** Proc. IMechE Vol. 220 Part C: J. Mechanical Engineering Science, 220 (C11), 1685-1696

Dörbecker C, Lubatschowski H, Lohmann S, Ruff C, Kermani O and Ertmer W, .1996.**Influence of the ablation plume on the removal process during the ArF-excimer laser photoablation**. Proceedings SPIE, Vol. 2632, pp 2-9

Eberl G, Hildebrand P, Kuhl M, Sutor U and Wrba P.1991. **New developments in the LASERCAVâ Technology.** ICALEO'91, Proceedings of the laser materials processing symposium, Laser Institute of America, Nov 3-8, San Jose, CA

References

Fahler, S. And Krebs, H. –U,1996. **Calculations and experiments of material removal and kinetic energy during pulsed laser ablation of metals**. Applied Surface Science, 1996, Vol.96-98, pp.61-65

Fiebig M, Kauf M, Fair J, Scaggs M, Endert H, Rahe M and Basting D, .1999. **Micromachining with 157 nm Radiation**. Euspen-Conference, Bremen, Germany, June 1999, pp 96-99

Foba-las - 1999, **operating manual, FOBA** GmbH Elektronik + Lasersysteme, Altenaer Strasse 168, D 58513 Luedenschied, Germany

Fraunhofer Institut Lasertechnik (ILT) website: http://www.ilt.fhg.de/eng/lasertypen.html Last visited: 29.01.211

Geiger M, Becker W, Rebhan T, Hutfless J and Lutz N, 1996. **Increase of efficiency for the XeCl excimer laser ablation of ceramics**. Applied Surface Science, Vol. 96-98, pp 309-315

Shirk M D and Molian P A, 1998. **A review of ultrashort pulsed laser ablation of materials**. Journal of Laser Applications, Vol. 10, No 1, pp 18-28

Good B. J., Jones R. D. And Howells J.N.H, 1998. **Ultrasonic pickling of steel strip**. Ultrasonics, Vol 36, 1998, p.79

References

Gotz, T.,Bergt, M., Hoheisel, W., Trager, F., Stuke, M.,1996. **Laser ablation of metals: the transition from non-thermal process to thermal evaporation**. Applied Surface Science, 1996,Volume96-98, pp.280-286

Haferkamp H and Seebaum D, 1994. **Material removal on tool-steel using high power CO2-lasers**. Laser Assisted Net shape Engineering, Meisenbach Bamberg, Proceedings of LANE'94, Vol. 1, pp 411-425

Harzic R. Le, Breitling D., Weikert M., Sommer S., Fohl C., Valette S., Donnet C., Audouard E. And Dausinger F.,2005**. Pulse width and energy influence on laser micromachining of metals in a range of 100fs to 5 ps**. Applied Surface Science. 2005

Hatano H. And Kanai S., 1996. **High-frequency ultrasonic clening tank utilising oblique incidence.** IEEE Transactions of Ultrasonics, Ferroelectrics, and Frequency Control, 1996, Vol43(4), pp.531-535

Hayl, P., Olschewski, T., Wijnaendts, R. W., (2001) **Manufacturing of 3D structures for micro-tools using laser ablation**. Microelectronic Engineering 57 – 58 (2001), pp. 775-780

Hellrung, D., Yeh, Li-Ya, Depiereux, Fr., Gillner, A., Poprawe, R., (1999) **High-accuracy micromachining of ceramics by frequency-tripled Nd:YAG lasers**. In Proceedings SPIE Vol. 3618 (1999), pp. 348-356

References

Heyl, P. Olchewski, T., Wijnaendts, R. W., 2001. **Manufacturing of 3D structures for micro tools using laser ablation**. Microelectronic Engineering, Volume 57-58, 2001, pp. 775-780

Hocheng H and Pa P.S, 2003.**Electropolishing of cylindrycal wokpiece of tool materials using disc form electrodes**. Journal of Materials Processing Technology Vol 142(2003), pp. 203-212

Hsu H.- T. And Lin J., 2005. **Thermal-mechanical analysis of the surface waves in laser cleanining**. International Jornal of Machine Tools & Manufacture, Vol.45(2005), pp.979-985

Surface Metrology Guide :http://www.predev.com/smg/standards.htm Last visited Jan2011

Ihlemann J and Rubahn K, 2000. **Excimer laser micro machining: fabrication and application of dielectric masks**. Applied Surface Science, Vol. 154-155, pp 587-592

International Organisation for Standards. http://www.iso.org.html, last visited: Jan, 2011

Jandeleit, J., Horn, A., Weichenhain, R., Kreutz, E. W., Poprawe, R., (1998) **Fundamental investigations of micromachining by nano- and picosecond laser radiation**. J. Applied Surface Science 127-129 (1998), pp. 885 – 891

References

Kao P Sand Hocheng H, 2003.**Optimizatin of electrochemical polishing of stainless steel by grey letaions analysis**. Journal of Materials Processing Technology, Vol. 140, 2003, pp.255-259

Karnakis D, Rutterford G, Knowles M, Dobrev T, Petkov P, Dimov SS, 2006. **High quality laser milling of ceramics, dielectrics and metals using nanosecond and picosecond lasers**, SPIE Photonics West LASE 2006, Volume 6106, San Jose CA, USA

Karnakis D.M., MRH Knowles, P. V.Petkov, T. Dobrev and S. S. Dimov (2007). **Surface integrity optimisation in ps-laser milling of advanced engineering materials**. Proc. 4th Int. WLT-Conference on Lasers in Manufacturing 2007, Germany, pp. 619-623

Kautek W and Krüger J, 1994. **Femtosecond pulse laser ablation of metallic, semiconducting, ceramic and biological materials**. Proceedings SPIE, Vol. 2207, pp 600-610

Kim J O, Choi S, Kim J H, 1999. **Vibroacoustic characteristics of ultrasonic cleaners**. Applied Acoustics, 1999, Vol. 58, pp.211-228

Knowles MRH, Rutterford G, Karnakis D, Dobrev T, Petkov P, Dimov SS,2006**. Laser micro-milling of ceramics, dielectrics and metals using nanosecond and picosecond lasers**. Proc. Of 4M, 2006, France, pp. 131 – 134

References

Koc A, Yilbas B S, Koc Y, Said S, Gbadebo S A and Sami M, 1998. **Material response to laser pulse heating: a kinetic theory approach**. Optics and Lasers in Engineering, Vol. 30, pp 327-350

Krüger J, Kautek W, Lenzner M, Sartania S, Spielmann C and Krausz F, 1998. **Laser micromachining of barium aluminium borosilicate glass with pulse durations between 20 fs and 3 ps**. Applied Surface Science, Vol. 127-129, pp 892-898

Lalev G, P Petkov, N Sykes, V Velkova, S Dimov, D Barrow,2008. **Template Fabrication incorporating different length scale features**. Proc. 4M, Cardiff, UK, pp261-264

Lasertech GmbH - 1999, presentations, operating manual, Gildemeister Lasertec GmbH, Tirolerstrasse 85, D 87459 Pfronten, Germany

Leong K, 2000.Drilling with lasers. **Industrial Laser Solutions for Manufacturing**,Vol. 15, No 9, pp 39

Li L. –F. And Celis J.-P,2003. **Pickling of austenitic stainless steel(a review)**. Canadian Metallurgical Quarterly, Vol. 42(2003), pp365-376

Lierath F., Pieper H.J., Wolf E., 2003. **Laser machining – a modern tooling process.** Proceedings of the CAMT Conference on Modern Trends in Manufacturing. Wroclaw, 2003, pp.433-446

References

Liu X, 2000. **Ultrafast lasers as a versatile processing tool**. Proceedings SPIE, Vol. 3888, pp 198-209

Liu, X., Du, D., and Mourou, G., 1997. **Laser ablation and micromachining with ultrashort laser pulses.** IEEE J. Quantum Electronics, 1997, Vol. 33, No. 10,pp.1706-1716

Lunney, J.G. and Jordan, R., 1998. **Pulsed laser ablation of metals**. Applied Surface Science, 1998, Vol.127,pp.941-946

Madou, M J, (2001). **Fundamentals of Microfabrication – The Science of Miniaturisation**. CRC Press, 2001

Meijer J., 2004**. Laser beam machining (LBM), state of the art and new opportunities.** Journal of Materials Processing Technology, Volume 149, Issues 1-3, 2004, pp2-17

Meiners E, Kessler A, Dausinger F and Hügel H, 1992. **Approaches in modelling of evaporative and melt removal processes in micro machining.** ECLAT'92, Proceedings of Laser Treatment of Material Conference, 1992 Göttingen, Germany, pp 705-710

Mendes M, Oliveira V, Vilar R, Beinhorn F, Ihlemann J and Conde O, 2000. **XeCl laser ablation of Al2O3-TiC ceramics.** Applied Surface Science, Vol. 154-155, pp 29-34

MicroXAM, 2003. MapVue software user manual. ADE Phaseshift, USA

References

Moldovan C ,Sosin S, Nedelcu Kaufmann U, Ritzhaupt-Kieissl H-J, Stefan Dimov, Petkov P, Dorey R, Persson K, Gormez D, Johander P, 2005. **Mixed technologies for gas sensors microfabrication,** Proc. 4M, Karlsruhe, Germany, pp.211-217

Momma C, Nolte S, Chichkov B N, von Alvensleben F and Tünnermann A, 1997.**Precise laser ablation with ultrashort pulses.** Applied Surface Science, Vol. 109-110, pp 15-19

Nantel M, Yashkir Y, Lee S K, Mugford C, and Hockley B S, 2001. **Laser micromachining of semiconductors for photonics applications.** Proceedings of SPIE- Vol. 4594, 2001, pp156-167

Nikumb S., Chen Q., Li C., Reshef H., Zheng H.Y, Qui H. And Low D., 2004. **Precision glass machining, drilling and profile cutting by short pulse lasers.** Thin Solid Films, Vol.477, Issues 1-2,2005, pp.216-221

Oliveira V, Vilar R and Conde O, 1998. **Excimer laser ablation of Al2O3-TiC ceramics: laser induced modifications of surface topography and structure.** Applied Surface Science, Vol. 127-129, pp 831-836

Petkov P V, S S Dimov, R M Minev and D T Pham,2008. **Laser milling: pulse duration effects on surface integrity.** 2008, Proceedings of IMechE Vol.222 PartB J Engineering Manufacture

References

Petkov P V, S Scholz and S Dimov, 2008 **. Strategies for material removal in laser milling**. Proc 4M, Cardiff, UK, 2008, pp249-252

Petkov P V, T Dobrev, D. T Pham and S Dimov (2007) .**Strategies for laser milling with microsecond pulses.** 8th Int. Conf. Lamdamap 2007, pp. 140-148

Petzoldt S., Reif J., Matthiias E., 1996**. Laser plasma threshold of metals**. Applied Surface Science, Vol. 96-98, 1996,pp.199-204

Pham D T, Dimov S S, Petkov P V, Petkov S P,2001**. Rapid manufacturing of ceramic parts.** Proceedings of 17th National Conference on Manufacturing Research, Cardiff, pp 211-216

Pham D T, S S Dimov, C Ji, P V Petkov and T Dobrev, (2003**). Laser milling as a "rapid" micro manufacturing process**, In Proc. 18th Int. Conference on Computer Aided Production Engineering, Edingburgh, Scotland

Pham D T, S S Dimov, P V Petkov and T Dobrev, 2005**. Laser milling for micro tooling.** LAMDAMAP'2005 7th International Conference and Exhibition on Laser Metrology, Machine Tool, CMM &Robotic Performance, Cranfield, UK, pp. 362 – 371

References

Pham D.T., S.S. Dimov and P.V. Petkov .**Laser milling of ceramic components .**International Journal of Machine Tools and Manufacture, Volume 47, Issues 3-4, March 2007, Pages 618-626

Pham, D. T., Dimov, S. S., Ji, C., Petkov, P. V., Dobrev, T., 2004**. Laser milling as a 'rapid' micromanufacturing process.** Proc. Institution of Mechanical Engineers, Volume 218 Part B: Journal of Engineering Manufacture, pp. 1 – 7

Pham, D. T., Dimov, S. S., Petkov, P. V., Petkov, S. P., (2002) .**Laser Milling**. In Proc Instn Mech Engrs Vol 216 Part B: J Engineering Manufacture (2002)

Preuss S, Demchuk A and Stuke M, 1995. **Sub-picosecond UV laser ablation of metals**. Applied Physics, A61, pp 33-37

Pronko P P, Dutta S K and Du D, November 1995. **Thermophysical effects in laser processing of materials with picosecond and femtosecond pulses**. Journal of Applied Physics, Vol. 78, No 10, pp 6233-6240

Pronko, P. P., Dutta, S. K., Squier, J., Rudd, J. V., Du, D., Mourou, G., (1995) **Machining of sub-micron holes using a femtosecond laser at 800 nm.** Optics Communications Vol. 114 (1995), pp. 106 – 110

QuickVision. QuickVision AccelPro user manual. Mitutoyo Corporation, Japan

References

Rizvi N.H. and Apte P., 2002. **Developments in laser micro –machining techniques**. Journal of Materials Processing Technology, Vol.127, Issue2, 2002, pp.206-210

Schubart D, Vollersten F and Kauf M, 1997. **Process modelling of laser ablating ferrous materials.** Modelling and Simulation in Materials Science and Engineering, Vol. 5, No 1, pp 79-92

Shao T.M., Hua M., Tam H.Y., E.H.M., 2005. **An approach to modelling of laser polishing of metals.** Surface and Coatings Technology, Vol.197, Issue 1, 2005,pp77-84

Steen W M, 1998. **Laser Materials Processing**. 2nd edition, London Springer

Tam A.C., Leung W.P., Zapka W. And Ziemlich W., 1992. **Laser cleaning techniiques for removal of surface particulates.** Journal of Applied Physics Volume 71(1992), pp 3515-3523

Toenshoff H K, Graumann K, Hessener H and Rinke M, 1998. **NC-controlled production of smooth 3-D surfaces in brittle materials with 193 nm-Eximer laser.** SPIE's International Symposium on Micromachining and Microfabrication, Santa Clara, USA, 20 - 24 Sept. 1998, pp 56-66

References

Toenshoff H K, Hesse D and Mommsen J, 1993. **Micromachining using excimer lasers.** Annals of CIRP, Vol. 42, No 1, pp 247-251

Toenshoff H K, von Alvensleben, Heekenjann P B and Willmann G, 1997. **Excimer laser machining of advanced materials**. SPIE Proceedings, Vol. 2992, pp 108-118

Toenshoff H K, von Alvensleben, Ostendorf A, Willmann G and Wagner T, 1999. **Precision machining using UV and ultrashort pulse laser.** SPIE Proceedings, Vol. 3680, pp 536-545

Tönshoff H K, Graumann C, Rinke M, Hesener H and Kulik C, 1998. **Comparison of 3-D surfaces produced by 248 nm- and 197 nm- excimer laser radiation**. Proceedings SPIE, Vol. 3519, pp 208-218

Tönshoff H K, Ostendorf A, Graumann C, Kral V and Thiessen B, 1998**. Minimising thermal cracking for laser cutting of ceramics by implementing a closed-loop control system**. Proceedings ECLAT'98, pp 391 – 39

Tönshoff H K, von Alvensleben F, Graumann C and Willman G, 1998. **High precision machining of ceramics.** Proceedings SPIE, Vol. 3414, pp 51-59

Tönshoff H K, von Alvensleben F, Ostendorf A, Körber K and Kulik C, 2000. **Microstructuring with F2 lasers.** Proceedings SPIE, Vol. 4075, pp 159-166

References

Tsai C.-H. And Chen H.-W., 2003. **Laser milling of cavity in ceramic substrate by fracture machining element technique.** Journal of Materials Processing Technology, Vol. 136, Issues 1-3, 2003, pp.158-165

von der Linde D and Sokolowski-Tinten K, 2000. **The physical mechanisms of short-pulse laser ablation.** Applied Surface Science, Vol. 154-155, pp 1-10

Weaver, J.H., Krafka, C., Lynch, D.W. and Koch, E.E., 1981. **Optical properties of metals,** Vol. I and Vol.II. Zentralstelle fur Atomkernenergie-Dkumentation, ZAED, 1981

Wilson, J. And Hawkes, J.F.B., 1987**. Lasers: principles and applications.** Prentice Hall-Europe, 1987

Yilbas B S, 1997. **Laser heating process and experimental validation**. International Journal of Heat and Mass Transfer, Vol. 40, No 5, pp 1131-1143

Yilbas B.S., Gbadebo S.A., and Sami M., 2000. **Laser heating: an electron-kinetic theory approach and induced thermal stresses.** Optics and lasers in Engineering, 2000, Vol.33, pp.65-79

Zhu X., 2000. **A new methood for determining critical pulse width in laser material processing.** Applied Surface Science, Vol.167, 2000, pp.230-242